Protective memory B cell response in controlled human malaria infection

D I S S E R T A T I O N

zur Erlangung des akademischen Grades

doctor rerum naturalium

(Dr. rer. nat.)

im Fach Biologie

eingereicht an der Lebenswissenschaftlichen Fakultät

der Humboldt-Universität zu Berlin

von

Master of Technology Rajagopal Ayyanar Murugan

Präsidentin der Humboldt-Universität zu Berlin

Prof. Dr.-Ing. Dr. Sabine Kunst

Dekan der Lebenswissenschaftlichen Fakultät

Prof. Dr. Bernhard Grimm

Gutachter/innen : 1. Prof. Dr. Arturo Zychlinsky

2. Prof. Dr. Hedda Wardemann

3. Prof. Dr. Anja Hauser

Tag der mündlichen Prüfung: 12th Feb 2018

Abstract

Antibodies against the major *Plasmodium falciparum* (Pf) sporozoite surface protein, circumsporozoite protein (CSP), can mediate sterile immunity thereby preventing malaria disease symptoms as shown by passive transfer in animal models. However, protective anti-CSP memory antibody responses are not efficiently induced by natural Pf exposure or vaccination. Affinity maturation, i.e. the diversification of antigen-activated naïve precursor B cells by a somatic immunoglobulin (Ig) gene mutation process and the subsequent selection of B cells expressing antigen receptors with improved antigen affinity in germinal center reactions is considered key to the formation of protective memory B cell responses. However, how the anti-PfCSP memory B cell response matures in humans is not known. To address this question, the clonal evolution of the human anti-Pf CSP memory B cell response over three successive controlled Pf infections under chemoprophylaxis was assessed at single cell level by high throughput paired full-length Ig gene sequencing and recombinant monoclonal antibody production. The work provides basic insights in the longitudinal development of human memory B cell responses and identified germline-encoded Ig gene features that were associated with high anti-CSP affinity and Pf inhibitory antibody activity. The clonal selection of germline B cells expressing such antibodies, rather than affinity maturation, was associated with high quality anti-PfCSP memory B cell responses. The data provide insights into the evolution of antibody response to a complex protein antigen during infection and a strong rational for the design of novel CSP immunogens to target naïve B cell precursors expressing potent anti-CSP antibodies for the induction of protective memory B cell responses by vaccination.

Zusammenfassung

Antikörper gegen Circumsporozoite protein (CSP), ein Oberflächenantigen von *Plasmodium falciparum* (Pf), können sterile Immunität hervorrufen und dadurch die Entwicklung von Malaria im Tierversuch verhindern. Im Menschen werden protektive B-Zell Gedächtnisantworten gegen CSP durch natürliche Malariaerkrankung bzw. Vakzinierung jedoch nur unzureichend erzeugt. - Für die Entwicklung von Gedächtnis-B-Zellen stellt die Affinitätsreifung, welche durch somatische Immungobulin Hypermutation sowie der nachfolgenden Selektion von B-Zellen mit verbesserter Antigenaffinität charakterisiert ist, eine Schlüsselfunktion in der Generierung von protektiven Immunantworten dar. Wie Affinitätsreifung gegen CSP im Menschen stattfindet ist jedoch nicht bekannt. In dieser Arbeit wird die Affinitätsreifung von CSP Gedächtnis B-Zellen auf Einzelzellebene im Menschen über drei kontrollierte Infektionen mit Pf Sporozoiten unter Chemoprophylaxe untersucht. Durch Hochdurchsatz-Einzelzell-Sequenzierung der Immunoglobulin (Ig) gene loci und der Produktion von rekombinanten monoklonalen Antikörpern gewährt diese Arbeit Einsicht in die Selektion und Affinitätsreifung von humanen Gedächtnis-B-Zell Antworten gegen komplexe Proteinantigene und identifiziert Keimbahn kodierte Immunglobulin Charakteristika, die mit hoher CSP-Affinität und Pf-Inhibition einhergehen. Überraschenderweise zeigen die Daten, dass initiale klonale Selektion von hochaffinen B Zellen eine weitaus wichtigere Rolle als Affinitätsreifung in dieser Infektion spielt. Diese Arbeit zeigt fundamentale Eigenschaften von humanen Gedächtnisantworten in einer komplexen Parasiteninfektion und liefert die Grundlage für ein mögliches Design von neuartigen Immunogenen um hoch-affine B-Zellen gegen CSP effizienter zu induzieren.

Abbreviations

7AAD	7-Aminoactinomycin D
ABTS	2,2'-azino-bis(3-ethylbenzthiazoline-6-sulphonic acid)
AID	activation-induced cytosine deaminase
AUC	area under curve
B cell	bone marrow derived cell
BCR	B cell receptor
BM	bone marrow
bp	base pairs
BSA	bovine serum albumin
CD	cluster of differentiation
cDNA	complementary DNA
CDR	complementarity determining region
CHMI	controlled human malaria infection
CSP	circumsporozoite protein
CSR	class-switch recombination
DENV	Dengue virus
DNA	deoxyribonucleic acid
dNTP	deoxynucleotide triphosphate
DTT	dithiothreitol
E.coli	*Escherichia coli*
EDTA	ethylenediaminetetraacetic acid
EDIII	Envelope domain III
EEF	exoerythrocytic form
ELISA	enzyme-linked immunosorbent assay
Fab	fragment antigen binding
FACS	fluorescence-activated cell sorting
Fc	fragment crystallizable
FCS	fetal calf serum
FITC	fluorescein isothiocyanate
FWR	framework region
GC	germinal center
gp140	glycoprotein 140
h	hour
HC-04 cells	human hepatocyte cells
HEK cells	human embryonic kidney cells
HEPES	4-(2-hydroxyethyl)-1-piperazineethanesulfonic acid
HIV	Human Immunodeficiency Virus
HRP	horseradish peroxidase
Ig	immunoglobulin
i.v.	intravenous

LB	lysogeny broth
LPS	lipopolysaccharide
MHC	major histocompatibility complex
min	minute
NANP	repeat peptide consisting of asparagine-alanine-asparagine-proline
OD	optical density
Pb	*Plasmodium berghei*
PBMC	peripheral blood mononuclear cell
PBS	phosphate-buffered saline
PCR	polymerase chain reaction
PE	phycoerythrin
PEI	polyetherimide
Pf	*Plasmodium falciparum*
PFA	paraformaldehyde
Pb-PfCSP	transgenic *Pb* expressing the CSP of *Pf*
RHP	random hexamer primers
RNA	ribonucleic acid
rpm	revolutions per minute
RPMI	Roswell Park Memorial Institute (medium)
RT	reverse transcriptase
RTS,S	R: stands for the central repeat region of *Pf* CSP T: stands for the T cell epitopes in the C-terminus of CSP S: stands for the hepatitis B surface antigen (HBsAg) [1]
sec	second
SHM	somatic hypermutations
T cell	thymus derived cell
Taq polymerase	thermos aquaticus polymerase
T_{FH}	T follicular helper cells
T_H	T helper cells
TB	terrific broth
TSR	thrombospondin-like type I repeat
ZIKV	Zika virus

Table of contents

Table of contents

1. Introduction

1.1 B cell mediated adaptive immunity:

The key features of the adaptive immune response to infection or vaccination are antigen specificity and long-term immune memory. Those are achieved by recruiting antigen-specific cells from the diverse pool of T or B lymphocytes and differentiating them to memory cells for immune recall[1].

1.1.1 Diversity of the B cell antigen receptor

A hallmark of the adaptive immune system is the diversity of antigen-receptors with every newly generated lymphocyte expressing a unique antigen-receptor. Antigen receptors are encoded by two genes and the receptor diversity relies on a random somatic gene recombination process that assembles both genes from a large number of small gene segments. Successful recombination of both genes leads to allelic exclusion, i.e. abrogation of the recombination process on the second chromosome, thereby ensuring the expression of only one kind of antigen-receptor. B cells undergo this process during their early development in bone marrow (BM) where they recombine variable (V), diversity (D) and joining (J) segments in the heavy chain locus and V and J segments in the light chain locus to form functional Ig heavy (IgH) and light (IgL) chain genes, respectively (Fig. 1). IgH and to lesser extent IgL gene segments are recombined in an imprecise fashion thereby increasing antigen-receptor diversity[2,3]. Further, IgL chain genes are generated from either of two light chain loci, Ig kappa (Igκ) and lambda (Igλ). In humans, the

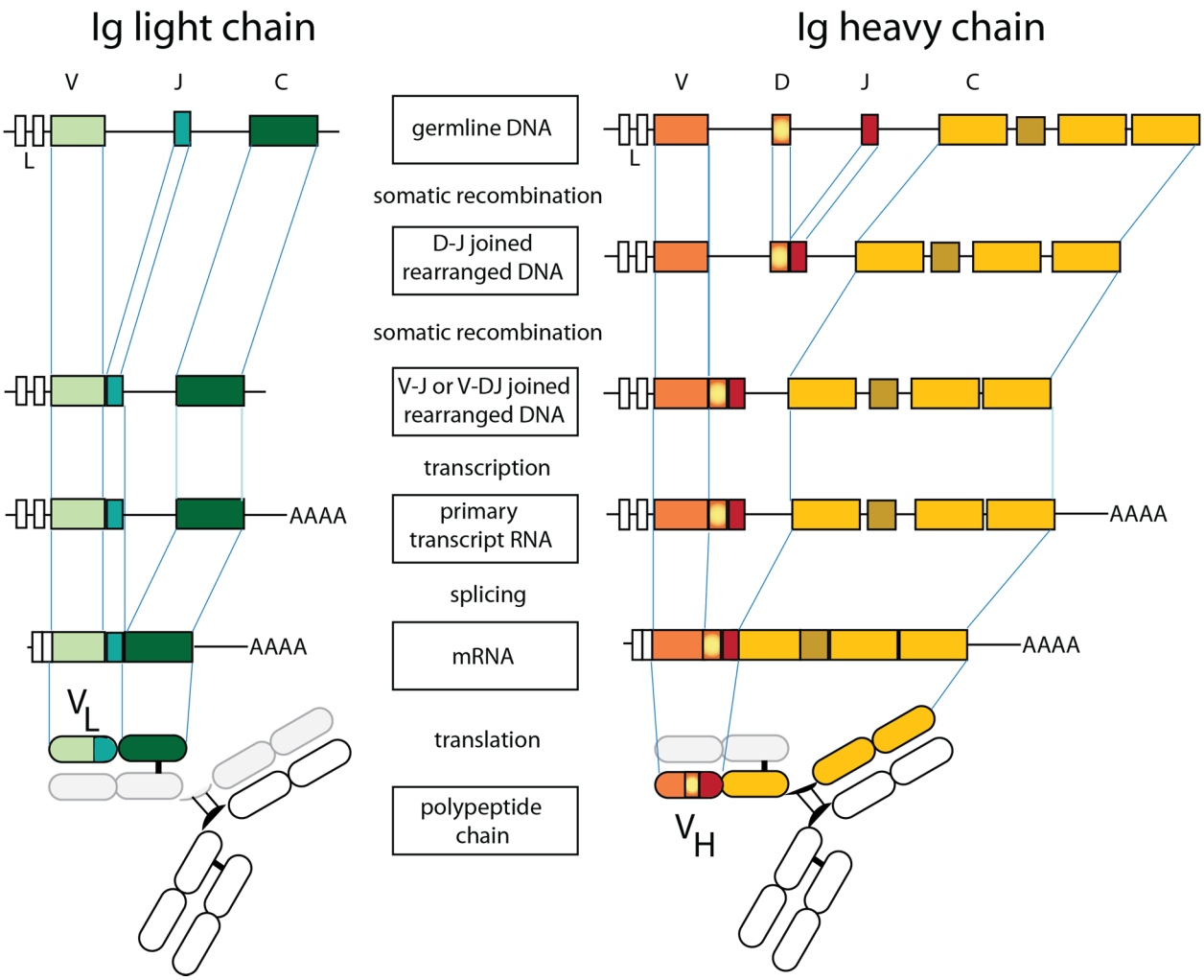

Figure 1. Immunoglobulin heavy and light chain gene recombination. In the heavy chain gene locus, random gene D and J segments recombine to form DJ which then recombines a random V gene segment to form VDJ. In the light chain locus, random V and J segments recombine to form VJ. Upon selection for being functional and non-autoreactive, they serve as BCRs of a mature naïve B cell. The figure is adapted from[4].

large number of individual Ig gene segments and the imprecise assembly process[5,6], together with IgL chain gene locus diversity generate a theoretical maximum diversity of $10^{12\text{-}14}$ different antigen-receptor specificities, which exceeds the actual number of B cells present at a given time in the whole organism (10^{12})[7,8]. Antigen-receptor diversity is key to the successful generation of protective immune responses against the plethora of potential pathogens that may be encountered during lifetime. However, cells expressing autoreactive B cell antigen receptors (BCRs) on the cell surface, which comprise the Ig and the signalling molecules Igα and Igβ[9], which are generated at high frequency due to the random nature of the Ig genes assembly process, are efficiently purged from the B cell pool at self-tolerance checkpoints in the BM and

periphery[10-14]. Therefore, the repertoire of B cells that remains in the system to respond to antigens expressed by invading pathogens may be considerably smaller than theoretically predicted. However, the diversity is still too large to allow for precise direct measurements.

1.1.2 B cell receptor: Structure and Function

BCRs are composed of Y-shaped IgH and paired Igκ or Igλ light chain homodimers linked by disulphide bridges and the associated Igα and Igβ signalling molecules[4]. The BCR is anchored in the cell membrane via a short transmembrane domain of the IgH chains[15]. However, upon antigen-mediated activation, B cells can also produce soluble antigen-receptors referred to as antibodies, which are composed of only the Ig part and lack the transmembrane region due to alternative splicing[16]. Antibodies are the effector molecules of B cell (humoral) immune responses. They are the product of antibody-secreting cells and are found at high concentrations in blood but also at mucosal surfaces. Here, they bind antigen and mediate defined effector functions through their IgH chains that interact with Ig receptors expressed on other immune cells as well as non-immune cells. Structurally, two fragments of antibodies can be distinguished, the Fab (fragment, antigen binding), which corresponds in large to the arms of Y-shaped molecule and mediates antigen-binding, and the stem or Fc (fragment, crystallizable) part, which determines the IgH-encoded effector function (Fig. 2).

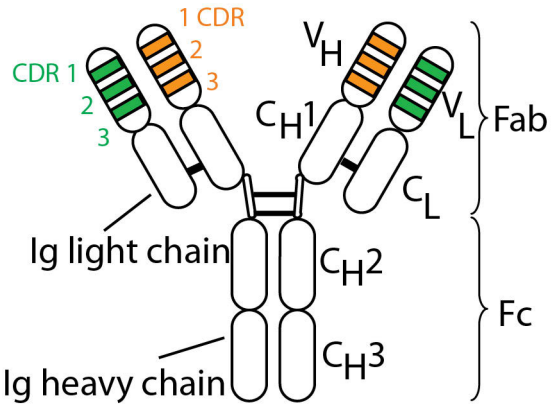

Figure 2. IgG antibody structure. Two units of heavy chain-light chain heterodimers linked by disulphite bridges form a single antibody molecule. The complementarity determining regions (CDR) of heavy and light chain variable regions (VH and VL, respectively) are indicated in orange and green, respectively. Antibody is functionally divided into antigen binding Fab and constant fragment Fc. The figure is adapted from[4].

IgH chains come in different flavors that are encoded by one of the following seven gene segments: *IGHM, IGHG1-4, IGHA1-2, IGHE,* and *IGHD* and show different effector functions based on interactions with specific Fc receptors[17,18]. The antigen-binding variable regions of the IgH and IgL chain genes are encoded by the joined V(D)J and VJ region of the fully rearranged IGH and IGK or IGL genes and therefore show high sequence variability. Structurally, the variable regions of both chains are divided into alternating framework and complementarity determining regions (FWRs and CDRs, respectively) (Fig. 2). While the FWRs mostly offer the frame for the protein structure and are overall more conserved in their sequence, CDRs show high sequence variability and strongly engage into antigen recognition.

1.1.3 B cell immune responses

Developing B cells that successfully passed the self-tolerance checkpoints and matured in the spleen circulate through the secondary lymphoid organs[11-14]. BCR-mediated interactions with a cognate antigen lead to their activation, proliferation and differentiation into either antibody secreting cells or resting memory B cells. Antigen-activated B cells internalize their BCRs thereby taking up antigen that is bound to the BCR. The uptake of protein antigens leads to their processing into small peptides that will be loaded onto so-called Major Histocompatability complex II (MHC-II) molecules for display on the cell surface. MHC molecules that present

these antigen peptides can be recognized by cognate T-helper cells (T_H)[19] (Fig. 3A). The direct interaction between B cells and T_H cells in secondary lymphoid organs is essential to induce the formation of germinal center reactions[20] (Fig. 3B).

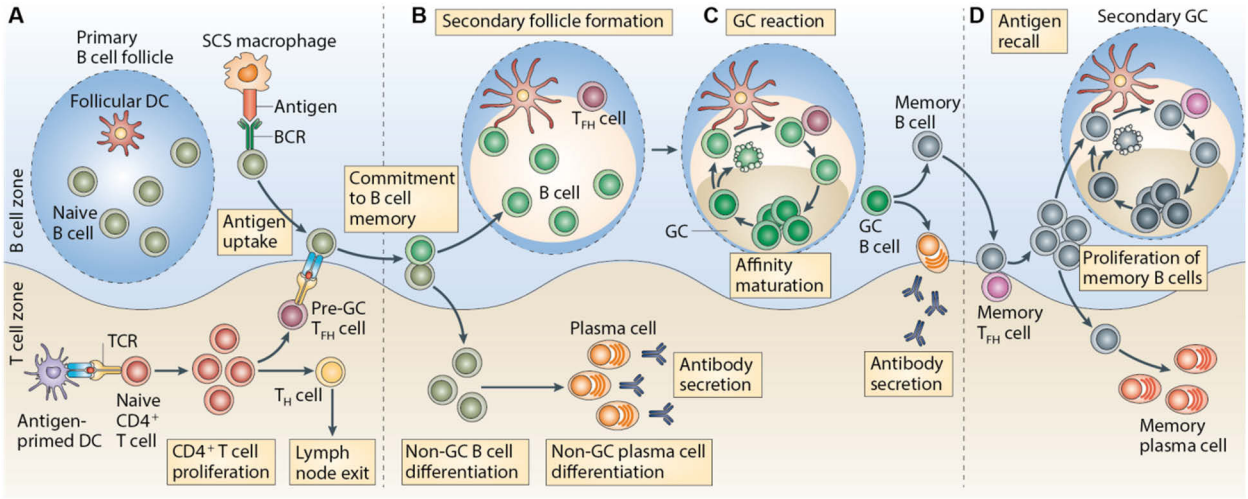

Figure 3. B cell mediated immune response. A. In response to protein antigen stimulation antigen specific naïve B cells engage in T cell - B cell contact. **B.** Non-GC dependent class switching and antibody secretion of B cells. Secondary follicular formation results in the generation and seeding of an germinal center (GC) by B cells, T_H cells and FDCs. **C.** GC reaction where B cells undergo affinity maturation through Ig gene diversification and selection by FDCs and TFH cells. Post GC, B cells differentiate into memory B cells or antibody secreting plasma cells. **D.** The memory B and TFH cells can take part in the secondary antigen encounter to seed new GCs. The figure is adapted from[21]

Germinal center reactions allow for the focused maturation of the B cell response to improve antigen-binding and thereby the quality of the humoral immune response by generating and selecting high-affinity antibody variants[22,23]. This process of affinity maturation is considered key for the development of potent long-lasting B cell memory to pathogens and has been shown to be essential for the induction of protective vaccine responses[24]. Germinal centers form in anatomically defined areas of secondary lymphoid organs, are clearly visible at around 6 days post primary immunization[25] and divide into two zones of proliferating (dark zone) and non-proliferating (light zone) cells[26]. Proliferating B cells in the dark zone are characterized by the somatic diversification of their Ig genes by random point mutations[27] (Fig. 3C). This process of somatic hypermutation (SHM) is regulated by the enzyme, Activation induced cytidine

deaminase (AID)[28]. *In vitro* experimental conditions estimate the mutation rate of AID as 10^3 per base pair per cell division, which is 10^6 fold higher than the normal somatic mutation rate[29,30]. The random point mutations generate B cells carrying variants of antibodies with altered or non-altered affinity. The Ig gene diversified GC B cells move to the light zone and compete for antigen presented by follicular dentritic cells (FDCs) and for help by the follicular T helper set, a specialized subset of T-helper cells (T_{FH})[20,31]. FDCs form a reticular network and can display antigen for extended periods of time[32,33]. GC B cells capture the antigen presented by FDCs through their BCR and present the processed antigenic peptides on MHC-II[34,35]. B cells with high affine antibodies compete better for antigens from the FDCs and will present more on MHC-II. This higher peptide-MHC-II density on the B cells with higher affine antibodies leads to the longest contact with the cognate T_{FH} cells[36,37]. The limitation of the antigen presented by the FDCs and key survival signals provided by the T_{FH} cells form the basis for antibody affinity maturation allowing the selection of B cells with high affine antibodies (Fig. 3C)[20,38,39]. The mentioned observations of GC dynamics come from extensive studies performed in the mouse model system[40]. The mechanistic details of the processes are less known in humans. The GC selection of high affine antibodies is extremely efficient for small molecules such as haptens[22,23,41] but more complex for protein antigens.

AID is not only essential to allow for affinity maturation through SHM, but also regulates class switch recombination (CSR), i.e. the exchange of Ig gene constant regions at genomic level. While AID catalyzes both, SHM and CSR, these processes can occur independently as both *IGHM* transcripts with SHMs[42-45] and non-mutated class-switched transcripts are found in GC B cells[31]. Upon positive selection by T_{FH} cells, B cells exit the GCs and differentiate into memory B cells or antibody secreting plasma cells. B cells carrying high affine antibodies are more likely to differentiate into plasma cells[46], whereas B cells with relatively lower affine antibodies differentiate into memory B cells, however the proportion of memory B cell to

plasma cell output may change over the GC life-time[47]. Memory B cells are quiescent B cells and do not contribute directly to the production of secreted antibodies. However, upon secondary antigen exposure they can get readily activated by antigen to differentiate into plasma cells or enter GCs for further diversification and affinity maturation[48] (Fig. 3D).

1.2 *Plasmodium falciparum*: Infection and Life cycle

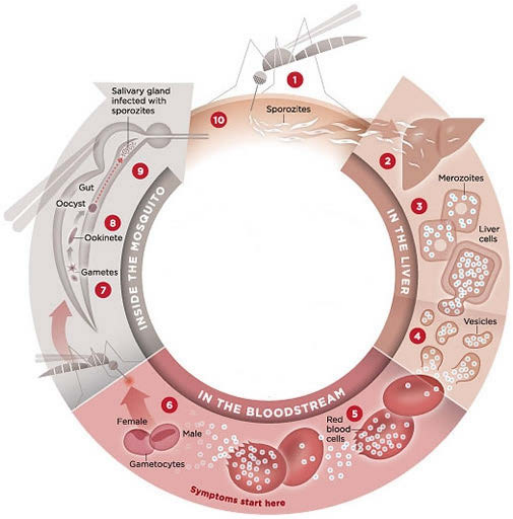

Figure 4. *Plasmodium falciparum* life cycle. Bite of the infected mosquito releases Pf sporozoites into the human host (1). The sporozoites travel to and infect hepatocytes (2) where they differentiate to merozoites (3). Once released from the hepatocytes (4), merozoites infect blood erythrocytes (5) and induce symptomatic malaria. The merozoites differentiate into female and male gametocytes (6) which when taken by the mosquitoes fertilize to form ookinete (7) and then oocyst (8) in the mosquito midgut. Upon oocyst differentiation, the resulting sporozoites travel to salivary gland (9) and are ready to be transmitted by the next mosquito bite (10). The figure is adapted from[49].

Malaria in humans is a mosquito vector born disease caused by *Plasmodium* parasites. Of the different species that cause clinical infection in humans, *Plasmodium falciparum* (Pf), which is most endemic in sub-Saharan Africa, causes the most severe form of the disease resulting in high mortality[50]. During a blood meal, Pf infected mosquitoes deposit sporozoites in the human skin from where they migrate to the nearest blood vessel and eventually home to the liver[51-54]. In the liver, sporozoites penetrate fenestrated endothelial cells and Kupffer cells to finally infect hepatocytes for their further development and differentiation into blood stage parasites (merozoites)[55,56]. Upon hepatocyte rupture, merozoites are released into the blood stream and infect circulating erythrocytes. After undergoing 48 h exponential replication inside the erythrocytes, merozoites and additional waste products are released into the blood stream

causing symptomatic disease. Inside erythrocytes, merozoites undergo either asexual expansion or differentiation into sexual male and female gametocytes. The sexual stage gametocytes are taken up during a blood meal by the *Anopheles* mosquito, wherein they fertilize to form the so called ookinete. The ookinete penetrates between basal lamina and midgut epithelium and differentiates into oocyst and then subsequently into sporozoites. The sporozoites invade the mosquito salivary glands and are released in the human host during the next blood meal for completion of the parasite life cycle[57,58].

1.2.1 Immune response to malaria

Wide range longitudinal studies in endemic areas reveal the acquisition of immunity to malaria disease with repeated parasite exposure[59,60]. This leaves newborns and young children at the most vulnerable end of the population, whereas adults encounter less severe forms of the disease[61]. The understanding for such phenomenon comes from the observation that the first parasite exposure, both in infants and humans with no previous exposure, almost always results in sickness. During the primary exposures, sudden systemic release of merozoites in the blood results in febrile illness. However, repeated parasite exposure over years generates antibody serum titers and controls the acute sickness[62-67]. While the immunity is established for homologous strains, several exposures with different strains build a broader, cross-strain immunity[68,69]. This however does not always guarantee sterile immunity, but rather prevents clinical illness and symptoms. The delay in the development of protective immunity and the lack of sterile immunity suggested that the immune memory formation is inefficient in malaria infection[70-72]. Contrary evidences for and against this suggestion have been reported and this conundrum underscores the pertinence to study the development of immune memory in malaria and how best to employ vaccines to meet that end.

1.2.2 Anti-sporozoite immunity and circumsporozoite protein

Seminal works in the 1970s by Nussenzweig and colleagues showed that immunization of mice with radiation attenuated *P. berghei* sporozoites provided sterile immunity against live *P. berghei* sporozoite challenge, but not against blood stage parasites[73]. This work established that sterile protection could be achieved and the findings that were later confirmed in humans using different attenuation strategies by radiation and genetic or chemical attenuation. Incubation of sporozoites with serum samples from mice immunized with irradiated sporozoites induced the so-called antibody-mediated "circumsporozoite precipitation". Nussenzweig *et al.*, later identified circumsporozoite protein (CSP), initially referred to as Pb44, as the sporozoite surface protein that was targeted by the antibodies, thereby inducing the precipitation reaction and active parasite inhibition[74-77].

CSP is structurally arranged in three domains, the N-terminal domain, a central region composed predominantly of NANP repeating units, and a GPI linked C-terminal domain that adheres the protein to the sporozoite surface[78] (Fig. 5). The N-terminal and C-terminal domains are polymorphic between different *P. falciparum* strains. In contrast, the central NANP repeat domain and

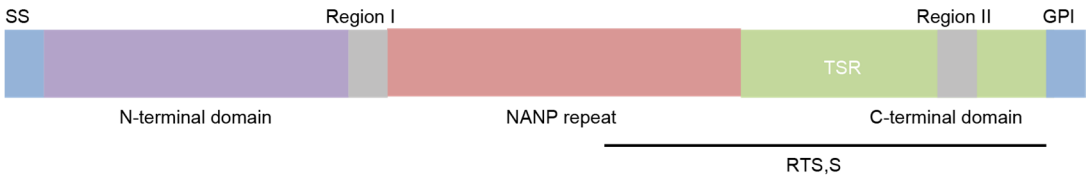

Figure 5. Schematic representation of PfCSP. PfCSP comprises of a signal peptide (SS), N-terminal domain, region I, NANP repeat units, and a C-terminal domain containing α-thrombospondin type-1 repeat (TSR), region II and a GPI anchor. The region constituting RTS,S vaccine is indicated by the black line.

immunodominant B-cell epitope is highly conserved and differs only in the number of repeating units[79,80]. Based on these findings, CSP has long been considered a promising subunit

vaccine candidate leading to the development of RTS,S AS01 (Mosquirix™), the leading malaria vaccine candidate. RTS,S contains 18.5 NANP repeat units and the entire C-terminal domain of CSP and aimed to induce protective humoral immune responses[81] (Fig. 5). However, recent Phase III clinical trials in endemic regions showed overall low protective efficacy ranging from 25% to 55% and no long-term protection, suggesting that protective memory responses did not develop efficiently[82,83].

2. Objectives

The overall goal of the thesis was to characterize the clonal evolution of the human anti-CSP memory antibody response over repeated *Plasmodium falciparum* infections and to determine the quality of the response at monoclonal antibodies level along the following specific aims,

1. To develop a high-throughput platform that would enable full length human immunoglobulin heavy and light chain gene (Ig) amplification from sorted single B cells compatible with direct cloning.

2. To determine the Ig gene features and clonal evolution of CSP-reactive memory B cells and corresponding plasmablasts after three controlled human malaria infections by high-throughput paired Ig gene amplification and sequencing at single cell level.

3. To assess the maturation of the anti-CSP memory B cell response over the repeated Pf infections by recombinant monoclonal antibody production and qualitative assessments of their CSP-reactivity as well as efficacy to inhibit Pf sporozoites.

3. Methods

3.1 Single B cell sorting and Ig gene amplification

Single cell Ig gene amplification and sequencing was performed using the protocols described here[84,85].

3.1.1 Fluorescence activated single cell sorting

Frozen PBMCs from liquid nitrogen storage was collected right before processing of the samples. The frozen vials were immediately transferred to 37 ºC water bath for 45 seconds until the frozen contents starts thawing. Before completely thawed, the contents of the vial was quickly transferred to 45 ml of RPMI medium in a 50 ml falcon tube and mixed well to ensure complete thawing took place in the tube and the residual DMSO was immediately diluted in the medium. The tubes were centrifuged at 350 x g for 5 min and the supernatant was discarded. The cell pellet was resuspended in 1ml of the cold FACS buffer (1% FCS in PBS) and transferred to 1.5 ml micro centrifuge tubes. The tubes were centrifuged at 1160 x g for 5 min at 4 ºC and the cell pellet was kept on ice after discarding the supernatant. Using manufacturer's instructions, AlexFluor 647 Protein labeling kit (Molecular Probes) was used for fluorescent labeling of recombinant PfCSP (Protein Potential, LLC). The pellet was resuspended in 100 µl of 30 ng/µl of labeled PfCSP and kept on ice for 30 min. After incubation, 1 ml of FACS buffer was added to the cell staining solution and the tubes were centrifuged at 1160 x g for 5 min at 4 ºC. After discarding the supernatant, the cell pellet was resuspended in 100 µl of the staining cocktail containing antibodies listed in Table 1 in FACS buffer and incubated on ice for 30 min. U-266 (DSMZ) cell lines were used for testing *IGHE* primers.

Table 1. Fluorochrome labeled monoclonal antibodies used in flow cytometry.

Mouse anti-human antibody	Clone	Manufacturer	Dilution used
CD19-BV786	SJ25C1	BD Biosciences	1:10
CD20-APC-H7	2H7	BD Biosciences	1:20
CD27-PE	M-T271	BD Biosciences	1:5
CD38-FITC	HIT2	BD Biosciences	1:5
IgG-BV510	G18-145	BD Biosciences	1:20
CD138-BV421	MI15	BD Biosciences	1:20
CD21-PE-Cy7	Bu32	BioLegend	1:20

After incubation, 100 µl of FACS buffer containing 7-aminoactinomycin (7-AAD) diluted to 1:200 was added to the cell suspension in staining cocktail and incubated on ice for 10 min. The tubes were washed once and the cell pellet was resuspended in 300 µl of FACS buffer and filtered through FACS tubes. FACS AriaII (BD) with the FACSDiVa software version 8.0.1 (BD) was used for analyzing the stained cell samples and single cell sorting. Single cells were selected using FSC and SSC height and width parameters. CSP binding memory B cells were defined as 7AAD- CD19+ CD27+ IgG+ CSP+, 7AAD- CD19+ CD27+ IgG CSP+ or 7AAD- CD19+ CD27- IgG+ CSP+ cell population. Plasmablasts were defined as 7AAD- CD19+ CD27+ CD38+ cell population. Due to the limitation of the samples, the above gates were defined using 100,000 recorded cells. The single cell sorting was performed using an OR gate set up between CSP memory B cells and plasmablasts. Index sorting option of the software was enabled during sorting, hence the sorted cells could be identified later for either of the two populations. The sorting was performed in 384well plates containing 2 µl of sort RHP mix above cooled sorting stage. The sort RHP mix consisted of NP-40 to enable cell lysis, DTT to denature RNA secondary structures, RNAsin as a RNAse inhibitor and RHP to bind to the RNA and prime reverse transcription.

Table 2. Concentration of the reagents used per well as sort RHP mix.

Reagent	Concentration	Volume (µl)
Nuclease free water	-	1.4813
PBS	10X	0.0500
DTT	100mM	0.1000
NP-40	10%	0.1375
RHP	300 ng/µl	0.1375
RNAsin	40 U/µl	0.0938
Total		**2.0000**

As soon as the sorting was finished, the plates were frozen down on dry ice to preserve the contents and transferred to -80 ºC freezer for long term storage.

3.1.2 Reverse Transcription Polymerase Chain Reaction (RT-PCR) mediated cDNA synthesis

The frozen PCR plates were thawed on ice and incubated at 68 ºC for 60 sec to enable RNA secondary structure denaturation. After the incubation, the plates were brought back on ice and 2 µl of RT master mix was added. The RT mix consisted of the following reagents, 1X RT buffer to provide ambient buffer condition, DTT for denaturing RNA secondary structures, dNTP for the synthesis reaction, RNAsin as RNAse inhibitor and monkey murine leukemia virus derived reverse transcriptase SuperScript III for the enzymatic reaction. The concentration used as are in the below table 3 and performed using the conditions listed in the table 4.

Table 3: Concentration of the reagents used per well as RT master mix for RT-PCR.

Reagent	Concentration	Volume (µl)
Nuclease free water	-	0.6375
RT buffer	5X	0.8000
DTT	100mM	0.3000
dNTP	25 mM each	0.1375
RNAsin	40 U/µl	0.0563
SuperScript III	200 U/µl	0.0688
Total		**2.0000**

Table 4. RT-PCR thermocycler program

Step	Temperature	Duration	Cycles
RNA denaturation	42 ºC	5 min	1
RHP annealing	25 ºC	10 min	1
Reverse Transcription	50 ºC	60 min	1
Ending reaction	94 ºC	5 min	1

3.1.3 Amplification of Ig gene transcripts using nested PCR

Ig gene amplification of heavy, kappa and lambda loci was performed using a nested PCR approach with primary and secondary PCRs for each locus[84, 85]. 1st PCR was performed using 1 µl of cDNA template in three different PCRs, each with locus specific primer sets, listed in the supplementary table S3 and the reagent concentration in Table 5. The resulting amplicons of the primary PCR were used as template in the 2nd PCR, using the primer sets listed in supplementary table S3 and the reagent concentration in Table 6. Both forward and reverse primers used in the 2nd PCR were barcoded with 16bp and the barcoded primers were used along the row or column to have unique combination in each well. The conditions of both the PCRs are listed in Table 7.

Table 5. Concentration of the reagents used per well in 1st (1° PCR).

Reagent	Concentration	Volume (µl)
Nuclease free water	-	7.5950
Buffer	10X	1.0000
5’ primer sets	50 µM	0.1300
3’ primer sets	50 µM	0.1300
dNTPs	25 mM each	0.1000
HotStart Taq	5 U/µl	0.0450
Template		1.0000
Total		**10.0000**

Table 6. Concentration of the reagents used per well in 2nd (2° PCR).

Reagent	Concentration	Volume (µl)
Nuclease free water	-	7.7900
Buffer	10X	1.0000
5’ primer sets	50 µM	0.0325
3’ primer sets	50 µM	0.0325
dNTPs	25 mM each	0.1000
HotStart Taq	5 U/µl	0.0450
Template		1.0000
Total		**10.0000**

Table 7. 1st (1°) and 2nd (2°) thermocycler program for the three loci

	Temperature				
Step	**Heavy**	**Kappa**	**Lambda**	**Duration**	**Cycles**
Activation of HotStart Taq	94 °C	94 °C	94 °C	15 min	1
DNA denaturation	94 °C	94 °C	94 °C	30 sec	50
Primer annealing	58 °C	58 °C	60 °C	30 sec	50
Elongation	72 °C	72 °C	72 °C	55 sec (1°) or 45 sec (2°)	50
End amplification	72 °C	72 °C	72 °C	10 min	1

3.1.4 Next generation sequencing (NGS) and sequence analysis

For a given locus, 1 µl of the 2nd PCR mixture per well was taken and pooled from all the wells processed. The pooled DNA was purified using PCR purification columns and later by running 2 % agarose gel using NucleoSpin® Gel and PCR Clean-up kit from Macherery-Nagel GmbH, following manufacturer's instructions. The purified amplicons were sequenced using 454 FLX+ sequencing (Roche) or MiSeq 300 bp Paired End (Illumina). The sequencing reads were processed through the published bioinformatics pipeline, sciReptor (version 1.0.1.-1-gad8bbdf or 1.0.2-0-gf70a308). The pipeline assembled the reads based on the barcodes present in the 5' and 3', built consensus sequence and used standalone version of IgBLAST to extract the gene segment usage, somatic hypermuation count and position and CDR3 features. The pipeline also linked the index data to the sequences. Using MySQL and R scripts, specific queries were coded and executed to do the analysis on functional matching heavy and light chains.

3.2 Ig gene cloning and monoclonal antibody expression

3.2.1 Ig gene specific PCR

To clone to the heavy and light chain gene sequences into the corresponding expression vectors, gene specific PCRs were performed. Based on the Ig gene analysis, specific V and J segment primers that carried restriction enzyme sites were used from the list available in the supplementary table S3. While the 5' V gene primer for all loci used AgeI restriction site, 3' J gene primers for heavy, kappa and lambda used SalI, BsiWi and XhoI restriction sites, respectively. 1st PCR product was used as a template and the concentration of other reagents are listed in the Table 8. The 2nd PCR program mentioned in the Table 7 was used for amplification.

Table 8. Concentration of the reagents used per well in Specific PCR.

Reagent	Concentration	Volume (µl)
Nuclease free water	-	29.40
Buffer	10X	4.00
5' primer sets	50 µM	2.00
3' primer sets	50 µM	2.00
dNTPs	25 mM each	0.40
HotStart Taq	5 U/µl	0.20
Template		2.00
Total		**40.00**

3.2.2 Preparation of chemo-competent bacteria

Escherichia coli DH10B strain was used in cloning. Frozen *E.coli* stock was streaked on a lysogeny broth (LB) agar plate and incubated at 37 °C overnight. Single colony from the LB plate was inoculated in a 5 ml LB medium and incubated at 37 °C in 180 rpm shaker overnight. 800 µl of the overnight grown culture was given as inoculum to 250 ml of LB medium and incubated at 37 °C in 180 rpm shaker. Absorbance was measured until the culture reached OD_{600} 0.5. The culture was then kept on ice for 30 min and centrifuged at 3000 rpm for 20 min at 0 °C. The bacterial pellet was resuspended in 80 ml of sterile 0.1 M $CaCl_2$ and incubated on ice under cold condition overnight. Next day, the contents were centrifuged at 3000 rpm for 20 min at 0 °C and the bacterial pellet was resuspended in 2 ml of 0.1 M $CaCl_2$ with 15 % glycerol. Aliquots of 50 µl bacterial suspensions were made, quickly frozen using liquid nitrogen and transferred to – 80 °C freezer for long term storage. Competency of the bacteria was determined by transforming them using plasmid at the following concentration: 1 ng, 0.25 ng, 0.0625 ng, and 0.015625 ng. Bacteria were used only when they yielded >=10^6 colonies/µg of DNA.

3.2.3 Transformation of chemo-competent *E. coli* for cloning vector generation

Igγ1, Igκ and Igλ vectors containing ampicillin resistance gene were used for cloning heavy, kappa and lambda genes, respectively (Supplementary Fig. S1). Frozen competent bacterial vials were incubated on ice for 20 min and thawed. To 10 µl of competent bacteria, 1 ng of cloning vector was added and incubated on ice for 20 min. After incubation, heat-shock was given by incubating the tubes at 37 °C for 2 min and bringing them back on ice for 5 min. After adding 100 µl of pre-warmed LB medium, the tubes were shaken at 650 rpm, 37 °C for 40 min. After incubation, 10 µl of the bacterial suspension was spread-plated in a LB agar plate containing ampicillin at 100 ng/µl and incubated at 37 °C overnight. Single bacterial colony from the plate was inoculated in 5 ml of LB medium containing 75 ng/µl ampicillin and incubated at 37 °C in 180 rpm overnight. 500 µl of the overnight grown culture was given as inoculum in 200 ml of LB medium containing 75 ng/µl ampicillin and incubated overnight at 37 °C in 180 rpm. The bacterial culture was centrifuged at 3000 rpm for 10 min and the pellet was used for plasmid purification using NucleoBond® Xtra Midi/Maxi kit from Macherey-Nagel GmbH following manufacturer's instructions. DNA concentration of the vectors was measured using Nanodrop.

3.2.4 Restriction endonuclease digestion of cloning vectors and PCR amplicons

The cloning vectors and PCR amplicons were double digested using the enzymes corresponding to the locus. AgeI was used for all three loci, whereas SalI, BsiWI and XhoI were used for heavy, kappa and lambda loci, respectively. Double digest recommendations from New England Biolabs were followed and the digestions were performed at 37 °C for 2 hr. After digestion of the PCR amplicons, the NucleoSpin® 96 PCR Clean-Up kit from Macherey-Nagel GmbH was used for purification. For the cloning vectors, the digested product was run 2 % agarose gel and the band corresponding to the linearized vectors were cut and

purified using the NucleoSpin® Gel and PCR Clean-up kit from Macherery-Nagel GmbH, following manufacturer's instructions. The linearized vectors were aliquoted and frozen at -20 °C freezer for long term storage.

3.2.5 Ligation of the digested cloning vectors and PCR amplicons

Digested and purified PCR amplicons were ligated to their corresponding linearized cloning vectors, using T4 DNA ligase. The reaction was performed as mentioned in the Table 9, and incubated overnight at 16 °C. After incubation, 6 µl of the ligation reaction mixture was mixed with 10 µl of chemo-competent bacteria and transformation was performed.

Table 9. Concentration of the reagents used per reaction for ligation.

Reagent	Concentration	Volume (µl)
Digested PCR amplicon	6-15 ng/µl	7.5
Ligation buffer	10X	1.0
Linearized cloning vector	25 ng/µl	1.0
T4 DNA Ligase	400 U/µl	0.5
Total		**10.00**

3.2.6 Screen for successful cloning by bacterial colony PCR and Sanger sequencing

To assess for successful cloning, three bacterial colonies were randomly chosen from, and the presence of PCR amplicon ligated to the cloning vector was verified through PCR. The primers used for the PCR annealed to the vector constructs and hence the resulting amplicon size served as an indicator for the presence of ligated PCR amplicon. PCR master mix was prepared as mentioned in the Table 10. The bacterial colony touched by a pipette tip was immersed into the reaction mix for 5 min. The PCR was performed using the conditions listed in the Table 11.

Table 10. Concentration of the reagents used per well in bacterial colony PCR.

Reagent	Concentration	Volume (µl)
Nuclease free water	-	18.6
Buffer	10X	2.5
5' primer	50 µM	0.2
3' primer	50 µM	0.2
dNTPs	1.25 mM each	2.5
Taq polymerase	5 U/µl	1.0
Total		**25.0**

Table 11. Bacterial colony PCR thermocycler program

Step	Temperature	Duration	Cycles
Activation of Taq polymerase	94 ºC	5 min	1
DNA denaturation	94 ºC	30 sec	72
Primers annealing	58 ºC	30 sec	72
Elongation	72 ºC	60 sec	72
End amplification	72 ºC	10 min	1

The size of the amplicons was assessed by running the products on 2% agarose gel. Successful amplified (~650 bp for Igγ1, ~700 bp for Igκ and ~590 bp for Igλ) products were commercially sequenced at Eurofins Genomics GmbH for sequencing service. The resulting sequences were compared to the secondary PCR sequences of the Ig genes. Sequences that showed any variation to the secondary PCR sequences were ignored from further analysis.

3.2.7 Preparation of cloned vector

Bacterial colonies that were screened and selected for successful Ig gene cloning were inoculated in 5 ml LB medium containing 75 ng/µl ampicillin and incubated overnight at 37 °C in 180 rpm shaker. After incubation, the bacterial culture was centrifuged at 4000 rpm for 5 min and the pellet was used for isolation of vector using NucleoSpin® Plasmid Kit from Macherey-Nagel, following manufacturer's instructions. Final elution of the vectors was performed using 150 µl Elution buffer and the DNA concentration was measured using Nanodrop. Until further use, the vectors were stored in -20 °C freezer.

3.2.8. Germline reversion of Ig genes

For the generation of germline reversion, Ig genes of all the mutated clusters members were aligned in Clustal Omega (https://www.ebi.ac.uk/Tools/msa/clustalo) and compared to the germline Ig gene downloaded from IMGT® (http://www.imgt.org/). The point mutations were reverted to the germline bp in the V regions. In the heavy chain CDR3 region, the most consensus bp at a given position from the cluster members was considered germline bp. In the light chain CDR3 region, the V and J sequences from the database was used for construction. The gene sequences carrying corresponding restriction sites were synthesized at MWG gene synthesis service and cloned into the corresponding cloning vector.

3.2.9 FreeStyle™ 293-F cell culture

FreeStyle™ 293-F cells were cultured using FreeStlye293 Expression Medium at 37 °C and 8 % CO_2 in 180 rpm shaker. The cells were seeded in 20 ml at 0.5 x 10^6 cells/ml in a 50 ml filtered culture tubes. The cells were regularly passaged when the cell count reached 3 x 10^6 cells/ml. The passaging steps included pelleting down the cells at 1500 rpm for 5 min,

discarding the spent medium, resuspending the cell pellet in the fresh medium and seeding them at the above mentioned concentration.

3.2.10 Cotransfection of FreeStyle™ 293-F cells using Polyethylenimine (PEI)

10 ml culture of 1.5 x 10^6 cells/ml were seeded a day before transfection and allowed to grow at 37 °C and 8 % CO_2 in180 rpm shaker. During the day of transfection, 15 µg of each heavy and light chain vectors were added to the culture and the tubes were placed back in the shaker for 10 min. After the incubation, 150 µl of 0.6 mg/ml sterile PEI was added to the culture and the tubes were placed back in the shaker. A day after the transfection, 10 ml of EX-CELL 293 Medium complemented with L-Glutamine was added and the tubes were incubated in the shaker. 5 days post transfection, the cell culture tubes were centrifuged at 4000 rpm at 4 °C for 30 min and the supernatant was carefully transferred into a clean tube. The antibody containing supernatants were stored at 4 °C, until further use.

3.2.11 Purification of recombinant monoclonal antibodies

Protein G Sepharose beads were used for purification of the recombinant antibodies. 100 µl of beads per 20 ml antibody supernatant was taken and washed with cold PBS. The beads were then added to the supernatant and mixed well by overnight incubation in tube rotator at 4 °C. After incubation, the tubes were centrifuged at 2000 rpm for 20 min at 4 °C and the supernatant was transferred to a clean tube. The pellet beads were resuspended in 1 ml cold PBS and transferred into equilibrated Biospin column. The beads were washed twice by letting 1 ml of cold PBS run through the column. The bound antibodies were thrice eluted using 200 µl of 0.1M glycine (pH 3.0) and the eluent was collected in 20 µl of 1 M Tris (pH 8.0). The purified antibodies were dialyzed in cold PBS using using Slide-A-Lyzer® Mini Dialysis Devices following manufacturer's instructions.

3.3 Biochemical and functional characterization of monoclonal antibodies

3.3.1 Antibody concentration determination

Concentration of the purified antibodies was determined using Enzyme Linked Immunosorbent Assay (ELISA). High binding 96 well ELISA plates were coated with 2 µg/ml goat anti-human IgG Fc-fragment in 50 µl/well of PBS at 4 °C overnight. The plates were washed with deionized water three times and 200 µl/well of PBS with 0.01% Tween and 0.01 M EDTA was added as blocking buffer and incubated at RT for 1 hr. 1:2.5 serial dilution of antibodies up to 8 steps were prepared in PBS with the starting dilution of 1 in 100. Purified human IgGs with known concentration was also similarly serially diluted to use as a standard with the starting concentration of 1 and 3 µg/ml. After blocking, the plates were washed thrice and incubated for 1.5 h with 50 µl /well the diluted antibodies and standard antibody. After incubation, the plates were washed thrice and incubated for 1 h with 50 µl/well of horseradish peroxidase conjugated goat anti-human IgG at 1 µg/ml in blocking buffer. The plates were washed and the bound antibodies were developed using 100 µl/well of ABTS 1-step solution (Roche) containing 1 µl/ml of H_2O_2. Absorbance was measured at OD_{405} using M1000 Pro platereader (Tecan) and the concentrations of the monoclonal antibodies were determined using the standard antibody absorbance.

3.3.2 Antibody reactivity assessment

High binding 96 well plates were coated with 40 ng/well CSP^{86} or 100 ng/well $NANP_{10}$ (Alpha Diagnostic Intl. Inc.) at 100 µl/well in PBS overnight at 4 °C. After incubation, the plates were washed with three times with deionized water and incubated with 200 µl/well blocking buffer containing 1 % BSA in PBS for 1 h. The monoclonal antibodies were serially diluted 1:4 up to 4 steps with the starting concentration 4 µg/ml in PBS. As positive and negative controls, the

monoclonal antibodies 2A10[87] and mGO53[88] were used. After blocking, the plates were incubated for 1.5 h with 50 µl/well of serially diluted antibodies. After incubation, the plates were washed thrice and incubated for 1 h with 50 µl/well of horseradish peroxidase conjugated goat anti-human IgG at 1 µg/ml in blocking buffer. The plates were washed and the bound antibodies were developed using 100 µl/well of ABTS 1-step solution (Roche) containing 1 µl/ml of H_2O_2. Absorbance was measured at OD_{405} using M1000 Pro platereader (Tecan). The reactivity of the monoclonal antibodies to a given antigen was determined by calculating area under the curve of absorbance measured for the 4 dilutions using GraphPad Prism 6.07.

3.3.3 Antibody poly-reactivity assessment

High binding 384 well ELISA plates were coated with 15 µl of recombinant human insulin (10 µg/ml), dsDNA (10 µg/ml) or LPS (5 µg/ml) at 4 °C overnight. The plates were washed thrice with deionized water and blocked with 50 µl/well blocking buffer (PBS with 0.01% Tween and 0.01 M EDTA) for 1 hr. After incubation, plates were thrice washed and incubated for 1.5 h with 15 µl of monoclonal antibodies at 4 µg/ml in PBS. Antibodies ED38[89] and mGO53[88] were used positive and negative controls. After incubation, the plates were washed thrice and incubated for 1 h with 15 µl/well of horseradish peroxidase conjugated goat anti-human IgG at 1 µg/ml in blocking buffer. The plates were washed and the bound antibodies were developed using 25 µl/well of ABTS 1-step solution (Roche) containing 1 µl/ml of H_2O_2. Absorbance was measured at OD_{405} using M1000 Pro platereader (Tecan). The reactivity of the monoclonal antibodies to a given antigen was determined by absorbance measured and analyzed using GraphPad Prism 6.07.

3.3.4 Serum ELISA

High binding 96 well plates were coated with 40 ng/well CSP at 100 µl/well in PBS overnight at 4°C. After incubation, the plates were washed with three times with deionized water and incubated with 200 µl/well blocking buffer containing 4 % BSA in PBS for 1 h. Serum samples were serially diluted 1:2 up to 4 steps with the starting concentration 1:100 in 2 % BSA in PBS. After blocking, the plates were incubated for 1.5 h with 50 µl/well of serially serum samples. After incubation, the plates were washed thrice and incubated for 1 h with 50 µl/well of horseradish peroxidase conjugated goat anti-human IgG at 2 % BSA in PBS. The plates were washed and the bound antibodies were developed using 100 µl/well of ABTS 1-step solution (Roche) containing 1 µl/ml of H_2O_2. Absorbance was measured at OD_{405} using M1000 Pro platereader (Tecan). The reactivity of the serum samples to CSP was determined by calculating area under the curve of absorbance measured for the 4 dilutions using GraphPad Prism 6.07.

3.3.5 Surface Plasmon Resonance (SPR)

SPR measurements were carried out in a BIACORE T200 (GE Healthcare) machine docked with a series S CM5 sensor chip (GE Healthcare). 10mM HEPES buffer with 150mM NaCl, 0.02 % Tween 20 and 0.05 % BSA at pH 7.4 was used as a running buffer. Using manufacturer's instructions, anti-human IgG antibody from the human antibody capture kit (GE Healthcare) was immobilized on the chip through amine-coupling. Antibody and control antibody mGO53 were captured in the sample and reference flow cell at equal concentration, respectively. After capture, both the flow cells were stabilized for 20 min at 10 µl/min flow rate. $NANP_5$ resuspended in the running buffer was injected into the flow cell at different concentrations in the order, 0, 0.015, 0.09, 0.55, 3.3 and 20 µM. Each injection followed 60 s association and 180 s dissociation at the flow rate of 30 µl/min at 25 °C. After each run, both

the flow cells were regenerated using 3M $MgCl_2$. BIACORE T200 software V2.0 was used for fitting the data in 1:1 binding model and performed steady state or kinetic analysis.

3.3.6 Sporozoite hepatocyte traversal assay

Human hepatocyte cell line (HC-04)[90] cells were seed in a 96 well plate at 6 x 10^4 cells/well in a volume of 150 µl/well and incubated at 37 °C and 5 % CO_2 for 24 h, until they reached 70 % confluency. 100,000 Pf NF54 sporozoites isolated from infected *Anopheles coluzzi* were incubated with 100 µg/ml monoclonal antibody in a volume of 27.5 µl on ice for 30 min. 27.5 µl of 1 mg/ml Dextran-rhodamine (Molecular Probes) was added to the sporozoites antibody mixture and 50 µl of this mixture was added to the cells. The cells treated with just dextran-rhodmine were used to measure the background noise. The cells treated with sporozoites and dextran-rhodamine were used for estimating the maximal traversal rate achieved. Monoclonal antibodies 2A10[87,91] and mGO53[88] were used as positive and negative controls, respectively. The plate was centrifuged at 3000 rpm for 10 min with no brakes and acceleration. After centrifugation, the plate was incubated at 37 °C and 5 % CO_2 for 2 h. After incubation, the cells in the plate were washed thrice with PBS and the detached using trypsinization and resuspended in 10% FCS in PBS. The contents were transferred into micro centrifuge tubes and centrifuged at 3600 rpm for 5 min at 4 °C. The cell pellet was resuspended in 1 % PFA in PBS. Flow cytometry was performed in LSR II instrument and the frequency of dextran-positive cells was estimated. After background noise detection, the inhibition of sporozoite traversal rate was estimated by normalizing the data to the maximal traversal rate achieved without antibody[91]. The data was analyzed in FlowJo V.10.0.8 (Tree Star).

3.4 Statistical analysis

Experimental data were analyzed on RStudio (version 3.2.2) or Prism 6.07 (GraphPad) using two-tailed Mann-Whitney assuming non-normal distribution, Chi-square test or Fisher's exact test. *P < 0.05; **P < 0.01; ***P < 0.001; ****P < 0.0001. All experiments were performed in independently performed replicates, a minimum of twice.

4. Results

4.1 Ig PCR primer establishment and validation

To develop a high throughput strategy for the human Ig gene amplification using a barcoded primer matrix, primers used in Ig gene amplification were altered to use minimum primers at the barcoding 2nd PCR step. In the *IGH* PCRs, the newly designed primer sets with 9 *IGHV* gene primers in the 1st PCR and a single *IGHV* gene primer in the 2nd PCR (Complete mix)[85] were compared to the published primer sets (Tiller et al)[84]. PCRs performed on single cell sorted IgG+ CD27+ memory B cells from healthy donors showed comparable amplification efficiency for both primer sets (Fig. 6A). To enable parallel amplification of the different isotypes in one PCR plate, performance of *IGHC* primers of the isotypes, IgM, IgG, IgA and IgE were compared in isolation (specific) or as a mixture (MEGA) in amplifying B cells of the corresponding isotypes. Comparable amplification efficiency indicated that the constant primers did not sabotage amplification of one another and could be used as a mixture (Fig. 6B). Similar to *IGH* PCRs, 2nd PCR primers in the *IGL* PCRs were reduced to two and the resulting *IGL* PCR amplification efficiency of ~30 % and the overall *IGK/IGL* PCR efficiency of ~ 80 % validated the primer sets (Fig. 6C).

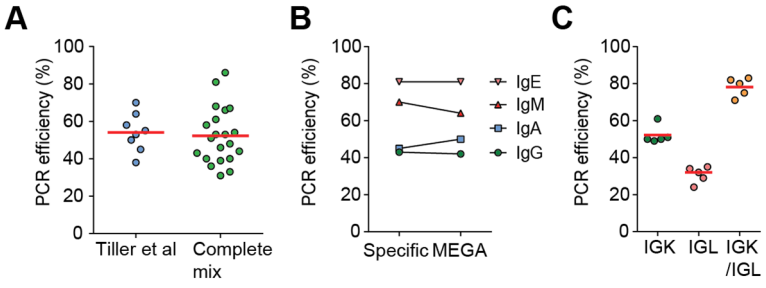

Figure 6. Comparison of Ig PCR primers. A. *IGH* PCR amplification efficiency using published primer sets (Tiller et al) and primer sets developed (Complete mix). **B.** *IGH* PCR efficiency using specific or mixed (MEGA) constant primers. **C.** PCR efficiency of *IGK* and *IGL* PCRs and the overall light chain PCR efficiency. Red line indicates mean. This figure is adapted from[85].

To summarize, the primers for Ig gene amplification designed to have minimum primer numbers at the barcoding steps amplified Ig genes with efficiency comparable to the published primer sets.

4.2 Performance of high-throughput matrix PCR

To test the performance of the human matrix PCR, the 2nd PCR primers were barcoded using 16 bp and were assigned to an individual row and column in a matrix, thus the individual reaction in each well would have a combination of uniquely barcoded forward and reverse primers[85,92]. IgG memory B cells from three healthy donors were single cell sorted and the barcoded primer matrix was used to amplify Ig genes. This strategy resulted in the amplification efficiency of 41%, 49% and 30% in heavy, kappa and lamdba PCRs. Taken together, 41% of the sorted cells were successfully amplified and sequenced in both heavy and light chain loci (Fig. 7A).

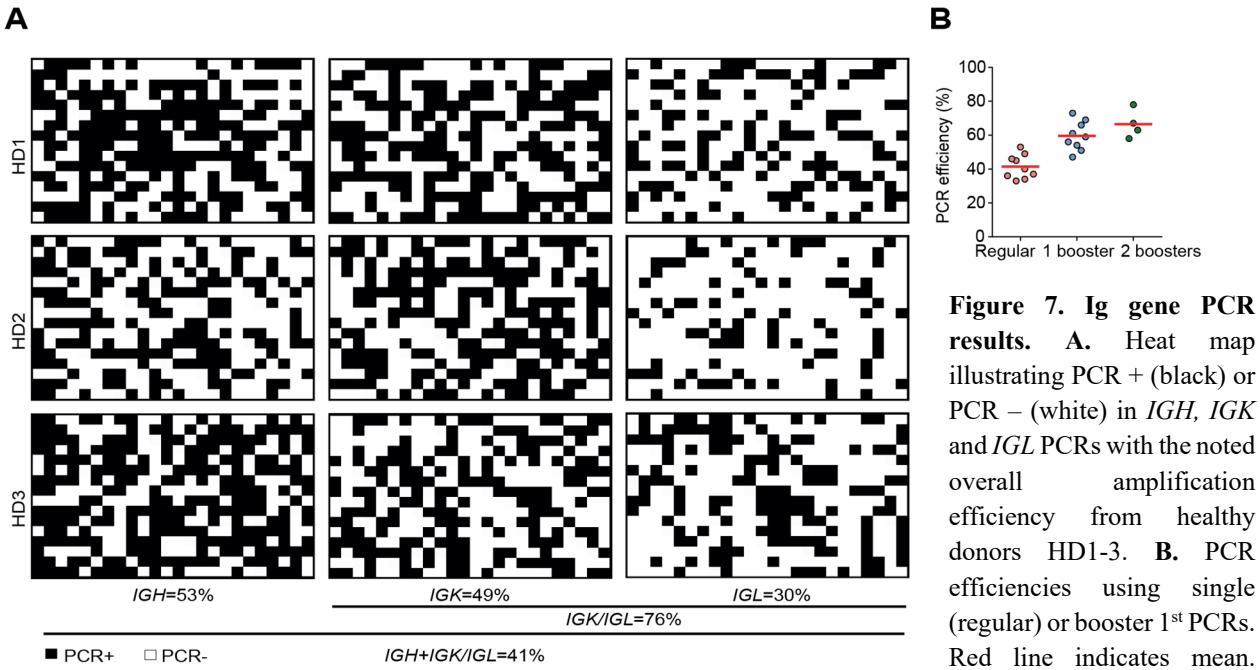

Figure 7. Ig gene PCR results. A. Heat map illustrating PCR + (black) or PCR – (white) in *IGH, IGK* and *IGL* PCRs with the noted overall amplification efficiency from healthy donors HD1-3. **B.** PCR efficiencies using single (regular) or booster 1st PCRs. Red line indicates mean. This figure is adapted from[85].

During the primer establishment, the 1st PCR was deduced to be crucial in the amplification step for Ig heavy genes[85]. Ig gene analysis of the resulting sequences showed results comparable to the previously published data (Supplementary Fig. S2). To boost the overall amplification efficiency, an additional booster 1st heavy PCR was performed. The amplicons from the two first PCRs were pooled and used as template for the second PCR. Under a single booster or two booster PCRs, overall Ig heavy gene amplification efficiency increase by an

average of ~20 % and ~25 %, respectively, compared to a single 1st PCR (Fig. 7B). Based on this observation, all further matrix PCRs employed two 1st PCRs and pooling them as template for a single 2nd PCR in heavy PCR, whereas the kappa and lambda chain PCRs were performed without repetition.

4.3 Controlled human malaria infection (CHMI) study cohort and sample collection

In the PfSPZ-CVac clinical trial TÜCHMI-2, 9 malaria naïve donors were recruited for the controlled human malaria infection[93]. The donors were infected three times with live 5.12 x 10^4 Pf NF54 sporozoites intravenously with an intervening period of 4 weeks. From the beginning of the trial period, the donors received nine doses of 5mg/kg chloroquine on a weekly basis as chemoprophylaxis against the Pf blood stage parasites (Fig. 8). 10 weeks after the third infection, the donors were challenged with 3.2 x 10^3 Pf NF54 sporozoites without chloroquine

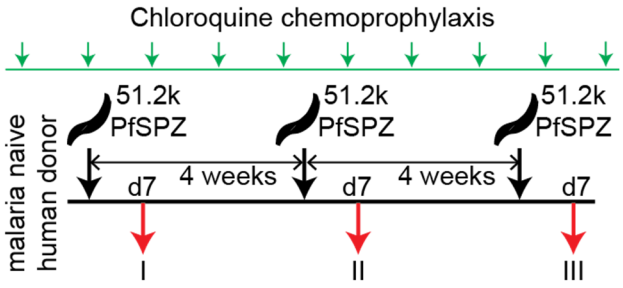

Figure 8. CHMI scheme. Pictorial representation of the trial scheme[93]. Malaria naïve human donors received three doses of 5.12 x 10^4 Pf sporozoites (PfSPZ) at the interval of 4 weeks under choloroquine chemoprophylaxis. Blood samples taken on day 7 post three infections (I, II and III) were analyzed and presented in this thesis. Green arrows and black arrows indicate the chloroquine and PfSPZ injection, respectively. Red arrows indicate the blood sample collection time points.

chemoprophylaxis and none of them developed blood parasitemia, indicating the establishment of sterile immunity. This thesis is based on the analysis performed on the samples collected from all donors at day 7 post each of the three controlled infections and challenge and the data analysis corresponding to the mentioned time periods will be referred to as I, II, III and C, respectively.

4.4 Anti-CSP serum response in CHMI

To understand the strength and the isotype usage of the CSP antibody response, serum collected from day7 post three infections of all 9 donors were assessed for CSP binding. Anti-CSP antibodies on day7 post first infection were undetectable in serum of all donors, indicating that in malaria naïve donors, a time span of seven days was too short to elicit detectable anti-CSP serum antibodies. However, at day7 post second infection, increased anti-CSP serum antibodies were found in T2_072 and T2_073 as IgM and T2_072 and T2_052 as IgG. Notably donor T2_072 also mounted strong anti-CSP IgA antibodies. In response to the third infection, all donors but T2_052 mounted anti-CSP IgM antibodies, albeit to various degrees. 5 out of 9 donors showed

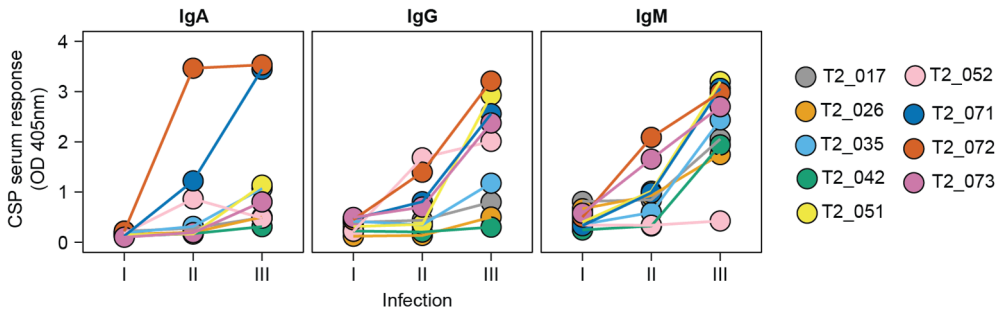

Figure 9. Serum anti-CSP antibodies. Serum ELISA results representing the detection of CSP binding serum antibodies of the isotypes IgA, IgG and IgM. Day 7 post each of the three infections are indicated as I, II and III. The individual donors are indicated in different colors.

a clear increase in anti-CSP IgG antibodies, whereas only two donors showed an increase in anti-CSP IgA antibodies. Although all donors showed an increase in anti-CSP serum antibodies over the course of three infections, there was a greater diversity in the strength and the isotypes detected.

4.5 Anti-CSP memory B cell and plasmablast response in CHMI

To characterize the frequency of CSP reactive memory B cells, flow cytometry was performed using the peripheral blood mononucleocytes (PBMCs) isolated on day7 post three infections.

Recombinantly expressed PfCSP was labelled with the fluorochrome Alexa 647 and used as a bait to detect CSP reactive memory B cells. After exclusion of dead cells using 7-AAD staining, live cells showing CD19 and CSP positivity with CD27 and/or IgG positivity were defined as CSP reactive memory B cells (Fig. 10A). Compared to non-infected malaria naïve donors, Pf infected donors showed significantly higher mean CSP reactive memory B cells frequency (Fig. 10B). However, CSP reactive memory B cell frequency showed greater variability among the 9 donors. Post three infections, three donors showed a strong CSP reactive memory B cell response mounting to >1% of all memory B cells, whereas three donors showed moderate response with ~1% of all memory B cells and three donors showed only weak response. It is noteworthy that in response to three infections, all 9 donors mounted CSP reactive memory B cell with frequencies greater than the observed mean CSP reactive memory B cell frequency in naturally exposed semi-immune African adults (0.14%)[91].

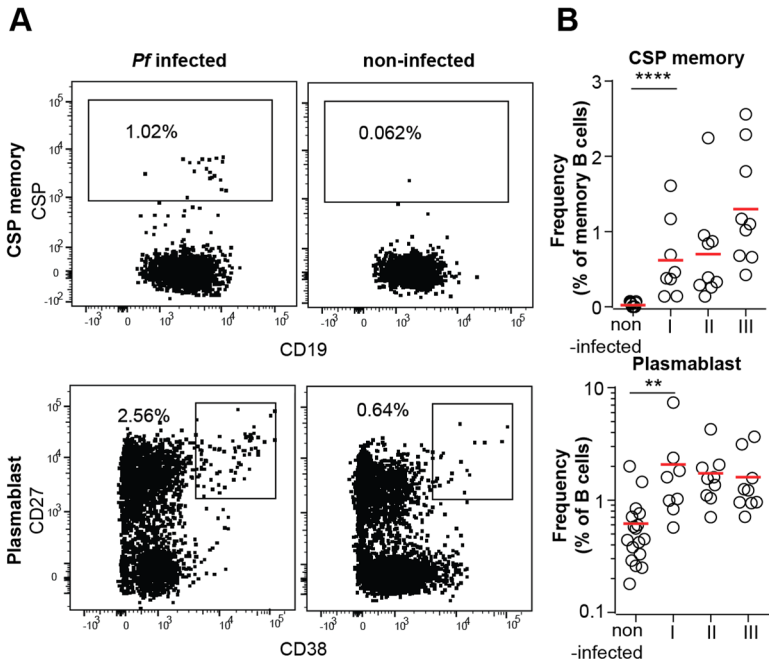

Figure 10. CSP memory B cell and plasmablasts frequency post Pf infection. A. Flow cytometry gates illustrating CSP binding memory B cells (top: 7AAD- CD19+ CSP+ B cells positive for CD27 and/or IgG) and plasmablasts (bottom: 7AAD- CD19+ CD27+ CD38+ B cells) in Pf infected donor (left) in comparison to non-infected donor (right). **B.** Frequency of CSP memory B cells (top) and plasmablasts (bottom) at d7 post three infections in 9 donors compared to non-infected healthy donors. **P<0.001, ****P<0.0001; two tailed Mann-Whitney test.

.

Independently, the frequency of plasmablasts in response to the Pf infections was estimated using CD27 and CD38 upregulation in live B cells (Fig. 10A). Interestingly, non-infected malaria naïve donors already had a mean plasmablast frequency of 0.6% among all B cells,

indicating the ongoing background B cell response in otherwise healthy adults. However, the Pf infected donors showed a significantly increased mean plasmablast frequency, compared to healthy adults (Fig. 10B). Similar to the CSP reactive memory B cells, the donors also showed greater variability in the plasmablast frequencies.

CSP reactive memory B cells and activated plasmablasts from day7 post three successive infections were single cell sorted. Index sorting function was used to record the fluorescent parameter of the individual cells that were sorted. The established high-throughput PCR strategy was used in single B cell Ig gene amplification[85]. The resulting amplicons were pooled and bulk sequenced using either 454-sequencing or Miseq Illumina sequencing platforms. The sequences were mapped to the wells and analyzed for Ig gene features using the published immune repertoire analysis platform, sciReptor[94]. B cells with the functional Ig heavy and light chains were further analyzed.

4.6 Ig heavy constant distribution

To assess the isotype distribution of CSP memory B cells in CHMI, *IGHC* regions of the functional Ig genes were identified and annotated for different constant genes (Fig. 11). While CSP memory B cells post first Pf infection predominantly carried *IGHM* genes in all donors, *IGHG* and *IGHA* CSP memory B cells were also observed. This indicates the recruitment of pre-existing class-switched and IgM memory B cells into the primary response against CSP. Surprisingly, post second and third infection, *IGHM* was still predominant in CSP memory B cells, whereas an increase in *IGHG* genes was found only in a subset of donors. This could be explained by the continuous recruitment of naïve B cells or IgM memory B cells. Taken together, CSP memory B cell response in CHMI was predominantly mediated through Ig genes carrying *IGHM*.

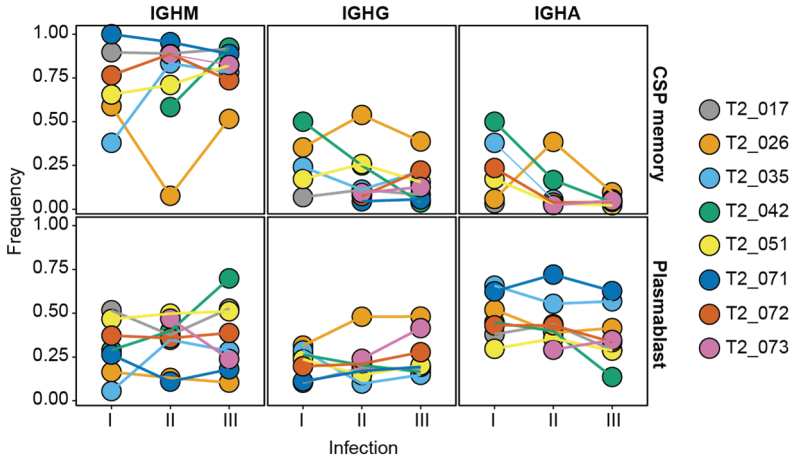

Figure 11. Ig heavy constant usage. Frequencies of three major IgH constants in CSP memory B cells (top) and plasmablasts (bottom) post three infections as identified by the PCR amplified *IGHV* sequence. The donors are indicated in different colors.

In contrast to CSP memory B cells, plasmablast response against Pf infection in all donors was diverse throughout all three constants (Fig. 11). No significant difference in the frequencies of constant regions was observed in the plasmblasts over the course of three infections, indicating a broad response against several Pf antigens, presumably with minimal background response.

4.7 Somatic hypermutation distribution

To understand the naïve or memory status of the B cells isolated, SHM counts in the *IGHV* genes were analyzed and compared to the known published sequences. Given the trial donors were diagnosed to be malaria naïve, the CSP memory B cells post first infection were expected to derive from a naïve B cell pool that carried little somatic hypermutations. Surprisingly, the B cells post first infection carried several mutations with an average of 10 mutations in *IGHV* genes (Fig. 12A). This SHM load is comparable to that of the reported resting memory B cell populations from healthy adults[95-98]. Together with the Ig gene constant regions distribution, the SHM counts also indicate the recruitment of pre-existing memory B cells during primary Pf infection. While the mean SHM count went down in response to the second and third infection, B cells with highly mutated antibodies were still observed (Fig. 12B). This indicates the continual recruitment of pre-existing memory B cells in the anti-CSP B cell response.

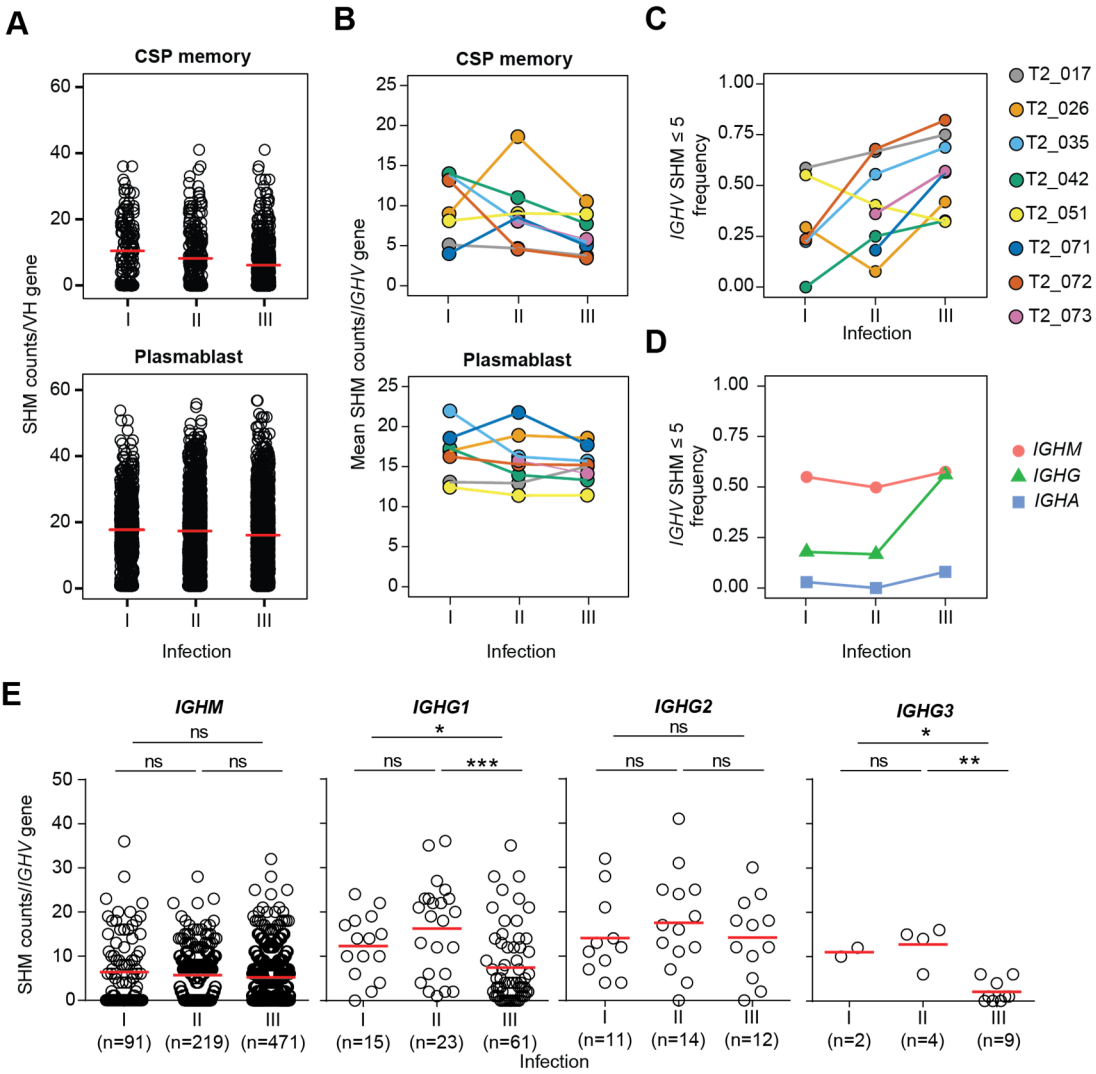

Figure 12. Somatic hypermutation (SHM) analysis in *IGHV* genes. A. Overall SHM counts per *IGHV* gene in CSP memory B cell (top) and plasmablast (bottom) antibodies of all donors post three Pf infections. **B.** Mean SHM counts/*IGHV* gene of CSP memory B cell and plasmablast antibodies isolated for each donor, indicated in different colors. **C-D.** Frequency of *IGHV* genes carrying < = 5 SHM counts in each donor (C) and their isotype distribution (D) in CSP memory B cells. **E.** SHM counts per *IGHV* gene of antibodies carrying indicated isotypes or subclasses in CSP memory B cells. A, E. Red lines indicate mean. *P<0.05, **P<0.001, ****P<0.0001, ns non-significant; two tailed Mann-Whitney test.

To compare the relative recruitment of naïve and memory B cells, the B cell frequency with a SHM count less than or equal to 5 in *IGHV* genes was estimated for all donors post each of the three infections (Fig. 12C). In all donors except T2_051, the frequency of B cells with low mutated antibodies was increased due to the enhanced recruitment and acquisition of mutations

by naïve B cells. To understand whether the recruited naïve B cells underwent class switching, *IGHC* regions were analyzed (Fig. 12D). Post third infection, frequency of less mutated antibodies with *IGHG* was increased compared to second infection. This was also observed by a drop in the mean SHM of Ig genes that carried the *IGHG1* constant region (Fig. 12E). In conclusion, CHMI in malaria naïve donors recruited pre-existing memory B cells from other infections. However, over the course of three infections, naïve B cells were recruited with increased frequency in the majority of donors and showed signs of class-switching to *IGHG1*.

4.8 Antibody R/S mutation ratio profile

To understand whether the isolated B cells underwent antigen mediated selection, the ratios of replacement to silent mutations (R/S) in the different antibody regions were compared (Fig. 13A). Increased frequency of replacement to silent mutations in the antibody complementarity determining regions (CDR) compared to its frame work regions (FWR) is reported to be a *bono fide* sign of antigen mediated selection[95,96]. As expected, the R/S ratios were higher in CDRs

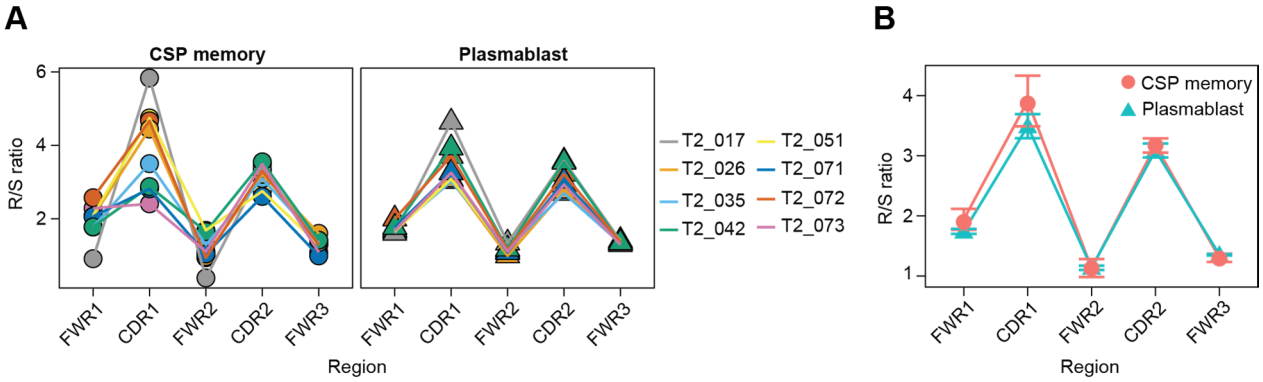

Figure 13. Replacement (R) to silent (S) ratio of different antibody regions. A,B. R/S ratio of frame work (FWR) and complementarity determining regions (CDR) calculated for CSP memory B cell and plasmablast antibodies represented for individual donors (A) or all donors pooled (B). Error bars indicate standard error mean.

compared to FWRs, both in CSP memory B cell and plasmablast antibodies (Fig. 13B). The calculated ratios were comparable to published ratios from the resting memory B cells in

healthy adults. This indicates the clear CSP mediated selection of mutations in the CSP memory B cell antibodies.

4.9 Degree of clonal expansion

A strong indication for antigen-specific selection is the presence of clonally-related cells within the antigen-specific population[99]. In order to characterize the degree of focused response towards CSP, clonally expanded B cell clusters were identified as B cells with the same Ig heavy and light chain genes with shared or non-shared somatic hypermutations. The Ig gene sequences from all time points, both in the CSP memory and plasmablasts, were analyzed and clonally expanded clusters were defined. In 5/8 donors, the degree of clonal expansion in CSP memory B cells was continually increased in response to each infection, leading to a total of up to ~ 50% of all CSP memory B cells post third infection (Fig. 14 A,B). Comparatively, the relative clonal expansion in 3/8 donors were weaker and showed variations in CSP memory B cell response in humans. Interestingly, maintenance and re-recruitment of memory B cell clusters from one infection to another was observed (Fig. 14C).

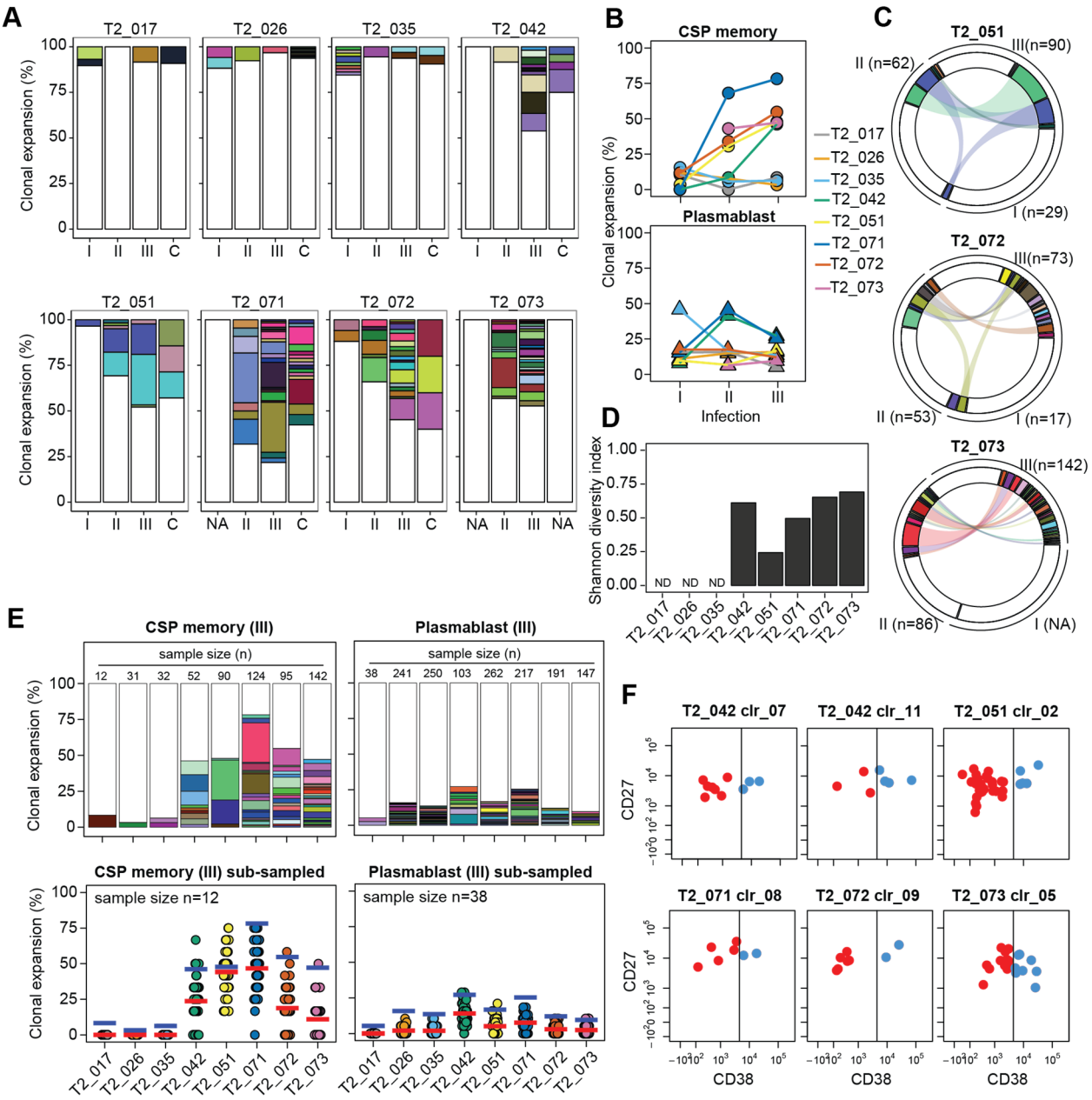

Figure 14. Analysis of clonally expanded B cell clusters. A. Bar plots depicting clonally expanded B cell clusters post three Pf infections and challenge. Expanded clusters are marked in unique colors and non-expanded B cells shown in white. **B,C.** Frequency of clonally expanded B cells observed for the donors (B) and circo plots of three representative donors where the B cell clusters that are recruited during later infections are linked (C). **D.** Shannon diversity index of the clusters measured at III. ND: non-determined. **E.** Clonal expansion in the overall data (top) or the subsampled data set (bottom) at III. Each dot indicates a given subsample, red line indicates the mean of at most 50 subsamples and blue line indicates the observed clonal expansion. F**.** Representative B cell clusters with members of memory B cell (red: CD27+CD38-) and plasmablast (blue: CD27+CD38+).

To measure the diversity of the clonally expanded cells, the Shannon diversity index was calculated, with 0 and 1 being entirely polyclonal and monoclonal responses, respectively (Fig. 14D). Among the 5 donors who showed strong clonal expansion, all except for donor T2_051

showed a higher diversity in recruiting and expanding B cells with diverse Ig genes. To account for the sample number variability between the donors, CSP memory B cells post third infection were sub-sampled (n=12) from each donor and clonal expansion was estimated (Fig 14E). The donors with higher overall clonal expansion still showed higher mean clonal expansion calculated from the 50 random sub-samples. Taken together, the donors showed a diverse degree of clonal expansion in CSP memory B cells with a strong response in 5/8 donors.

Compared to CSP memory, clonal expansion in the plasmablast compartment was lower in all donors. In contrast to subunit vaccines, live Pf sporozoite infection provides the immune system with a diverse set of antigens (Fig. 14B,E). Because plasmablasts were not selected for a given antigen, the individual antigen specific clones would be diluted. Hence, the lower degree of clonal expansion in plasmablasts reflects the response against diverse Pf antigens.

To check whether the B cell clusters identified in CSP memory compartments also shared a plasmablast phenotype, clonally expanded B cells were assessed for CD38 expression, an activation marker upregulated in plasmablasts (Fi. 14F). In several CSP binding B cell clusters, a part of the cluster members showed a memory B cell phenotype (CD27+CD38-), while the rest showed a plasmablast phenotype (CD27+CD38+). This evidence underlines the potential of a single ancestor B cell to take part in a germinal center reaction and potentially contribute to both memory B cell and plasmablast compartments.

4.10 Ig gene repertoire analysis

To identify an enrichment of molecular signatures, VH genes of CSP memory B cells were compared to those of plasmablasts (Fig. 15). Given that plasmablasts are presumably mounted against several antigens, they were used as internal controls to assess the specific nature of CSP memory B cell Ig genes., CSP memory B cells in 4/8 donors showed a higher enrichment of Ig

genes with gene segments of the VH3 family, compared to those of plasmablasts. Interestingly, these 4 donors showed strong clonal expansion by recruiting and expanding B cells with diverse Ig genes as identified in Fig. 14, post three infections. In these 4 donors, the enrichment in VH3 gene segments was driven mostly by either *IGHV3*-33 and/or *IGHV3-23,* and the gene segments were recorded in several of the clonally expanded B cell Ig genes. In contrast, donor T2_051 showed an enrichment of VH1 and VH4 family gene segments and the majority of this enrichment was due to strong clonal expansion of only two B cell clusters. While individual donors showed enrichment in a given family of segments, there was greater diversity in the light chains regarding the segments used amongst the donors, both in CSP memory B cells and in plasmablasts (Supplementary Fig. S3).

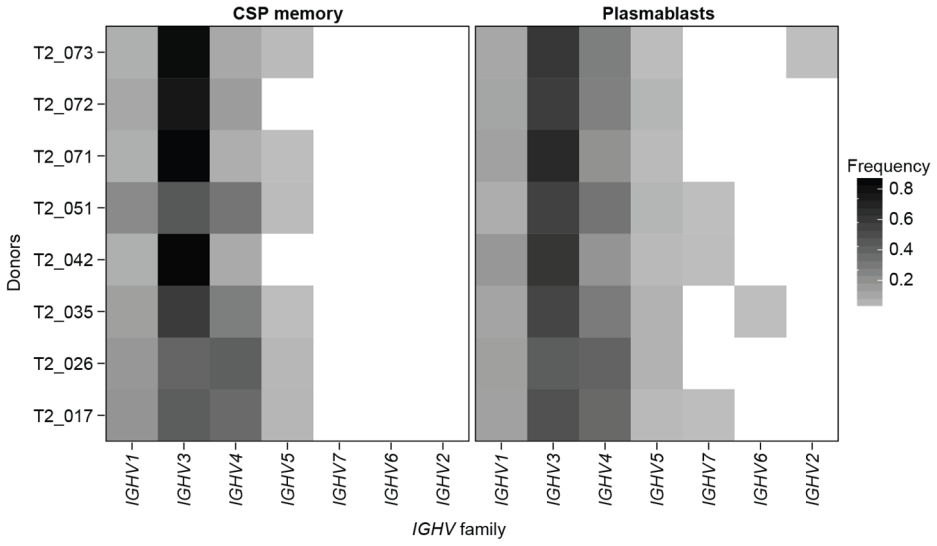

Figure 15. *IGHV* family usage. Heat map illustrating frequency of antibodies with different *IGHV* families in CSP memory B cells (left) and plasmablasts (right) in indicated donors.

Overall, the Ig heavy gene repertoire showed distinct gene signatures that were enriched in CSP memory B cells among the donors that showed strong clonal expansion. In the majority of the donors, this enrichment was due to the recruitment and expansion of several B cell clusters carrying these Ig genes.

4.11 CSP binding quality of memory B cells

To characterize the antigen binding quality of the antibodies, Ig genes from 422 CSP memory B cells and clonally related plasmablasts, with special focus on clonally expanded cells, were cloned and expressed as recombinant monoclonal antibodies. To compare the antibodies for CSP binding, Enzyme Linked Immunosorbant Assay (ELISA) was performed using recombinantly expressed CSP at several dilutions of the monoclonal antibodies (Fig. 16A). Only 6% of the antibodies post first infection showed detectable CSP binding in ELISA, indicating that it was too early to generate high CSP binding antibodies after seven days post first infection (Fig. 16B). However, the frequency of CSP binding antibodies post second and third infection increased to 47% and 66%, respectively. This significant increase in CSP binding antibodies indicates the global affinity maturation towards CSP over the course of three *Pf* infections.

NANP repeat units are reported to be the immunodominant B cell epitope in CSP. To assess if the antibodies targeted the NANP repeat, ELISA was performed using $NANP_{10}$ repeat units at several dilutions of the monoclonal antibodies (Fig. 16C). This assay confirmed that the majority of the CSP binding antibodies targeted the NANP repeat units.

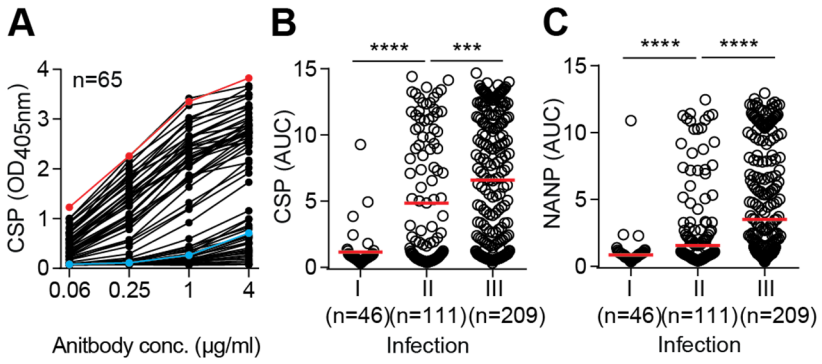

Figure 16. Antibody reactivity assessment. A. Binding of memory B cell antibodies to CSP in ELISA detected by absorbance at indicated antibody concentration. 2A10[87, 91] (red) and mGO53[88] (blue) are used as positive and negative controls. **B, C.** Area under the curve values of antibodies binding to CSP (B) and $NANP_{10}$ (C) post three Pf infections. Data is representative of two independent experiments. ***P<0.001, ****P<0.0001; two tailed Mann-Whitney test.

To summarize, at least two Pf infections were required to generate high CSP binding antibodies and the third infection increased the frequency of high CSP binding antibodies even further. The globally increased high CSP binding antibodies targeted NANP repeat units, the reported immunodominant B cell epitope.

4.12 Poly-reactivity of CSP memory B cell antibodies

To determine whether the antigen binding in CSP memory B cell antibodies is specific or poly-reactive, antibodies were tested in ELISA for binding to three structurally different antigens: dsDNA, insulin and LPS (Fig. 17A). Antibodies that bound at least two of the three antigens were defined as poly-reactive. The assay showed that 30% of antibodies cloned from memory B cells post first infection showed poly-reactivity (Fig. 17B). However, in response to the second infection, the frequencies of poly-reactive antibodies were significantly decreased. To summarize, the poly-reactive features of the antibodies provided an added advantage in recruiting the B cells post first infection. The relative decrease in the frequency of poly-reactive antibodies post second and third infection indicates an efficient recruitment and selection of B cells with CSP specific antibodies.

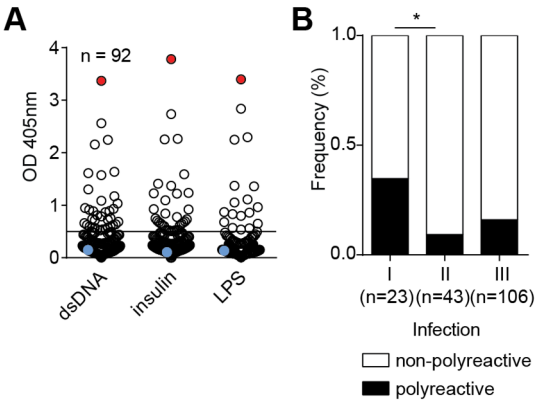

Figure 17. Antibody poly-reactivity assessment. A. Poly-reactive nature of antibodies assessed by binding to the indicated antigen at 1 µg/ml measured by absorbance at 405nm. ED38[89] (red) and mGO53[88] (blue) are used as positive and negative controls. **B.** Frequency of poly-reactive antibodies detected at the three infection time points. Data is representative of two independent experiments. *P<0.05, 2 × 2 Fischer exact test.

4.13 *In vitro* functional characterization of CSP memory B cell antibodies

To determine the functional capacity of the antibodies in inhibiting sporozoite traversal activity, the antibodies were assessed in an *in vitro* hepatocyte traversal assay[91] (Fig. 18A). Comparable to CSP binding, antibodies from CSP memory B cells post first infection did not inhibit sporozoite traversal. However, the monoclonal antibodies from the later infection time points showed significantly increased sporozoite traversal inhibition compared to first infection. The *Pf* sporozoite traversal inhibition had a remarkable correlation with the CSP binding nature of the monoclonal antibodies (Fig. 18B). To summarize, over the course of three infections, high CSP binding antibodies that were enriched in CSP memory B cells showed remarkable functionality regarding their Pf sporozoite inhibitory capacity in an *in vitro* traversal assay.

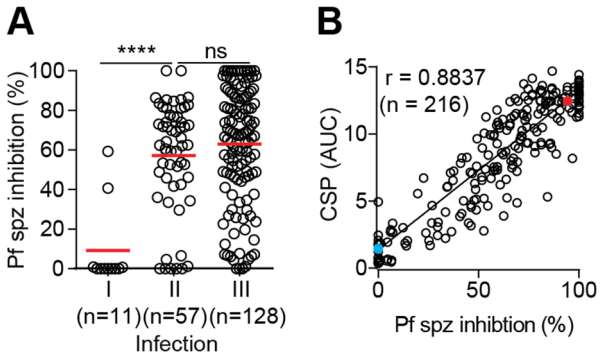

Figure 18. Antibody *in vitro* functional assessment. A,B. Pf sporozoites hepatocyte traversal inhibition of monoclonal antibodies measured in the *in vitro* traversal assay (A) and the inhibition compared to the antibody CSP binding indicated by ELISA AUCs (B). Red line indicates mean. 2A10[87,91] (red) and mGO53[88] (blue) are used as positive and negative controls. Data is representative of two independent experiments. ****P<0.0001, ns: non-significant; two tailed Mann-Whitney test. r indicates Spearman correlation coefficient.

4.14 Kinetic parameters of CSP memory B cell antibodies

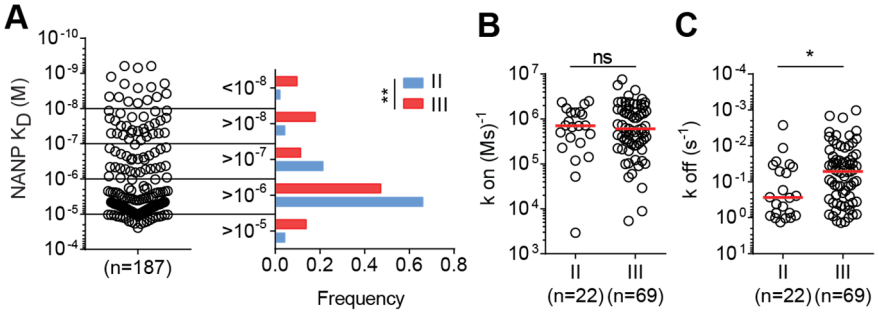

Figure 19. Antibody affinity and kinetic parameters assessment. A. Range of antibody affinity to $NANP_5$ measured by SPR (left) and comparison of antibody frequencies with the indicated affinity ranges between infection time points II and III (right). **P<0.01; Chi-square test. **B, C.** Kinetic on (B) and off rates (C) compared between antibodies from infection time points II and III. *P<0.05, ns: non-significant; two tailed Mann-Whitney test.

To characterize the binding affinity and deduce kinetic parameters of CSP binding antibodies, a $NANP_5$ repeat unit was used as a minimal epitope in the Surface Plasmon Resonance (SPR). The affinity measurement showed the overall range of NANP affinity to be that of the reported range of antigen-antibody interactions: 10^{-5} to 10^{-10} M [100,101](Fig. 19A). It is important to note that the overall antibody affinity to CSP may be increased due to the repetitive presence of the minimal epitope in the full length protein. To qualitatively compare the affinity maturation, frequencies of antibodies with different affinity ranges were compared between the second and the third infection (Fig. 19A). Interestingly, antibodies post third infection showed a higher frequency in both the low affinity range (> 10^{-5} M) and the high affinity range (<10^{-8} M). To better understand the enrichment, the kinetic on and off rates of the antigen-antibody interaction were compared (Fig. 19B,C). While the kinetic on rates did not show any significant difference between the second and third infections, there was a significant reduction in the kinetic off rates explaining the enrichment of higher affinity antibodies in the third infection. In summary, the kinetic affinity of NANP targeting antibodies was in the reported range and the kinetic maturation of the antibodies between second and third infection occurred due to the significant reduction in the kinetic off rates of the interaction.

4.15 Clonal evolution of CSP memory B cells

To characterize the affinity maturation on single expanded B cell cluster level, clonally related antibodies that were diversified through SHM were grouped and their affinities were compared. Surprisingly, cluster members with different mutations showed a similar affinity in the majority of the clusters (Fig. 20A). Interestingly, memory B cells with a germline antibody configuration (0 mutations in heavy and light chain) isolated in some clusters already possessed an affinity that was comparable to its mutated counterparts. To check whether the germline binding also existed in the clusters, unmutated common ancestors (UCA) were made by reverting the

observed mutations back to the germline (Fig. 20B). In the analyzed clusters, the generated UCA showed similar affinity compared to the mutated variants, confirming the previous observation. While affinity maturation was indeed observed while the antibody affinity increased by 100 folds, this observation was found only in a few clusters and restricted to individual antibodies in the clusters (Fig. 20C). Affinities of clonally related antibodies that were isolated post different infections were also comparable to each other (Fig. 20D). To summarize, the global increase in CSP binding antibody quality was not observed in several of the diversified antibody clusters. In the majority of the clusters, the germline antibodies already possessed an affinity that was maintained in the mutated variants throughout the evolution of response.

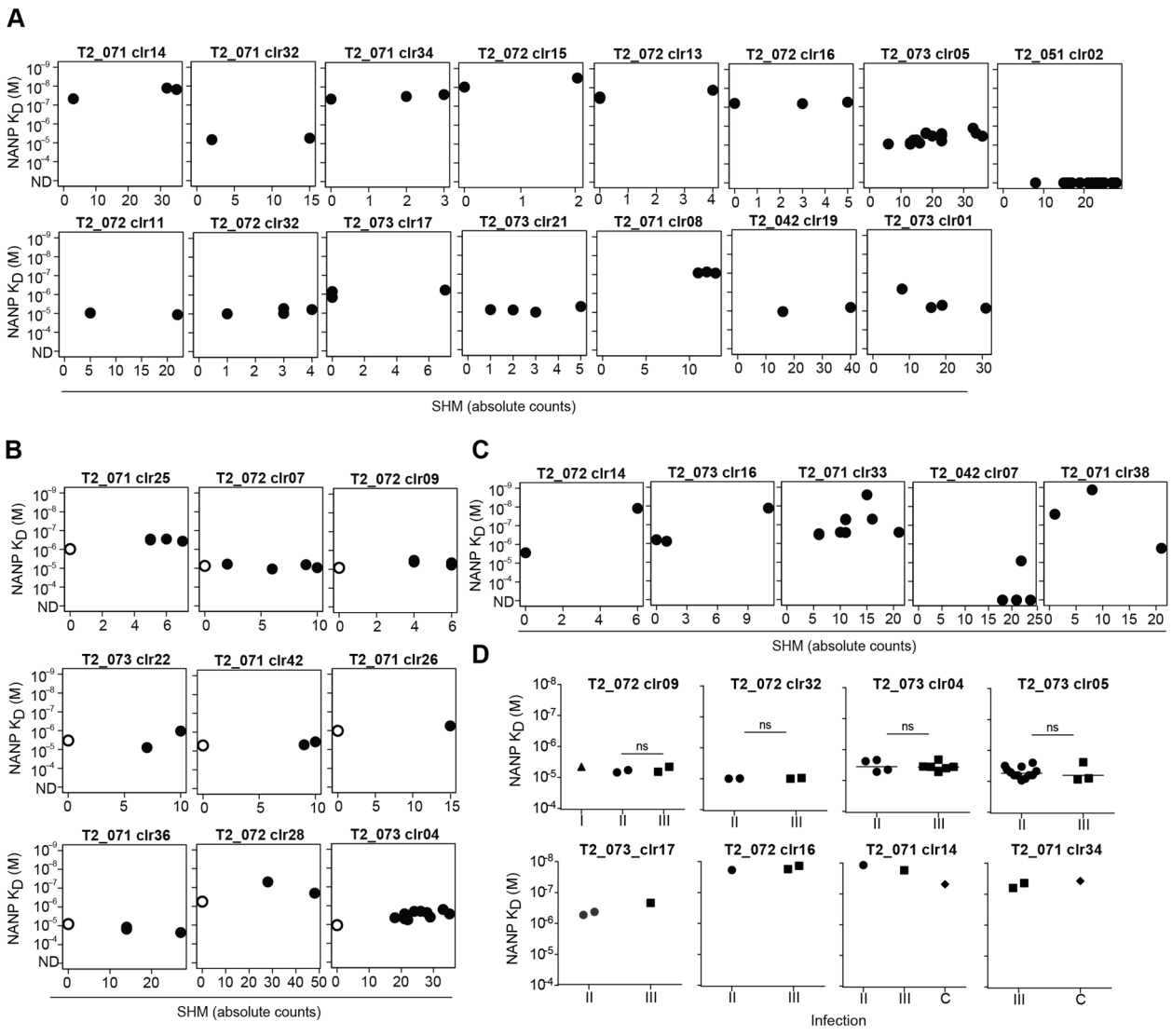

Figure 20. Inefficient antibody affinity maturation in CSP response. A,B. Antibody affinities of diversified B cell clusters towards the minimal epitope $NANP_5$ showing no appreciable difference amongst the clonal members (black circle) (A) and when compared to the germline version of the cluster (white circle) (B). **C.** B cell clusters with individual members showing >100 x affinity maturation. A-C. Sum mutations in the heavy and light chain are represented in x-axis. **D.** Affinity of cluster members compared across Pf infection time points I, II and III and the challenge C. Data is representative of at least two independent experiments. ns non-significant; two tailed Mann-Whitney test.

4.16 SHM pattern of high CSP binding antibodies

The observation that germline or less mutated antibodies in the cluster already had a high affinity prompted for the analysis of SHM patterns in antibodies that showed CSP binding. Fig. 21A compares the total SHMs present in *IGHV* and *IGKV/IGLV* of the monoclonal antibodies to their

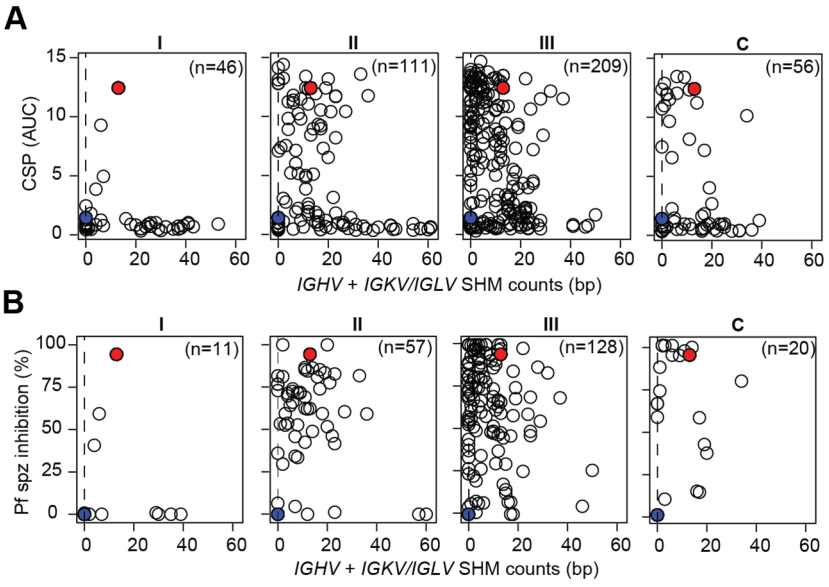

Figure 21. SHM profile compared to antibody binding and functional characteristics. A,B. CSP binding of the antibodies indicated by ELISA AUC (A) and Pf sporozoites traversal inhibitory capacity of the antibodies (B) compared to their sum mutations in the *IGHV* and *IGKV/IGLV* genes, post indicated infection time points. Red and green dots indicate the positive (2A10)[87,91] and negative control (mGO53)[88]. Data is representative of at least two independent experiments.

binding to CSP defined by ELISA AUC. This plot showed that although there were mutated antibodies that exhibited CSP binding, the majority of the high CSP binding antibodies carried few mutations in the heavy and light chain genes. This plot also revealed that these high binding, less mutated antibodies were recruited even more often after second and third infections and performed better inhibition in the *in vitro* hepatocyte traversal assay (Fig. 21B). Interestingly, this observation was true for the antibodies cloned from day7 post challenge as

well. To summarize, the majority of the high CSP binding antibodies generated in response to CHMI carried little to no SHMs, indicating that the role of germline residues in the antibodies lies in mediating CSP binding.

4.17 Ig gene features of high CSP binding antibodies

Given the observation that the high CSP binding was not mediated through SHM, Ig gene features such as Ig gene segments and CDR3 length were assessed to define CSP binding features. Comparing CSP binding through ELISA of antibodies carrying Ig gene segments of different families showed the enrichment of high CSP binding in antibodies with segments of the VH3 gene family (Fig. 22A). Also, comparing the CDR3 amino acid (aa) length of the kappa chain showed the enrichment of high CSP binding in antibodies with a KCDR3 length of 8 aa (Fig. 22B). This significant enrichment was clearly visible while comparing the $NANP_5$ affinities of the antibodies with a KCDR3 length of 8 or 9 aa (Fig. 22C). The frequency of antibodies with NANP affinity $<10^{-7}$ M was enriched in the antibodies with a KCDR3 length of 8 aa. To summarize, VH3 gene family usage and an 8 aa long KCDR3 enriched for high CSP binders as detected by CSP ELISA and SPR measurements for $NANP_5$ repeat units.

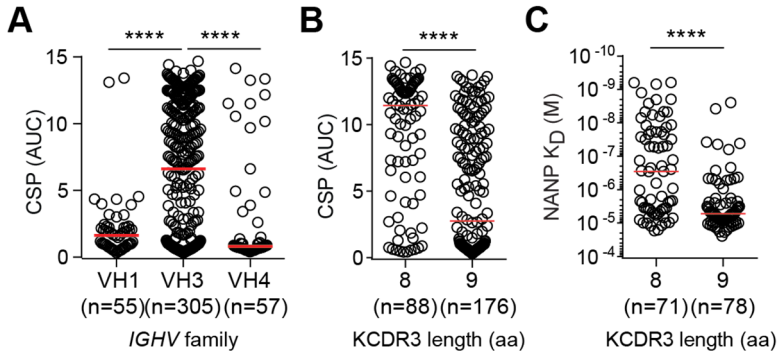

Figure 22. Ig genes features compared to antibody CSP binding. A, B. CSP binding indicated by ELISA AUC of the antibodies compared to their *IGHV* gene families (A) and KCDR3 amino acid length (B). **C.** $NANP_5$ affinities of the antibodies with 8 or 9 amino acid long KCDR3. Red lines indicate mean. ****P<0.0001; two tailed Mann-Whitney test. A,B. Data is representative of two independent experiments.

4.18 Ig heavy and light chain genes of high affine antibodies

To identify the Ig gene segments that contribute to better NANP binding, antibodies with detectable $NANP_5$ affinity by SPR were assessed for their gene segments in the heavy and kappa chain (Fig. 23). Based on the clear enrichment of high affinity antibodies ($NANP_5$ K_D < 10^{-7} M) in those that carried an 8 aa long KCDR3, CSP binding antibodies were sorted for high and low NANP binding ($NANP_5$ K_D < 10^{-7} M and $NANP_5$ K_D > 10^{-7} M, respectively) and for having an 8 or 9 aa long KCDR3. Association of the heavy and light chain V gene of these groups identified *IGHV3-33* and *IGKV1-5 / 3-11 / 3-20* with 8 aa KCDR3 as the gene configurations of the high affine antibodies. Antibodies with these gene features were isolated from 4 donors who showed strong clonal expansion in CSP memory B cells, indicating the prevalence of high quality antibodies in malaria naïve donors. Furthermore, antibodies with the mentioned gene segments and a 9 aa CDR3 length did not exhibit high affinities ($NANP_5$ K_D< 10^{-7} M), highlighting the restriction placed by the KCDR3 length.

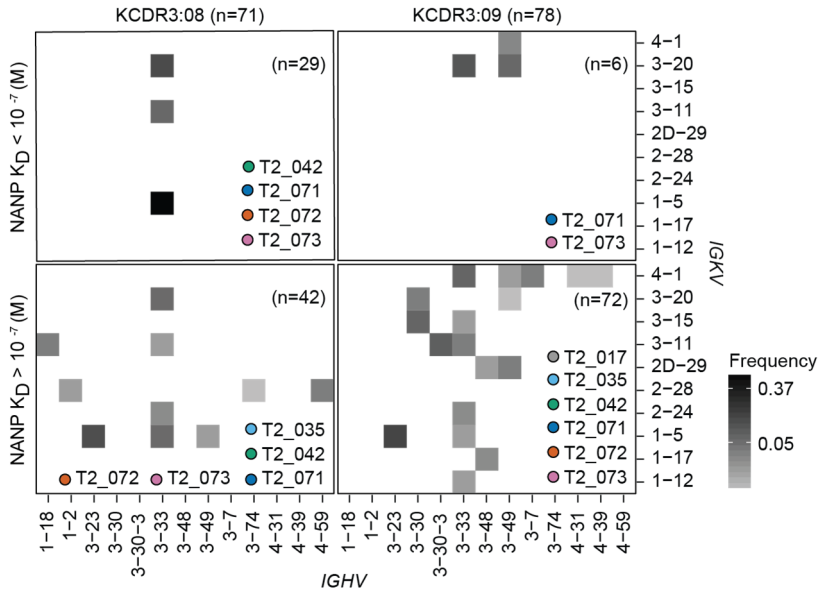

Figure 23. V gene repertoire of CSP binding antibodies. Frequencies of VH-Vk gene association of antibodies with KCDR3 amino acid length of 8 (left) and 9 (right), and with $NANP_5$ affinity K_D < 10^{-7} M (top) or K_D > 10^{-7} M (bottom). Donors with the observed gene associations are listed.

4.19 Comparison of donors based on high CSP binding Ig gene features

VH3 gene segment usage and an 8 aa long KCDR3 in CSP memory B cells enriched for high CSP binding. Besides, the degree of clonal expansion served as an indicator of focused B cell response over three *Pf* infections. Considering these three features as signs of a qualitative CSP response, Ig sequences of CSP memory B cells were analyzed to estimate the frequency of VH3 family genes, 8 aa long KCDR3 and mean clonal expansion post three infections from the multiple subsampled data set. Principal Component Analysis (PCA) performed on the above three Ig gene parameters to compare the donors clustered the donors, T2_071, T2_072 and T2_073 into one group and T2_017, T2_026 and T2_035 into another. Donor T2_042 was present in-between these groups, whereas donor T2_051 was separated from the rest (Fig. 24A).

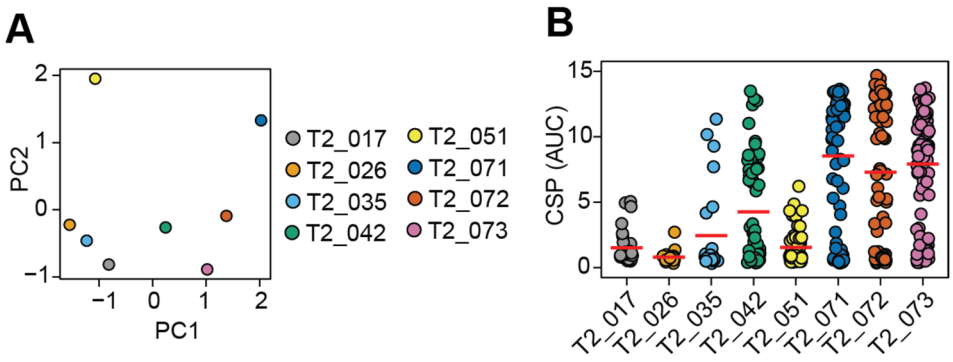

Figure 24. Inter-donor variability in CSP response. A. Principal component analysis of the donors based on, VH3 family frequency and antibodies with 8 amino acids long KCDR3 frequency in overall CSP memory B cells, mean clonal expansion of the subsampled data set from CSP memory B cells post third Pf infection (Figure. 12D). Individual donors are indicated in different colors. **B.** CSP binding of antibodies cloned from the 8 donors indicated by ELISA AUCs. Red lines indicate mean. B. Data is representative of two independent experiments.

Interestingly, the distinct pattern of clustering was also reflected in the mean CSP AUC of the monoclonal antibodies cloned from these donors (Fig. 24B). Donors T2_071, T2_072 and T2_073 had a higher frequency of high CSP binders, whereas T2_017, T2_026 and T2_035 had very few, if any, high CSP binders. The quality of the antibodies from donor T2_042 was in-between the high and weak responders. While the degree of clonal expansion in T2_042 was

comparable to the high responders, the frequency of high CSP binders was low. It is noteworthy, that the high binders in these donors were the ones that carried fewer mutations. Donor T2_051 was distinct in the expansion of clones with high CSP binding gene features and hence had no high CSP binding antibodies. To summarize, high CSP binding Ig gene features enabled distinguishing donors with high and low quality CSP response.

5. Discussion

5.1 High throughput Ig gene amplification strategy

The high throughput platform reported here for the amplification of full length Ig genes on single cell level provides a significant improvement on the existing strategies. The limitations of the bulk sequencing strategies which lose Ig heavy and light chain gene pairing[102-104] and the other single cell approaches[105] which do not provide full length Ig gene information are overcome here[85]. The throughput offered by the barcoded primer matrix in combination with the NGS bulk sequencing results in the efficient generation of Ig gene sequence information of several thousand cells at a much reduced cost and time[92]. The power of this strategy relies in deep sampling rare populations, identifying clonally expanded cells, understanding gene signatures and enabling Ig gene cloning and characterization of monoclonal antibodies. The application of the strategy is further exemplified in this thesis in following the onset and longitudinal evolution of CSP reactive memory B cells to understand how the selection of B cells with high affine antibodies develops in CHMI. Additionally, random hexamers used in cDNA library synthesis leaves room for further development of tools to analyze the transcriptome on the single cell level and characterizing the cell types.

5.2 Recruitment of pre-existing memory B cells in CSP response

Highly mutated memory B cells were recruited throughout the course of the three infections, although the overall mean mutation count decreased due to increased recruitment of naïve B cells[95-97]. While the antibodies from some mutated memory B cells show CSP binding, the majority of them carry antibodies with affinity below the ELISA detection threshold. The higher prevalence of poly-reactive cells within this population may partly explain this observation[96,106]. Further, due to the lower threshold needed for activation[107-109], pre-existing memory B cells from non-Pf infections were re-recruited in to the Pf response. Studies using

mouse model report the BCR extrinsic and intrinsic stimulation of memory B cells[110]. Transcriptional and epigenetic changes during memory B cell differentiation prepare the cells to be more responsive[111]. This provides the explanation for the high recruitment of mutated memory B cells during primary Pf infection presumably through BCR extrinsic mechanisms. Nonetheless, naïve B cells carrying high affine antibodies selected during the second and third infection out-compete the less affine B cells. The efficient clonal selection based on BCR intrinsic stimulation results in the generation of high quality antibodies preferentially in the clonally expanded B cells[40].

Interestingly, some CSP binding antibodies at later infections carried relatively high Ig gene mutations (SHM count > 20), indicating the corresponding memory B cells were less likely to have been recruited as naïve B cells[95-97]. Although their affinity was not as high as the naive B cell antibodies, they still exhibited significant *Pf* spz inhibition. The most likely explanation is that these are memory B cells from non-Pf response, but were nevertheless recruited during Pf infection due to their cross-binding to CSP. Although NANP repeat units are exclusively present only in CSP, it is possible that the antibodies from the pre-existing memory B cells recognize a structurally similar epitope. This notion is supported by a recent study that reported the memory B cells generated in response to DENV1 infection to actively take part during ZIKA infection due to the structural overlap of the envelope domain present in both viruses[112].

5.3 Coexistence of B cells with high and low affine antibodies

While the average antibody affinity improved during three Pf infections, B cells with high and low affine antibodies were maintained throughout. This could be the result of minimum affinity required to reach the threshold BCR signaling and hence positive selection. For monovalent antigens, the reported minimum antigen-antibody affinity required for antigen uptake and presentation for T_{FH} help is 10^{-6} M [100]. However, for antigens with repetitive epitopes like CSP,

this minimum threshold could be lowered and allows for permissive selection of low affine antibodies, as suggested by the anti-CSP antibodies with ~10^{-5} M affinity. Although the overall CSP response was initiated by the low affine antibodies, over the course of three infections, GC competition selects for B cells with high affine antibodies (~10^{-7} M), and such B cells are enriched. A recent study using multi-photon microscopy of GCs suggested that although the average affinity of GC B cell antibodies increases, homogenizing selection takes place to a lesser extent[99]. The study reported the presence of B cell clones with diverse affinities selected in several GCs, ensuring parallel affinity maturation. Although this study focused on GC B cells, the CSP memory B cells generated during CHMI show a similar picture. Maintenance of B cells with a broad range of antibody affinities in the memory B cell pool rescues the system from narrowing the response to a few high affinity clones. Such diverse affinity clones could be re-recruited in a future response and still undergo affinity maturation. While the impact of antibody clones targeting different epitopes has been studied by following the evolution of gp140 antibody responses in HIV infection[113], the implication of antibodies with a broader affinity ranges for functional vs non-functional immune responses remains to be studied.

5.4 High affine CSP antibodies are germline encoded

CHMI with high sporozoite dosages may have provided an ideal environment for the selection of antibodies with desired gene features (*IGHV3-33* + *IGKV1-5*) and high affinity from the extensively diverse naïve B cell pool. Other studies also present the enrichment of gene signatures in several responses such as *IGHV3-23* + *IGKV1-5* in DENV1 and ZIKV envelope domain binding antibodies[112], *IGHV3-30* in antibodies against Pneumovax®23 cell wall polysaccharide[114] and *IGHV1-2* and *IGHV1-69* in HIV gp140 binding antibodies[115,116]. It is important to note that these responses generated mutated antibodies with the indicated gene signatures[112,117,118]. The CSP response in CHMI remains unique in generating high affine

germline antibodies with the mentioned gene features in humans. Mouse immunization studies with the protein antigens *Bacillus anthracis* protective antigen and influenza hemagglutinin reported the recruitment of GC B cells with near germline antibodies and prominent gene signatures[119]. A mechanistic explanation for the dominance of clonal selection of B cells with high affine germline antibodies over generating them through SHM comes from the mathematical modeling with an immunization scheme similar to CHMI (Buchauer and Hoefer, unpublished results). The model predicted that the higher the complexity of an antigen, requiring more mutations by the antibody to increase affinity, the lesser the likelihood of intra-clonal affinity maturation. Much like the experimental observation in CHMI, B cells with high affine antibodies were predominantly selected from the naïve B cell pool, the effect compounded by the high antigen dose and increased GC life time. In this respect, the evolution of the CSP response in CHMI offers significant insight in the onset and development of antibody response against complex protein antigens in humans.

5.5 Role of IgM memory B cells in CSP response

Predominant usage of IgM isotype in CSP response would indicate the origin of the B cells in the naïve B cell compartment or in IgM memory B cells. Intravenous (i.v) immunization should target antigens to the spleen. Therefore i.v injection of sporozoites should induce strong immune response in the spleen[120], a residential place of IgM memory B cells[121,122]. The overall dominance of VH3 gene family antibodies is reported in the splenic IgM memory B cells[122], a feature shared by high CSP binding antibodies. However, individual members of the expanded IgM memory B cell clusters showed isotype class-switching to IgG, indicating the plasticity of IgM memory B cells. Further, high R/S ratios in CDRs compared to FWRs in CSP-memory B cells from all donors, suggesting that the antibodies had developed in *bona fide* GC responses[95,96] and not from extra-follicular responses and that there was no major effect of

chloroquine on GC reactions. Studies following IgM memory cells report that in response to secondary antigen exposure, IgM memory B cells are more likely to be recruited in the germinal center[48,123] while IgG memory B cells are more likely to differentiate into antibody secreting plasmablasts[111,124,125]. This however does not exclude IgM memory B cells from differentiating into plasmablasts or IgG memory B cells being recruited into secondary germinal centers. Perhaps this explains the serum IgM and IgG antibodies seen post second and third Pf infections. Additionally, serum IgM antibodies, secreted either as pentamers or hexamers, offer enhanced binding through avidity even when the individual paratope-epitope interaction is of less affinity. Although this provides no evidence for selection of IgM isotype in CSP memory B cells, multimeric binding of IgM antibodies might be more suited for NANP targeting antibodies, due to the repetitive nature of the NANP epitope in CSP and the protein on the parasite surface. Given that the IgM memory B cell antibodies were recombinantly expressed as IgG in this study, the overall avidity and potency of these antibodies could be underestimated. A recent study showed that the IgM memory B cell antibodies against CSP isolated from semi-immune African adults offered significant protection in *in vitro* and *in vivo* infection models[91]. A functional role of IgM antibodies in malaria has been reported in murine models in controlling the asexual stage of erythrocytic parasites[126]. These studies, along with the one presented in this thesis, shed light on the previously underappreciated role of IgM memory B cells in malaria.

5.6 Inter-donor variability in anti-CSP antibody response

The variability seen in the degree of clonal expansion was also reflected in the CSP binding quality of the memory B cell antibodies in the majority of the donors, as CSP binding antibodies are more frequently found in the clonally expanded B cells than in the non-expanded B cells. It is important to note that, although CSP is predominantly expressed on the sporozoite surface,

sporozoite infection may also present other Pf antigens to the immune system[127]. Analysis of serum antibodies in the Pf antigen proteome array detected binding to several antigens in the 9 donors[93]. Based on the degree of expansion and repertoire usage, the plasmablast response showed no significant difference among the 9 donors, indicating that random cloning and characterizing of plasmablasts would identify the antigens targeted in a donor. The fact that all the donors were protected during the challenge infection indicates that protection may not be mediated only through the anti-CSP antibodies. Studies on irradiated sporozoite immunization in non-human primates report the protective capacity of liver resident CD8 T cells[128]. This shows the diverse ways in which protection can be established. The repertoire diversity of B cells and T cells amongst donors might initiate and lead the response in different directions, particularly in successive infections.

5.7 Generation of high affine CSP antibodies

In comparison to natural infections, control of blood parasitemeia using chloroquine chemoprophylaxis in CHMI might have focused the immune response towards sporozoites antigens. This is supported by a recent report where mice infected with parasites that did not differentiate from sporozoites to merozoites, either through genomic mutations or chemoprophylaxis, showed stronger response against sporozoites antigens compared to mice infected with wildtype sporozoites[129]. Given that the recruitment of high affine antibodies occurred in three donors after 2 Pf infections (T2_071, 072 and 073) and in one donor after challenge infection (T2_042), their generation may depend on the precursor B cell frequency in the highly diverse naïve B cell pool. The dynamic changes of the antibody repertoire within naïve B cell population in healthy adults and how it changes during inflammatory conditions is not known. A potential vaccine would need to maximize the change of eliciting a functional antibody response in every donor even if there are changes in the antibody repertoire. The

recently developed HIV gp140 CD4 binding site epitope based on germline targeting immunogen (eOD-GT8) predicted the precursor B cell frequency in naïve B cell population to be 0.0056% in HIV uninfected donors[130]. Little is known about the precursor B cell frequencies of other vaccine antigens. Similar studies estimating the precursor B cell frequencies binding to NANP repeat units would provide significant insight in vaccine design and in establishing dose and time frame of immunizations.

6. Outlook

Passive immunization with CSP binding antibodies in *in vivo* animal models shows protection against the infection. The CSP binding antibodies reported in this thesis could be used as a preventive measure for travelers by passive vaccination. NANP affinity measurements indicate the strong potential of the antibodies in offering *in vivo* protection. A murine antibody targeting the N-terminal domain of CSP (5D5) showed better *in vivo* protection than NANP binding antibody (2A10)[131], indicating the presence of additional functional epitopes in CSP. Thus, binding to those non-NANP epitopes should be assessed. To identify the most potent antibody, a panel of high affine antibodies targeting different CSP epitopes should be titrated and assessed for their inhibitory capacity while infecting humanized mice by Pf or C57BL/6 mice by *P. berghei* expressing PfCSP.

One of the major goals in the field is to develop a vaccine candidate that offers sterile immunity and long-term protection. The leading CSP based vaccine candidate RTS,S offers protection with only with a low efficacy and the protection waned rapidly[67]. The study presented here identified germline high affine antibodies that were elicited in CHMI. Understanding their mode of epitope binding through antigen-antibody co-crystals would allow the identification of protective epitopes for CSP based immunogen designs. Using the immunogens, the frequency of precursor naïve B cells with high CSP affine antibodies in malaria naïve donors can be estimated. Further, the minimum dose, duration and booster vaccination scheme should be designed and tested to recruit the precursor B cells in all donors. In the end, the finding should also be corroborated in the target population, such as the African infants and pre-exposed semi immune adults.

The study presented here focused on memory B cells, but the serum antibody titers that offer sporozoites inhibition come from plasmablasts and plasma cells. Blocking of sporozoites during the transitory period they spend in blood before liver infection could be only achieved

by ensuring high antibody titers. It is also crucial to maintain stable high titers during the time of infection. While this can be achieved through passive immunization, a functional vaccine response determined by the immunogen design and adjuvant choice should aim at not only inducing high quality antibodies but maintaining the titers through long lived plasma cells.

7. References

1. Cooper, M. D., Peterson, R. D. A. & Good, R. A. Delineation of the thymic and bursal lmphoid systems in the chicken. *Nature* **205,** 143–146 (1965).
2. Roth, D. B. V(D)J Recombination: Mechanism, Errors, and Fidelity. *Microbiol. Spectr.* **2,** 1–11 (2014).
3. Hozumi, N. & Tonegawa, S. Evidence for somatic rearrangement of immunoglobulin genes coding for variable and constant regions. *Proc. Natl. Acad. Sci.* **73,** 3628–3632 (1976).
4. Janeway, C. A., Murphy, K., Travers, P., Walport, M. & Shlomchik, M. J. *Immunobiology: The Immune System in Health and Disease. Taylor & Francis, Inc.* **5,** (2001).
5. Desiderio, S. V *et al.* Insertion of N regions into heavy-chain genes is correlated with expression of terminal deoxytransferase in B cells. *Nature* **311,** 752–755 (1984).
6. Lafaille, J. J., DeCloux, A., Bonneville, M., Takagaki, Y. & Tonegawa, S. Junctional sequences of T cell receptor gamma delta genes: Implications for gamma delta T cell lineages and for a novel intermediate of V-(D)-J joining. *Cell* **59,** 859–870 (1989).
7. Xu, J. L. & Davis, M. M. Diversity in the CDR3 Region of VH Is Sufficient for Most Antibody Specificities. *Immunity* **13,** 37–45 (2000).
8. Yaari, G. & Kleinstein, S. H. Practical guidelines for B-cell receptor repertoire sequencing analysis. *Genome Med.* **7,** 121–134 (2015).
9. Kim, KM., Alber, G., Weiser, P., & Reth, M. Differential signaling through the Ig-alpha and Ig-beta components of the B cell antigen receptor. *Eur J Immunol*. **4**, 911-916 (1993).
10. Rajewsky, K. Clonal selection and learning in the antibody system. Nature 381, 751–758 (1996).
11. Wardemann, H. & Yurasov, S. Predominant autoantibody production by early human B cell precursors. *Sci*. **301**, 1374–1377 (2003).
12. Nemazee, D. & Buerki, K. Clonal deletion of autoreactive B lymphocytes in bone marrow chimeras. *Proc. Natl. Acad. Sci. U. S. A.* **86**, 8039–43 (1989).
13. Hartley, S. B. et al. Elimination of self-reactive B lymphocytes proceeds in twostages: arrested development and cell death. *Cell* **72**, 325–35 (1993).
14. Carsetti, R. Transitional B cells are the target of negative selection in the B cell compartment. *J. Exp. Med.* **181**, 2129–2140 (1995).
15. Reth, M. Antigen receptors on B lymphocytes. *Annu. Rev. Immunol.* **10**, 97–121(1992).
16. Fagraeus, A. The plasma cellular reaction and its relation to the formation of antibodies in vitro. *J. Immunol.* **58,** 1–13 (1948).
17. Nimmerjahn, F. & Ravetch, J. V. Fcgamma receptors as regulators of immune responses. *Nat. Rev. Immunol.* **8**, 34–47 (2008).
18. Wells, T. J. et al. Increased severity of respiratory infections associated with elevated anti-LPS IgG2 which inhibits serum bactericidal killing**.** *J. Exp. Med.* **211**, 1893–904 (2014).
19. Schwickert, T. A. et al. A dynamic T cell-limited checkpoint regulates affinity-dependent B cell entry into the germinal center. *J. Exp. Med.* **208**, 1243–1252 (2011).
20. Allen, C. D., Okada, T., Tang, H. L. & Cyster, J. G. Imaging of germinal center selection events during affinity maturation. *Science* **315**, 528–531 (2007).
21. McHeyzer-Williams, M. G., Okitsu, S., Wang, N., McHeyzer-Williams, L. Molecular programming of B cell memory. *Nat. Reviews.* **12**, 24-34 (2009).
22. J, KelsoeG, Rajewsky K, Weiss U. Intraclonal generation of antibody mutants in germinal centres. *Nature* **354**,389–392 (1991)
23. BerekC, BergerA, ApelM. Maturation of the immune response in germinal centers. *Cell* **67**, 1121– 1129 (1991)
24. Sallusto, F., Lanzavecchia, A., Araki, K. & Ahmed, R. From vaccines to memory and back*. Immunity* **33**, 451–63 (2010)
25. Jacob J, Kassir R, Kelsoe G. In situ studies of the primary immune response to (4-hydroxy- 3-nitrophenyl) acetyl. I. The architecture and dynamics of responding cell populations. *J. Exp. Med.* **173**, 1165–1175 (1991).
26. Nieuwenhuis P, Opstelten D. Functional anatomy of germinal centers. *Am. J. Anat.* **170**, 421–435 (1984).
27. Di Noia, J. M. & Neuberger, M. S. Molecular mechanisms of antibody somatic hypermutation. *Annu. Rev. Biochem.* **76**, 1–22 (2007).
28. Muramatsu M, Kinoshita K, Fagarasan S, Yamada S, Shinkai Y, Honjo T. Class switch recombination and hypermutation require activation-induced cytidine deaminase (AID), a potential RNA editing enzyme. *Cell* **102**, 553–563 (2000).
29. McKean D, Huppi K, Bell M, Staudt L, Gerhard W, Weigert M. Generation of antibody diversity in the immune response of BALB/c mice to influenza virus hemagglutinin. *Proc. Natl. Acad. Sci. USA* **81**, 3180–3184 (1984).
30. BerekC,Milstein C. Mutation drift and repertoire shift in the maturation of the immune response. *Immunol. Rev.* **96**, 23–41 (1987).
31. N. S. De Silva, U. Klein, Dynamics of B cells in germinal centres. *Nat. Rev. Immunol*. **15**, 137–148 (2015).
32. Mandel TE, Phipps RP, Abbot AP, Tew JG. Long-term antigen retention by dendritic cells in the popliteal lymph node of immunized mice. *Immunology* **43**, 353–362 (1981).

33. Hanna MG Jr. An autoradiographic study of the germinal center in spleen white pulp during early intervals of the immune response. *Lab. Investig*. **13**, 95–104 (1964).
34. Batista FD, Iber D, Neuberger MS. B cells acquire antigen from target cells after synapse formation. *Nature* **411**, 489–494 (2001).
35. Batista FD, Arana E, Barral P, Carrasco YR, DepoilD, et al. The role of integrins and coreceptors in refining thresholds for B-cell responses. *Immunol. Rev.* **218**:197–213 (2007).
36. Shulman, Z. et al. T follicular helper cell dynamics in germinal centers. *Science* **341**, 673–677 (2013).
37. Shulman, Z. et al. Dynamic signaling by T follicular helper cells during germinal center B cell selection. *Science* **345**, 058–1062 (2014).
38. Liu D, Xu H, Shih C, Wan Z, Ma X, Ma W, Luo D, Qi H: T-B-cell entanglement and ICOSL-driven feed-forward regulation of germinal centre reaction. *Nature*, **517,** 214-218 (2015).
39. Janeway CA Jr. The discovery of T cell help for B cell antibody formation: a perspective from the 30th anniversary of this discovery. *Immunol. Cell Biol.* **77,** 177–79 (1999).
40. G. D. Victora, M. C. Nussenzweig, Germinal Centers. *Annu. Rev. Immunol*. **30**, 429–457 (2012).
41. Takahashi, Y., Dutta, P.R., Cerasoli, D.M., and Kelsoe, G. In situ studies of the primary immune response to (4-hydroxy-3-nitrophenyl) acetyl. V. Affinity maturation develops in two stages of clonal selection. *J. Exp. Med.* **187**, 885–895 (1998).
42. Klein, U., Kuppers, R. & Rajewsky, K. Evidence for a large compartment of IgM-expressing memory B cells in humans. *Blood* **89**, 1288–1298 (1997).
43. Dogan, I. et al. Multiple layers of B cell memory with different effector functions. *Nature Immunol.* **10**, 1292–1299 (2009).
44. Jacob, J., Miller, C. & Kelsoe, G. In situ studies of the antigen-driven somatic hypermutation of immunoglobulin genes. *Immunol. Cell Biol*. **70**, 145–52 (1992).
45. Bergqvist, P., Gärdby, E., Stensson, A., Bemark, M. & Lycke, N. Y. Gut IgA class switch recombination in the absence of CD40 does not occur in the lamina propria and is independent of germinal centers. *J. Immunol*. **177**, 7772–83 (2006).
46. Phan, T. G. et al. High affinity germinal center B cells are actively selected into the plasma cell compartment. *J. Exp. Med.* **203**, 2419–24 (2006).
47. Weisel, F. J., Zuccarino-Catania, G. V., Chikina, M. & Shlomchik, M. J. A Temporal Switch in the Germinal Center Determines Differential Output of Memory B and Plasma Cells. *Immunity* **44**, 116–130 (2016).
48. McHeyzer-Williams LJ, Milpied PJ, Okitsu SL, McHeyzer- Williams MG: Class-switched memory B cells remodel BCRs within secondary germinal centers. *Nat Immunol*, **16**,296-305 (2015).
49. http://www.malariavaccine.org
50. White, N. J. et al. Malaria. *Lancet* **383**, 723–735 (2014).
51. Amino, R. et al. Quantitative imaging of Plasmodium transmission from mosquito to mammal. *Nat. Med*. **12**, 220–224 (2006).
52. Vanderberg, J. P. & Frevert, U. Intravital microscopy demonstrating antibody-mediated immobilisation of Plasmodium berghei sporozoites injected into skin by mosquitoes. *Int. J. Parasitol*. **34**, 991–996 (2004).
53. Formaglio, P., Tavares, J., Ménard, R. & Amino, R. Loss of host cell plasma membrane integrity following cell traversal by Plasmodium sporozoites in the skin. *Parasitol. Int*. **63**, 237–244 (2014).
54. Hopp, C. S. et al. Longitudinal analysis of Plasmodium sporozoite motility in the dermis reveals component of blood vessel recognition. *Elife* **4**, e07789 (2015).
55. Shin, S. C. J., Vanderberg, J. P. & Terzakis, J. A. Direct Infection of Hepatocytes by Sporozoites of Plasmodium berghei. *J. Protozool*. **29**, 448–454 (1982).
56. Yuda, M. & Ishino, T. Liver invasion by malarial parasites - How do malarial parasites break through the host barrier? *Cell. Microbiol*. **6**, 1119–1125 (2004).
57. Silvie, O., Mota, M. M., Matuschewski, K. & Prudêncio, M. Cell biology and immunology of malaria. Curr. Opin. Microbiol. **11**, 352–359 (2008).
58. Hafalla, J. C., Silvie, O. & Matuschewski, K. Cell biology and immunology of malaria. *Immunol Rev*. **240**, 286–296 (2011).
59. Bousema, T., Okell, L., Felger, I. & Drakeley, C. Asymptomatic malaria infections: detectability, transmissibility and public health relevance. *Nat. Rev. Microbiol*. **12**, 833–840 (2014).
60. Langhorne, J., Ndungu, F. M., Sponaas, A.-M. & Marsh, K. Immunity to malaria: more questions than answers. *Nat. Immunol*. **9**, 725–732 (2008).
61. Males, S., Gaye, O. & Garcia, A. Long-Term Asymptomatic Carriage of Plasmodium falciparum Protects from Malaria Attacks: a Prospective Study among Senegalese Children. *Clin. Infect. Dis.* **46**, 516–522 (2008).
62. Collins, W. E., Skinner, J. C. & Jeffery, G. M. Studies on the persistence of malarial antibody response. *Am. J. Epidemiol.* **87**, 592–598 (1968).
63. Kinyanjui, S. M., Conway, D. J., Lanar, D. E. & Marsh, K. IgG antibody responses to Plasmodium falciparum merozoite antigens in Kenyan children have a short half-life. *Malar. J.* **6**, 82–89 (2007).
64. Weiss, G. E. et al. The Plasmodium falciparum-specific human memory B cell compartment expands gradually with repeated malaria infections. *PLoS Pathog*. **6**, e1000912 (2010).

65. Cavanagh, D. R. et al. A longitudinal study of type-specific antibody responses to Plasmodium falciparum merozoite surface protein-1 in an area of unstable malaria in Sudan. *J. Immunol*. **161**, 347–359 (1998).
66. Dorfman, J. R. et al. B Cell Memory to 3 Plasmodium falciparum Blood-Stage Antigens in a Malaria-Endemic Area. *J. Infect. Dis.* **191**, 1623–1630 (2005).
67. Stoute, J. a et al. Long-term efficacy and immune responses following immunization with the RTS,S malaria vaccine. *J. Infect. Dis.* **178**, 1139–1144 (1998).
68. John, C. C., Zickafoose, J. S., Sumba, P. O., King, C. L. & Kazura, J. W. Antibodies to the Plasmodium falciparum antigens circumsporozoite protein, thrombospondin-related adhesive protein, and liver-stage antigen 1 vary by ages of subjects and by season in a highland area of Kenya. *Infect. Immun*. **71**, 4320–4325 (2003).
69. Noland, G. S. et al. Low prevalence of antibodies to pre erythrocytic but not blood-stage Plasmodium falciparum antigens in an area of unstable malaria transmission compared to prevalence in an area of stable malaria transmission. *Infect. Immun*. **76**, 5721–5728 (2008).
70. Muellenbeck, M. F. et al. Atypical and classical memory B cells produce Plasmodium falciparum neutralizing antibodies. *J. Exp. Med*. **210**, 389–399 (2013).
71. Portugal, Silvia, Crompton, P. Malaria-associated atypical memory B cells exhibit markedly reduced B cell receptor signaling and effector function. *Elife* **4**, e07218 (2015).
72. Sullivan, R. T. et al. FCRL5 Delineates Functionally Impaired Memory B Cells Associated with Plasmodium falciparum Exposure. *PLoS Pathog*. **11**, e1004894 (2015).
73. Nussenzweig, R. S., Vanderberg, J., Most, H. & Orton, C. Protective immunity produced by the injection of x-irradiated sporozoites of Plasmodium berghei. Nature 215, 25–30 (1967)
74. P. Potocnjak, N. Yoshida, R. S. Nussenzweig, V. Nussenzweig, Monovalent fragments (Fab) of monoclonal antibodies to a sporozoite surface antigen (Pb44) protect mice against malarial infection. *J. Exp. Med*. **151**, 1504–1513 (1980).
75. Hollingdale, M. R., Nardin, E. H., Tharavanij, S., Schwartz, A. L. & Nussenzweig, R. S. Inhibition of entry of Plasmodium falciparum and P. vivax sporozoites into cultured cells; an in vitro assay of protective antibodies. J. Immunol. 132, 909–913 (1984).
76. Hollingdale, M. R., Zavala, F., Nussenzweig, R. S. & Nussenzweig, V. Antibodies to the protective antigen of Plasmodium berghei sporozoites prevent entry into cultured cells. J. Immunol. 128, 1929–1930 (1982).
77. Yoshida, N., Nussenzweig, R. S., Potocnjak, P., Nussenzweig, V. & Aikawa, M. Hybridoma produces protective antibodies directed against the sporozoite stage of malaria parasite. Science 207, 71–73 (1980).
78. Dame, J.B., J.L. Williams, T.F. McCutchan, J.L. Weber, R.A. Wirtz, W.T. Hockmeyer, W.L. Maloy, J.D. Haynes, I. Schneider, D. Roberts, and et al. Structure of the gene encoding the immunodominant surface antigen on the sporozoite of the human malaria parasite Plasmodium falciparum. *Science* **225**,593-599 (1984).
79. Godson, G.N., J. Ellis, P. Svec, D.H. Schlesinger, and V. Nussenzweig. Identification and chemical synthesis of a tandemly repeated immunogenic region of Plasmodium knowlesi circumsporozoite protein. *Nature* **305**, 29-33 (1983).
80. Zavala, F., A.H. Cochrane, E.H. Nardin, R.S. Nussenzweig, and V. Nussenzweig. Circumsporozoite proteins of malaria parasites contain a single immunodominant region with two or more identical epitopes. *J Exp Med* **157**,1947-1957 (1983).
81. Neafsey, D.E., et al. Genetic Diversity and Protective Efficacy of the RTS,S/AS01 Malaria Vaccine. *N Engl J Med* **373**,2025-2037 (2015).
82. Agnandji ST, et al. First results of phase 3 trial of RTS,S/AS01 malaria vaccine in African children. *N Engl J Med* **365**:1863-1875 (2011).
83. Olotu, A. et al. Seven-Year Efficacy of RTS,S/AS01 Malaria Vaccine among Young African Children. *N. Engl. J. Med*. **374**, 2519–2529 (2016).
84. Tiller, T. et al. Efficient generation of monoclonal antibodies from single human B cells by single cell RT-PCR and expression vector cloning. *J. Immunol. Methods* **329**, 112–124 (2008).
85. Murugan, R., Imkeller, K., Busse, C. E. & Wardemann, H. Direct high-throughput amplification and sequencing of immunoglobulin genes from single human B cells. *Eur. J. Immunol.* **45**, 2698–700 (2015).
86. Tewari, K. et al. Poly(I:C) is an effective adjuvant for antibody and multi-functional CD4+ T cell responses to Plasmodium falciparum circumsporozoite protein (CSP) and αDEC-CSP in non human primates. *Vaccine* **28**, 7256–7266 (2010).
87. F. Zavala, A. H. Cochrane, E. H. Nardin, R. S. Nussenzweig, V. Nussenzweig, Circumsporozoite proteins of malaria parasites contain a single immunodominant region with two or more identical epitopes. *J. Exp. Med*. **157**, 1947–1957 (1983).
88. Wardemann, H. et al. Predominant autoantibody production by early human B cell precursors. *Science* **301**, 1374– 1377 (2003).
89. Meffre, E. et al. Surrogate light chain expressing human peripheral B cells produce self-reactive antibodies. *J. Exp. Med.* **199**, 145–150 (2004).
90. J. Sattabongkot et al., Establishment of a human hepatocyte line that supports in vitro development of the exo-erythrocytic stages of the malaria parasites Plasmodium falciparum and P. vivax. *Am. J. Trop. Med. Hyg.* **74**, 708–715 (2006).

91. G. Triller et al., Natural parasite exposure induces protective human anti-malarial antibodies. *Immunity.* in Press (2017).
92. Busse, C. E., Czogiel, I., Braun, P., Arndt, P. F. & Wardemann, H. Single-cell based high-throughput sequencing of full-length immunoglobulin heavy and light chain genes. *Eur. J. Immunol*. **44**, 597-603 (2013).
93. Mordmüller, B. et al. Sterile protection against human malaria by chemoattenuated PfSPZ vaccine. *Nature* **542**, 445–449 (2017).
94. K. Imkeller, P. F. Arndt, H. Wardemann, C. E. Busse, sciReptor: analysis of single-cell level immunoglobulin repertoires. *BMC Bioinformatics*. **17**, 67 (2016).
95. M. Tsuiji et al., A checkpoint for autoreactivity in human IgM+ memory B cell development. *J. Exp. Med.* **203**, 393–400 (2006).
96. T. Tiller et al., Autoreactivity in Human IgG+ Memory B Cells. *Immunity*. **26**, 205–213 (2007).
97. M. A. Berkowska et al., Circulating Human CD27-IgA+ Memory B Cells Recognize Bacteria with Polyreactive Igs. *J Immunol*. **195**, 1417–1426 (2015).
98. J. Prigent et al., Scarcity of autoreactive human blood IgA+ memory B cells. *Eur. J. Immunol*. **46**, 2340–2351 (2016).
99. G. D. V. Jeroen M. J. Tas, Luka Mesin, Giulia Pasqual, Sasha Targ, Johanne T. Jacobsen, Yasuko M. Mano, Casie S. Chen, Jean-Claude Weill, Claude-Agnès Reynaud, Edward P. Browne, Michael Meyer-Hermann, Visualizing antibody affinity maturation in germinal centers. *Science* **351**, 1048–1054 (2016).
100. F. D. Batista, M. S. Neuberger, Affinity dependence of the B cell response to antigen: A threshold, a ceiling, and the importance of off-rate. *Immunity*. **8**, 751–759 (1998).
101. J. Foote, H. N. Eisen, Kinetic and affinity limits on antibodies produced during immune responses. *Proc. Natl. Acad. Sci. U. S. A.* **92**, 1254–1256 (1995).
102. Weinstein, J.A. et al. High-throughput sequencing of the zebrafish antibody repertoire. *Science* **324**, 807–810 (2009).
103. Khan, T.A. et al. Accurate and predictive antibody reper- toire profiling by molecular amplification fingerprinting. *Sci. Adv*. **2**, e1501371 (2016).
104. Lavinder, J.J. et al. Systematic characterization and comparative analysis of the rabbit immunoglobulin repertoire. *PLoS One* **9**, e101322 (2014).
105. DeKosky, B.J. et al. High-throughput sequencing of the paired human immunoglobulin heavy and light chain repertoire. *Nat. Biotechnol*. **31**, 166–169 (2013).
106. Scheid, J. F. et al. Differential regulation of self-reactivity discriminates between IgG+ human circulating memory B cells and bone marrow plasma cells. *Proc. Natl. Acad. Sci. U. S. A.* **108,** 18044–8 (2011).
107. Kometani, K. et al. Repression of the transcription factor Bach2 contributes to predisposition of IgG1 memory B cells toward plasma cell differentiation. *Immunity* **39**, 136–147 (2013).
108. Weill, J.-C., Le Gallou, S., Hao, Y. & Reynaud, C.-A. Multiple players in mouse B cell memory. *Curr. Opin. Immunol*. **25**, 334–338 (2013).
109. Kasturi, S. P. et al. Programming the magnitude and persistence of antibody responses with innate immunity. *Nature* **470**, 543–547 (2011).
110. Kurosaki T, Kometani K, & Ise W. Memory B cells. *Nat. Rev. Immunol.* 15, 149–159 (2015).
111. Kometani, K. et al. Repression of the transcription factor Bach2 contributes to predisposition of IgG1 memory B cells toward plasma cell differentiation. *Immunity* **39**, 136–147 (2013).
112. Davide F. Robbiani et al., Recurrent Potent Human Neutralizing Antibodies to Zika Virus in Brazil and Mexico. *Cell* **169**, 597–609 (2017).
113. Hua-Xin Liao et al., Co-evolution of a broadly neutralizing HIV-1 antibody and founder virus, *Nature* **496**, 469-476 (2013).
114. Smith K, Muther JJ, Duke AL, McKee E, Zheng NY, Wilson PC, James JA. Fully human monoclonal antibodies from antibody secreting cells after vaccination with Pneumovax®23 are serotype specific and facilitate opsonophagocytosis. *Immunobiology*. **218**, 745-754 (2013).
115. Peter D Kwong & Ian A Wilson. HIV-1 and influenza antibodies: seeing antigens in new ways. *Nat Immunol.* **10**, 573-578 (2009).
116. Scheid J F., et al., Broad diversity of neutralizing antibodies isolated from memory B cells in HIV-infected individuals. *Nature.* **458**, 636-640 (2009/0.
117. Klein F et al., Somatic Mutations of the Immunoglobulin Framework Are Generally Required for Broad and Potent HIV-1 Neutralization. *Cell* **153**, 126–138 (2013).
118. L. Pappas et al., Rapid development of broadly influenza neutralizing antibodies through redundant mutations. *Nature*. **516**, 418–422 (2014).
119. Kuraoka et al., Complex Antigens Drive Permissive Clonal Selection in Germinal Centers. *Immunity*. **44**, 542–552 (2016).
120. Lau et al., CD8+ T Cells from a Novel T Cell Receptor Transgenic Mouse Induce Liver-Stage Immunity That Can Be Boosted by Blood-Stage Infection in Rodent Malaria. *Plos Path.* **5**, e1004135 (2014).
121. Good-Jacobson KL, Tarlinton DM. Multiple routes to B-cell memory. *Int Immunol*. **24**, 403-408 (2012).
122. Bagnara et al., A reassessment of IgM memory subsets in humans. *J Immunol.* **195**, 3716-3724 (2016).

123. Seifert et al., Functional capacities of human IgM memory B cells in early inflammatory responses and secondary germinal center reactions. *Proc. Natl. Acad. Sci. U. S. A.* **112,** E546-545 (2015).
124. Kallies, A. et al. Initiation of plasma-cell differentiation is independent of the transcription factor Blimp-1. *Immunity* **26**, 555–566 (2007)
125. Martin, S. W. & Goodnow, C. C. Burst-enhancing role of the IgG membrane tail as a molecular determinant of memory. *Nature Immunol*. **3**, 182–188 (2002).
126. Krishnamurty et al., Somatically Hypermutated Plasmodium-Specific IgM+ Memory B Cells Are Rapid, Plastic, Early Responders uponMalaria Rechallenge. *Immunity.* **45**, 1-13 (2016).
127. Swearingen et al., Interrogating the Plasmodium Sporozoite Surface: Identification of Surface-Exposed Proteins and Demonstration of Glycosylation on CSP and TRAP by Mass Spectrometry- Based Proteomics. *PLOS Pathog.***12**, e1005606.
128. Ishizuka et al., Protection against malaria at 1 year and immune correlates following PfSPZ vaccination. *Nat Med*. **6**, 614-623 (2016).
129. G. J. Keitany et al., Blood Stage Malaria Disrupts Humoral Immunity to the Pre-erythrocytic Stage Circumsporozoite Protein. *Cell Rep*. **17**, 3193–3205 (2016).
130. Jardine et al., HIV-1 broadly neutralizing antibody precursor B cells revealed by germline-targeting immunogen. *Science*. **351**, 1458-1463 (2016).
131. Espinosa et al., Proteolytic Cleavage of the Plasmodium falciparum Circumsporozoite Protein Is a Target of Protective Antibodies. *J Infect Dis.* **212**, 1111-1119 (2015).

8. Supplementary Material

8.1 Antibodies

ELISA capture antibody

Goat anti-human IgG, Fcγ	Jackson, ImmunoResearch Laboratories, West Grove, PA, USA

ELISA secondary antibodies

Goat anti-human IgG, Fcγ (HRP conjugated)	Jackson, ImmunoResearch Laboratories, West Grove, PA, USA
Goat anti-human IgM, Fc5µ (HRP conjugated)	Jackson, ImmunoResearch Laboratories, West Grove, PA, USA
Goat anti-human IgA, α Chain (HRP conjugated)	Jackson, ImmunoResearch Laboratories, West Grove, PA, USA

ELISA standard and control antibodies

2A10 (chimeric antibody)	87,91
ED38 (highly poly-reactive antibody)	89
Human IgG1, kappa	Sigma Aldrich Chemie GmbH, Steinheim, Germany
mGO53 (non-poly-reactive antibody)	88

FACS analysis antibodies & reagents

7-AAD	Invitrogen GmbH, Karlsruhe, Germany
Mouse anti-human CD19 (BV786-conjugated)	BD Biosciences GmbH, Heidelberg, Germany
Mouse anti-human CD21 (PE-Cy7conjugated)	BioLegend GmbH, Fell, Germany
Mouse anti-human CD27 (PE-conjugated)	BD Biosciences GmbH, Heidelberg, Germany
Mouse anti-human IgG (BV510-conjugated)	BD Biosciences GmbH, Heidelberg, Germany
Mouse anti-human CD20 (APC-H7-conjugated)	BD Biosciences GmbH, Heidelberg, Germany
Mouse anti-human CD38 (FITC-conjugated)	BD Biosciences GmbH, Heidelberg, Germany
Mouse anti-human CD138 (BV421-conjugated)	BD Biosciences GmbH, Heidelberg, Germany

8.2 Antigens

CSP	Kind gift of Dr. Kim Lee Sim, Protein Potential LLC, Rockville, MD, USA
Δ-NCSP	Kind gift of Dr. Silvia Boscardin, Department of Parasitology, University of São Paulo, Brazil [199]
DNA sodium salt from salmon testes	Sigma Aldrich Chemie GmbH, Steinheim, Germany
Human recombinant insulin	Sigma Aldrich Chemie GmbH, Steinheim, Germany
LPS, *E.coli* 055:B5	Sigma Aldrich Chemie GmbH, Steinheim, Germany
$NANP_5$, $NANP_{10}$	Alpha Diagnostic Intl. Inc., Texas, USA

8.3 Bacteria

E.coli DH10B	Clonetech Inc., Palo Alto, CA, USA

8.4 Bacterial culture media

LB agar (35 g/l)	Carl Roth GmbH & Co. KG, Karlsruhe, Germany
Lysogeny broth (LB) (25 g/l)	Carl Roth GmbH & Co. KG, Karlsruhe, Germany
Terrific broth (TB)	Life Technologies GmbH, Karlsruhe, Germany

8.5 Buffers, solutions and chemicals

5x loading buffer gel electrophoresis	60 % (w/v) sucrose 1 mM cresol red
50x TAE buffer	2 M Tris 0.05 % (v/v) Tween®20 1 mM EDTA
ABTS self-made buffer	0.1 M citric acid 0.2 M disodium phosphate 1 ABTS tablet/91 ml ABTS buffer
ABTS tablets	Roche Diagnostics GmbH, Mannheim, Germany

Acetic acid (CH_3COOH)	Sigma Aldrich Chemie GmbH, Steinheim, Germany
Ammonium chloride (NH_4Cl_2)	Sigma Aldrich Chemie GmbH, Steinheim, Germany
Ammonium sulfate ($(NH_4)_2SO_4$)	Sigma Aldrich Chemie GmbH, Steinheim, Germany
Bovine serum albumin fraction V (BSA)	Carl Roth GmbH & Co. KG, Karlsruhe, Germany
Calcium chloride ($CaCl_2$)	Sigma Aldrich Chemie GmbH, Steinheim, Germany
Citric acid ($C_6H_8O_7$) (≥ 99.5 %)	Sigma Aldrich Chemie GmbH, Steinheim, Germany
Coomassie Brilliant Blue G-250	BioRad Laboratories GmbH, München, Germany
Coomassie Destaining Buffer	100 ml methanol 400 ml acetic acid 500 ml deionized water
Coomassie Incubation Buffer	50% (v/v) methanol 2% (v/v) phosphoric acid 17% (m/v) ammonium sulfate ad 1000 ml deionized water
Coomassie Staining Buffer	0.66 g Coomassie Brilliant Blue G-250/1l ad 1l Coomassie Incubation buffer
Criterion™ TGX™ Precast Gels	Bio-Rad Laboratories GmbH, München, Germany
Cytochalasin D	Sigma Aldrich Chemie GmbH, Steinheim, Germany
Dextran-rhodamine	Thermo Fisher Scientific Inc., Darmstadt, Germany
Dimethyl sulfoxide (DMSO)	Sigma Aldrich Chemie GmbH, Steinheim, Germany
Disodium phosphate (Na_2HPO_4)	Sigma Aldrich Chemie GmbH, Steinheim, Germany
Disodium phosphate (Na_2HPO_4)	Carl Roth GmbH & Co. KG, Karlsruhe, Germany
ELISA blocking buffer (concentration ELISA)	1x PBS 0.05% (v/v) Tween®20 1 mM EDTA
ELISA blocking buffer 2 (antigen ELISA)	1% BSA/PBS
ELISA blocking buffer 3 (serum ELISA)	1x PBS 0.05% (v/v) Tween®20 4% BSA
Elution buffer pH 3 (antibody purification)	0.1 M glycine pH 3.0
Ethanol	Sigma Aldrich Chemie GmbH, Steinheim, Germany
Ethidium bromide ($C_{21}H_{20}BrN_3$)	Sigma Aldrich Chemie GmbH, Steinheim, Germany
Ethylenediaminetetraacetic acid (EDTA)	Carl Roth GmbH & Co. KG, Karlsruhe, Germany
GIBCO™ 10x PBS (pH 7.4)	Life Technologies GmbH, Karlsruhe, Germany
GIBCO™ 1x PBS (pH 7.4)	Life Technologies GmbH, Karlsruhe, Germany
GIBCO™ Trypan Blue Stain 0.4%	Life Technologies GmbH, Karlsruhe, Germany
Giemsa's stain improved R66 solution Gurr®	VWR International, Leicestershire, UK
Glycerol ($C_3H_8O_3$)	Carl Roth GmbH & Co. KG, Karlsruhe, Germany
Glycine ($C_2H_5NO_2$)	Sigma Aldrich Chemie GmbH, Steinheim, Germany
H_2O_2	Th. Geyer GmbH & Co. KG, Renningen, Germany
Neutralization buffer pH 9.0 (antibody purification)	1M Tris
Paraformaldehyde (PFA)	Alfa Aesar, Thermo Fisher (Kandel) GmbH, Karlsruhe, Germany
Percoll®	GE Healthcare Life Sciences, Freiburg, Germany
Polyethyleneimine (PEI)	Sigma Aldrich Chemie GmbH, Steinheim, Germany
Protein G Sepharose™ Fast Flow	GE Healthcare Life Sciences, Freiburg, Germany
Rat collagen	Sigma Aldrich Chemie GmbH, Steinheim, Germany
SeaKem® LE Agarose	Cambrex Inc., Rockland, ME, USA
Sodium chloride (NaCl)	Sigma Aldrich Chemie GmbH, Steinheim, Germany
Triton X-100	Sigma Aldrich Chemie GmbH, Steinheim, Germany
Trizma® base ($C_4H_{11}NO_3$)	Sigma Aldrich Chemie GmbH, Steinheim, Germany
Tween® 20 ($C_{58}H_{114}O_{26}$)	Carl Roth GmbH & Co. KG, Karlsruhe, Germany

8.6 Cell lines

U-266	DSMZ (ACC 9)

HC-04	BEI Resources, NIAID, NIH, Manassas, VA, USA: HC-04, Hepatocyte (human), MRA-975, contributed by Jetsumon Sattabongkot Prachumsri
FreeStyle™ 293-F	Thermo Fisher Scientific Inc., Darmstadt, Germany

8.7 Cell culture media

Ampicillin	Sigma Aldrich Chemie GmbH, Steinheim, Germany
GIBCO™ DMEM	Life Technologies GmbH, Karlsruhe, Germany
GIBCO™ HEPES	Life Technologies GmbH, Karlsruhe, Germany
GIBCO™ L-glutamine	Life Technologies GmbH, Karlsruhe, Germany
GIBCO™ MEM	Life Technologies GmbH, Karlsruhe, Germany
GIBCO™ PenStrep	Life Technologies GmbH, Karlsruhe, Germany
GIBCO™ RPMI	Life Technologies GmbH, Karlsruhe, Germany
GIBCO™ RPMI with L-glutamine	Life Technologies GmbH, Karlsruhe, Germany
GIBCO™ Trypsin EDTA 1x	Life Technologies GmbH, Karlsruhe, Germany
Human serum	Haema, Berlin
FreeStyle293 Expression media	Thermo Fisher Scientific Inc., Darmstadt, Germany
EX-CELL® 293 Serum-Free Medium	Thermo Fisher Scientific Inc., Darmstadt, Germany

8.8 Experimental parasites

Pf NF54	Kind gift of Dr. Robert Sauerwein, Radboud University Medical Centre, NL

8.9 Commercial kits

AlexaFluor® 647 Antibody Labeling Kit	Thermo Fisher Scientific Inc., Darmstadt, Germany
NucleoBond® Xtra Midi / Maxi	Macherey-Nagel GmbH & Co. KG, Düren, Germany
NucleoSpin® 96 PCR Clean-Up	Macherey-Nagel GmbH & Co. KG, Düren, Germany
NucleoSpin® Gel and PCR Clean-up	Macherey-Nagel GmbH & Co. KG, Düren, Germany
NucleoSpin® Plasmid Kit	Macherey-Nagel GmbH & Co. KG, Düren, Germany

8.10 Enzymes and additives

Cloning

AgeI, BsiWI, SalI, XhoI	New England Biolabs GmbH, Frankfurt am Main, Germany
Buffer 1 10x	New England Biolabs GmbH, Frankfurt am Main, Germany
Cutsmart buffer 10x	New England Biolabs GmbH, Frankfurt am Main, Germany
T4 DNA Ligase	New England Biolabs GmbH, Frankfurt am Main, Germany
T4 DNA Ligase buffer 10x	New England Biolabs GmbH, Frankfurt am Main, Germany

RT and PCRs

10x PCR buffer	Quiagen AG, Hilden, Germany
5x First strand buffer (RT)	Life Technologies GmbH, Karlsruhe, Germany
DTT	Life Technologies GmbH, Karlsruhe, Germany
Hotstart *Taq* DNA polymerase	Quiagen GmbH, Hilden, Germany
NP-40	Sigma Aldrich Chemie GmbH, Steinheim, Germany
Nuclease free water	Eppendorf AG, Hamburg, Germany
RNAsin®	Promega Inc., Madison, WI, USA
RT buffer	Life Technologies GmbH, Karlsruhe, Germany
SuperScript™ III Reverse Transcriptase	Life Technologies GmbH, Karlsruhe, Germany
Taq DNA polymerase	Self-made

8.11 Expression vectors

Vectors (with γ1-, κ- and λ-chain C regions)	Kind gift of Dr. J. Ravetch, Rockefeller University, New York City, USA

8.12 Nucleotides and nucleic acids

1kb Plus DNA marker	New England Biolabs GmbH, Frankfurt am Main, Germany
Desoxynucleotide Triphosphates (dNTPs)	Life Technologies GmbH, Karlsruhe, Germany
Oligonucleotides	MWG Biotech AG, Ebersberg, Germany
Random Hexamer Primers	Roche Diagnostics GmbH, Mannheim, Germany

8.13 Instruments and consumables

1.5 ml reaction tubes	Sarstedt AG, Nümbrecht, Germany
2 ml reaction tubes	Sarstedt AG, Nümbrecht, Germany
13 ml tubes	Sarstedt AG, Nümbrecht, Germany
96-well Multiply®-PCR plate	Sarstedt AG, Nümbrecht, Germany
96-well skirted twintech PCR plate	Eppendorf AG, Hamburg, Germany
Alpha Imager™ 1220	Alpha Innotech Corporation Inc., San Leandro, CA, USA
Aluminum foil seal	4titude, Surrey, UK
AxioObserver Z1 fluorescence microscope	ZEISS Microscopy, Oberkochen, Germany
BD Aria II™	BD Biosciences GmbH, Heidelberg, Germany
BD LSR II™	BD Biosciences GmbH, Heidelberg, Germany
BD Microlance™ 3 30G x 1/2”	BD Biosciences GmbH, Heidelberg, Germany
BioPhotometer	Eppendorf AG, Hamburg, Germany
Bio-Spin® chromatography columns	Bio-Rad Inc., Hercules, CA, USA
Cell culture 48-well plate	TPP, Trasadingen, Switzerland
Cell culture 96-well plate	TPP, Trasadingen, Switzerland
Cell culture 96-well plate (transparent bottom)	TPP, Trasadingen, Switzerland
Cell culture dish (150 mm)	BD Biosciences GmbH, Heidelberg, Germany
CellStar sterile serological pipettes 2 ml, 5 ml, 10 ml, 25 ml, 50 ml	Greiner Bio-One GmbH, Frickenhausen, Germany
Centrifuge 5180R (rotor A-4-81)	Eppendorf AG, Hamburg, Germany
Centrifuge 5417R (rotor F-45-30-11)	Eppendorf AG, Hamburg, Germany
CO_2 Incubator CB210	Binder GmbH, Tüttlingen, Germany
Cover slips	Menzel-Gläser GmbH, Braunschweig, Germany
CryoTube™ Vials	Thermo Fisher Scientific Inc., Darmstadt, Germany
Domed 12-cap strips (PCR tube strips)	Bio-Rad Laboratories GmbH, München, Germany
Electrophoresis chamber D3 (horizontal)	Thermo Scientific Inc., Rochester, NY, USA
ELISA plates (96-well, flat bottom)	Costar Inc., Corning, Action, MA, USA
FluoNunc Plates	Costar Inc., Corning, Action, MA, USA
FrameStar® 384	4titude, Surrey, UK
Heraeus B5042 (Bacteria incubator)	Kendro Laboratory Products, Weaverville, NC, USA
Inoculating loops/needles, polystyrene	VWR International Inc., Brigdgeport, NJ, USA
Leica DM2000 LED	Leica Microsystems GmbH Wetzlar, Germany
M1000Pro plate reader	Tecan, Crailsheim, Germany
Mastercycler® ep Gradient S	Eppendorf AG, Hamburg, Germany
Mastercycler® Pro 384	Eppendorf AG, Hamburg, Germany
MiniVE vertical electrophoresis unit	Höfer Inc., Holliston, MA USA
Multichannel Pipet-Lite® LTS 2-20 µl, 20-200 µl, 100-1200 µl	Rainin Instrument Inc. LLC, Woburn, MA, USA
Multipette plus	Eppendorf AG, Hamburg, Germany
Multitron Pro (Bacteria shaker)	Infors HT, Bottmingen, CH
Nanodrop™ 1000	Thermo Scientific Inc., Wilmington, DE, USA
Neubauer Counting Chamber by Marienfeld	Carl Roth GmbH & Co. KG, Karlsruhe, Germany
Omnican® 50 Insulin Syringes, 12 mm 30 G	B. Braun Medical Ltd, Sheffield, UK
PC	LG Electronics Deutschland GmbH, Ratingen, Germany
Petri dishes (100 mm)	Greiner Bio-One GmbH, Frickenhausen, Germany
Pipetboy acc	Integra Biosciences GmbH, Fernwald, Germany

Pipet-Lite® LTS 0.1-2 µl, 2-20 µl, 20-200 µl, 100-1000 µl	Rainin Instrument Inc. LLC, Woburn, MA, USA
Polypropylene tubes (15 ml, 50 ml)	Sarstedt AG, Nümbrecht, Germany
Polystyrene round bottom tube (5 ml) with cell strainer cap	BD Biosciences GmbH, Heidelberg, Germany
Slide-A-Lyzer® Mini Dialysis Devices	Thermo Scientific, Rockford, IL, USA
S-Monovette® EDTA K	Sarstedt, Nümbrecht, Germany
SpectraMax 190 Microplate Reader	Molecular Devices Inc., Sunnyvale, CA, USA
Stemi 2000 Stereomicroscope	ZEISS Microscopy, Oberkochen, Germany
Stuart® Gyro rocker SSL3	Sigma Aldrich Chemie GmbH Steinheim, Germany
T75 cm^2 flask	BD Biosciences GmbH, Heidelberg, Germany
Thermomixer comfort	Eppendorf AG, Hamburg, Germany
Vortex genie 2	Scientific Industries Inc., Bohemia, NY, USA
Water bath with thermostat	JULABO Labortechnik GmbH, Seelbach, Germany
Wax seal	4titude, Surrey, UK

8.14 Software

FlowJo v10.0	Treestar Systems Inc., Ashland, USA
GraphPad Prism 6.07	GraphPad Software Inc., La Jolla, USA
Illustrator® CS5	Adobe Inc., San Jose, CA, USA
Mendeley Desktop	Mendeley Ltd, London, UK
Microsoft® Office 2011	Microsoft GmbH, Stuttgart, Germany
Pearl	Version 12.5, open source distribution
PhotoShop® CS5	Adobe Inc., San Jose, CA, USA
Rstudio version 0.99.484	RStudio, Inc., Boston, MA USA
SoftMax Pro	Molecular Devices, Sunnyvale, CA, USA

8.15 Web Resources

Clustal Omega	http://www.ebi.ac.uk/Tools/msa/clustalo/
Ensemble Genome Browser	http://www.ensembl.org/index.html
Expasy SIB Bioinformatics Resource Portal	http://expasy.org/
IMGT®	http://www.imgt.org/
NCBI Ig Blast	http://www.ncbi.nlm.nih.gov/igblast/
PlasmoDB	http://plasmodb.org/plasmo/

9. Supplementary Figures

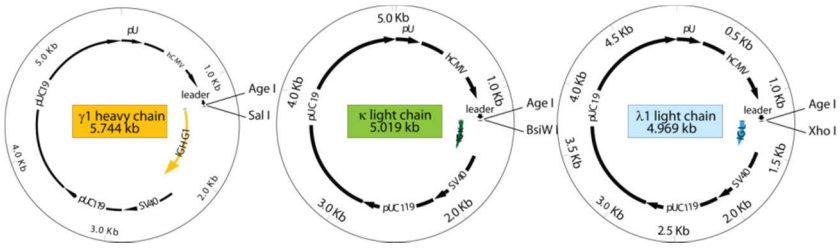

Supplementary Figure 1: Human expression vector maps. Human Igγ1, Igκ and Igλ expression vectors with the human Igγ1, Igκ and Igλ constant regions where corresponding Ig genes can be cloned in the multiple cloning site. The restriction sites used for cloning in a given vector are indicated. Upstream to the multiple cloning site, a murine leader sequence is located. Human cytomegalovirus (hCMV) promotor is used for expression. Ampicillin resistance allows for the screening of the vectors. Figure is adapted from Tiller (Tiller, T. The frequency of Self-Reactive Human and Mouse IgG$^+$ B Lineage Cells in Health and Autoimmunity (Humboldt Universität zu Berlin, 2009)).

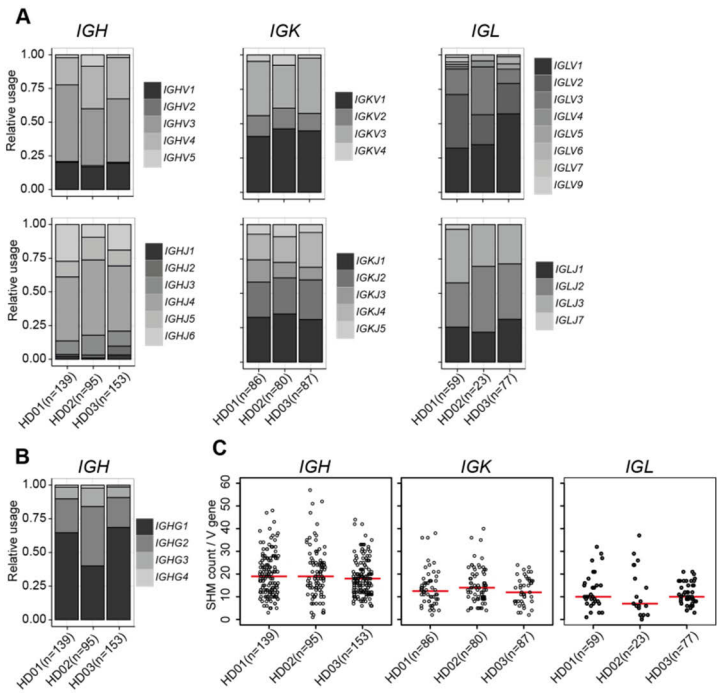

Supplementary Figure 2. Ig gene sequence analysis. A, B. Frequencies of *IGHV, IGKV* and *IGLV* gene families (A) and isotype subclass (B) in the healthy donors HD1-3. **C.** SHM count per V gene of *IGHV, IGKV* and *IGLV* genes. This figure is adapted from[85].

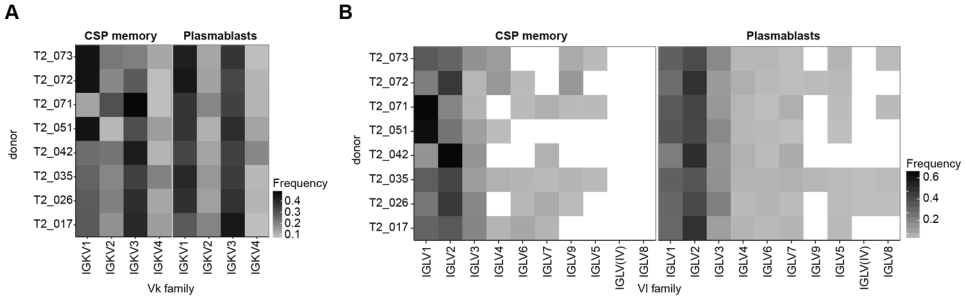

Supplementary Figure 3. Vk and Vl family usage. A,B. Frequency of Vk (A) and Vl (B) gene family usage in CSP memory B cells antibodies compared to that of plasmablasts in individual donors represented as a heatmap.

10. Supplementary Tables

Table S1. Number of CSP memory B cell antibodies sequenced and cloned after infection I, II and III

CSP memory						
	Antibody sequences*			Antibodies cloned		
donors	I	II	III	I	II	III
T2_017	29	9	12	10	6	12
T2_026	17	13	31	4	3	9
T2_035	58	18	32	8	4	10
T2_042	2	12	52	1	8	29
T2_051	29	62	90	15	22	28
T2_052	5	6	1	0	0	0
T2_071	1	22	124	1	16	33
T2_072	17	53	95	7	23	37
T2_073	NA	86	142	NA	29	51

Table S2. Number of plasmablast antibodies sequenced after infection I, II and III

Plasmablast			
	Sequences*		
donors	I	II	III
T2_017	58	64	38
T2_026	73	229	241
T2_035	181	316	250
T2_042	38	123	103
T2_051	165	211	262
T2_052	246	226	23
T2_071	72	283	217
T2_072	137	109	191
T2_073	NA	209	147

*paired functional *IGH* and *IGK/IGL* genes

NA: Not available

Supplementary Table 3: Primer Sequences[84,85].

1st heavy PCR:

Forward primer

hIGHV-1/7-066-fw	ACAGGTGCCCACTCCCAGGTGCAG
hIGHV-1/7-017-fw	ATGGACTGGACCTGGAG
hIGHV-1/7-041-fw	TCCTCTTTGTGGTGGCAGCAGC
hIGHV-2-035-fw	TCCACGCTCCTGCTRCTGAC

Supplementary table

hIGHV-3-066-fw	AAGGTGTCCAGTGTGARGTGCAG
hIGHV-3-057-fw	TAAAAGGTGTCCAGTGT
hIGHV-4/6-066-fw	CCCAGATGGGTCCTGTCCCAGGTGCAG
hIGHV-4-022-fw	ATGAAACACCTGTGGTTCTTCC
hIGHV-5-066-fw	CAAGGAGTCTGTTCCGAGGTGCAG
Reverse primer	
hIGHA-111-rv	GTCCGCTTTCGCTCCAGGTCACACT
hIGHE-140-rv	AAGGTCATAGTTGTCCCGTTGAGG
hIGHG-137-rv	GGAAGGTGTGCACGCCGCTGGTC
hIGHM-082-rv	GGAAGGAAGTCCTGTGCGAGGC

2nd heavy PCR:

Forward primer	
hIGHV-pan-080-fw	AGGTGCAGCTGCTGGAGTCKGG
Reverse primer	
hIGHA-076-rv	GGAAGAAGCCCTGGACCAGGC
hIGHE-070-rv	CCAGGCAGCCCAGAGTCACGG
hIGHG-074-rv	AGTCCTTGACCAGGCAGCCC
hIGHM-031-rv	GGGAATTCTCACAGGAGACGA

Specific heavy PCR:

Forward primer	
5’ AgeI VH 1	CTGCAACCGGTGTACATTCCCAGGTGCAGCTGGTGCAG
5’ AgeI VH 1-18	CTGCAACCGGTGTACATTCCCAGGTTCAGCTGGTGCAG
5’ AgeI VH 1-24	CTGCAACCGGTGTACATTCCCAGGTCCAGCTGGTACAG
5’ AgeI VH 3	CTGCAACCGGTGTACATTCTGAGGTGCAGCTGGTGGAG
5’ AgeI VH 3-9	CTGCAACCGGTGTACATTCTGAAGTGCAGCTGGTGGAG
5’ AgeI VH 3-23	CTGCAACCGGTGTACATTCTGAGGTGCAGCTGTTGGAG
5’ AgeI VH 3-33	CTGCAACCGGTGTACATTCTCAGGTGCAGCTGGTGGAG
5’ AgeI VH 4	CTGCAACCGGTGTACATTCCCAGGTGCAGCTGCAGGAG
5’ AgeI VH 4-34	CTGCAACCGGTGTACATTCCCAGGTGCAGCTACAGCAGTG
5’ AgeI VH 4-39	CTGCAACCGGTGTACATTCCCAGCTGCAGCTGCAGGAG
5’ AgeI VH 6-1	CTGCAACCGGTGTACATTCCCAGGTACAGCTGCAGCAG
5’ AgeI VH 7	CTGCAACCGGTGTACATTCTCAGGTGCAGCTGGTGCAATCTGG
Reverse primer	
3’ SalI JH 1/2/4/5	TGCGAAGTCGACGCTGAGGAGACGGTGACCAG
3’ SalI JH 3	TGCGAAGTCGACGCTGAAGAGACGGTGACCATTG
3’ SalI JH 6	TGCGAAGTCGACGCTGAGGAGACGGTGACCGTG

1st kappa PCR

Forward primer	
5’ L-Vκ 1/2	ATGAGGSTCCCYGCTCAGCTGCTGG
5’ L-Vκ 3	CTCTTCCTCCTGCTACTCTGGCTCCCAG
5’ L-Vκ 4	ATTTCTCTGTTGCTCTGGATCTCTG
Reverse primer	
3’ Ck 543	GTTTCTCGTAGTCTGCTTTGCTCA

2nd kappa PCR:

Forward primer	
5’ Pan-Vκ	ATGACCCAGWCTCCABYCWCCCTG
Reverse primer	
3’ Ck494	GTGCTGTCCTTGCTGTCCTGCT

Supplementary table

Specific kappa PCR:

Forward primer

5' AgeI Vκ 1-5	CTGCAACCGGTGTACATTCTGACATCCAGATGACCCAGTC
5' AgeI Vκ 1-9	TTGTGCTGCAACCGGTGTACATTCAGACATCCAGTTGACCCAGTCT
5' AgeI Vκ 1D-43	CTGCAACCGGTGTACATTGTGCCATCCGGATGACCCAGTC
5' AgeI Vκ 2-24	CTGCAACCGGTGTACATGGGGATATTGTGATGACCCAGAC
5' AgeI Vκ 2-28	CTGCAACCGGTGTACATGGGGATATTGTGATGACTCAGTC
5' AgeI Vκ 2-30	CTGCAACCGGTGTACATGGGGATGTTGTGATGACTCAGTC
5' AgeI Vκ 3-11	TTGTGCTGCAACCGGTGTACATTCAGAAATTGTGTTGACACAGTC
5' AgeI Vκ 3-15	CTGCAACCGGTGTACATTCAGAAATAGTGATGACGCAGTC
5' AgeI Vκ 3-20	TTGTGCTGCAACCGGTGTACATTCAGAAATTGTGTTGACGCAGTCT
5' AgeI Vκ 4-1	CTGCAACCGGTGTACATTCGGACATCGTGATGACCCAGTC

Reverse primer

3' BsiWI Jk 1/4	GCCACCGTACGTTTGATYTCCACCTTGGTC
3' BsiWI Jk 2	GCCACCGTACGTTTGATCTCCAGCTTGGTC
3' BsiWI Jk 3	GCCACCGTACGTTTGATATCCACTTTGGTC
3' BsiWI Jk 5	GCCACCGTACGTTTAATCTCCAGTCGTGTC

1st lambda PCR:

Forward primer

5' L-Vλ 1	GGTCCTGGGCCCAGTCTGTGCTG
5' L-Vλ 2	GGTCCTGGGCCCAGTCTGCCCTG
5' L-Vλ 3	GCTCTGTGACCTCCTATGAGCTG
5' L-Vλ 4/5	GGTCTCTCTCSCAGCYTGTGCTG
5' L-Vλ 6	GTTCTTGGGCCAATTTTATGCTG
5' L-Vλ 7	GGTCCAATTCYCAGGCTGTGGTG
5' L-Vλ 8	GAGTGGATTCTCAGACTGTGGTG

Reverse primer

3' hCl-057	CACCAGTGTGGCCTTGTTGGCTTG

2nd and specific lambda PCR:

2nd PCR Forward primer

hIGLV-pa1-fw CAGYCTGYSCTGACTCA
hIGLV-pa2-fw TCCTATGAGCTGACWCAG

Specific PCR Forward primer

5' AgeI Vλ 1	CTGCTACCGGTTCCTGGGCCCAGTCTGTGCTGACKCAG
5' AgeI Vλ 2	CTGCTACCGGTTCCTGGGCCCAGTCTGCCCTGACTCAG
5' AgeI Vλ 3	CTGCTACCGGTTCTGTGACCTCCTATGAGCTGACWCAG
5' AgeI Vλ 4/5	CTGCTACCGGTTCTCTCTCSCAGCYTGTGCTGACTCA
5' AgeI Vλ 6	CTGCTACCGGTTCTTGGGCCAATTTTATGCTGACTCAG
5' AgeI Vλ 7/8	CTGCTACCGGTTCCAATTCYCAGRCTGTGGTGACYCAG

Reverse primer

3' hCl-040-XhoI	CTCCTCACTCGAGGGYGGGAACAGAGTG

Insert check PCR:

Forward primer

5' Absense	GCTTCGTTAGAACGCGGCTAC

Reverse primer

3' IgG-Internal	GTTCGGGGAAGTAGTCCTTGAC
3' hCl-057	CACCAGTGTGGCCTTGTTGGCTTG

3’ Ck494	GTGCTGTCCTTGCTGTCCTGCT

Table S3. Ig gene and functional features of CSP memory B cell antibodies cloned

I, II, III and C indicate three infection and challenge time points, respectively.

Light: K and L indicate kappa and lambda light chain, respectively.

SHM are counted in nucleotide base pairs.

AUC: area under the curve.

ND: Not determined.

Supplementary Tables

antibody	infection	V	J	light	IGKV/IGLV	IGKJ/IGLJ	IGH	cluster	V SHM	IGKV/IGLV SHM	CSP (AUC)	NANP (AUC)	NANP KD (M)	Pf spz inhibition (%)
L1517x0059	I	4-39	1	K	3D-20	5	M	0	0	0	0.812	0.7238		
L1517x0075	I	4-59	6	K	3-20	1	G2	19	4	3	4.948	0.6146	ND	0
L1517x0105	I	5-51	4	K	4-1	1	M	0	0	0	1.273	1.392		
L1517x0143	I	4-59	3	K	3-20	3	M	0	0	0	0.879	1.112		
L1517x0146	I	3-11	4	K	3-20	2	M	0	6	0	1.242	1.236		
L1517x0181	I	1-18	3	K	1D-8	2	M	0	0	1	0.5103	0.4172		
L1517x0185	I	4-59	4	K	1-39	2	M	0	16	12	1.026	1.04		
L1517x0456	II	3-11	5	K	1-39	4	M	0	5	2	1.938	2.206	ND	4.6
L1517x0604	III	1-69	3	K	4-1	1	G1	0	0	0	1.021	0.9525		
L1517x0618	III	3-33	4	K	1-12	4	M	0	7	3	5.051	5.351	1.17E-05	47.8
L1517x0661	III	1-2	6	K	3D-15	2	M	0	5	0	0.9658	1.119		
L1517x0679	III	5-51	4	K	3-15	1	M	0	0	0	1.248	2.41	ND	0
L1517x0683	III	4-39	5	K	1-39	5	M	0	0	0	0.7037	0.9761		
L1517x0687	III	3-23	6	K	4-1	4	M	0	0	0	0.6514	0.7386		
L1517x0692	III	3-33	4	K	4-1	1	M	0	0	0	4.665	3.101	3.52E-06	26.9
L1517x0704	C	4-59	4	K	2-30	1	A1	0	16	9	1.01	0.9034		
L1517x0705	C	3-21	4	K	1-39	2	G2	0	5	0	1.195	1.208		
L1517x0715	C	3-23	4	K	2-28	4	M	0	19	5	0.961	0.7638		
L1517x0716	C	1-2	3	K	1-9	2	M	0	12	6	0.9323	0.8971		
L1517x0738	C	3-23	6	K	3-11	4	M	0	0	0	1.117	1.195		
L1426x0237	I	1-8	4	K	3-20	1	M	0	4	3	0.7789	1.005		
L1426x0302	I	4-61	6	K	1-39	4	M	0	0	0	0.9879	1.044		
L1426x0397	II	4-61	4	K	3-20	2	G2	0	16	12	0.537	0.526		
L1426x0725	II	4-39	6	K	2-28	4	G1	0	25	6	0.8774	0.5734		
L1426x0775	III	3-33	4	K	4-1	2	M	0	0	0	0.6182	0.6485		
L1426x0845	III	4-61	6	K	2-28	3	G1	0	7	1	0.7167	0.5105		
L1426x0864	III	3-7	4	K	2-30	2	M	0	1	0	2.711	3.095	9.13E-06	6.1
L1426x0910	III	1-69	4	K	3-20	2	M	17	2	0	0.3353	0.365		
L1426x1003	III	4-4	6	K	2-28	1	M	0	15	5	0.6416	0.4933		
L1426x1020	III	3-23	4	K	3-15	4	M	0	0	1	0.625	1.04		
L1426x1040	III	4-30-2	5	K	3-20	2	G1	0	21	6	0.8341	0.5862		
L1426x1100	III	1-3	4	K	2-28	3	M	0	0	0	0.7704	1.008		
L1426x1186	C	3-15	4	K	3-20	4	M	0	8	9	0.6288	0.8907		
L1426x1416	C	1-8	4	K	2D-29	1	G2	3	9	12	0.5748	0.8011		
L1426x1479	C	3-30	4	K	1-16	3	M	0	0	0	0.752	0.8581		
D0835x0459	I	3-74	3	K	2-28	2	A1	33	12	13	0.8972	1.063		
D0835x0465	I	3-33	4	K	2-24	1	M	0	6	0	9.284	10.9	6.78E-06	59.3
D0835x0473	I	3-74	3	K	2-28	2	A2	33	24	13	0.4824	0.6254		

D0835x0507	I	3-64	4	K	1-9	3	A2	23	25	18	0.6833	0.5391		
D0835x0516	I	1-46	4	K	1-6	1	M	47	19	3	0.5193	0.6878		
L1435x1741	C	4-39	4	K	4-1	1	G1	0	26	8	10.17	7.959	1.80E-06	79
L1435x1943	I	3-7	6	K	3-20	1	G2	28	11	9	0.8241	0.8729		
L1435x2011	I	3-74	3	K	2-28	2	G2	33	17	5	0.3297	0.3747		
L1435x2239	I	3-7	6	K	3-20	1	A2	28	15	7	0.5247	0.6119		
L1435x2353	II	1-2	4	K	1-39	4	M	0	15	11	1.051	1.106		
L1435x2354	II	3-73	6	K	1-39	1	M	0	0	0	0.6079	0.7869		
L1435x2690	III	3-30-3	4	K	3-11	1	M	0	4	1	7.704	6.509	7.30E-06	67
L1435x2867	III	3-30-3	4	K	3-11	1	M	0	2	0	11.35	11.78	1.24E-05	67.7
L1435x2887	III	3-23	4	K	4-1	1	M	0	0	0	0.7131	0.7086		
L1435x2889	III	3-30-3	3	K	1-17	1	M	0	1	0	0.6975	0.8907		
L1435x2991	III	3-33	4	K	3-20	2	M	0	0	0	4.178	5.794	1.59E-05	33.5
L1435x2998	III	1-46	4	K	1-6	1	G2	47	19	9	0.5034	0.6399		
L1435x3008	III	3-33	4	K	1-5	1	M	0	0	0	4.643	1.988	1.18E-05	54.6
h2088_k4041	C	3-23	4	K	1-17	4	M	0	14	2	1.668	2.646	ND	14
L1542x0898	I	3-30-3	2	K	3-15	1	G1	0	17	9	1.016	0.7371		
L1542x1238	II	3-30	4	K	3-15	1	M	11	7	6	8.46	7.179	ND	62.4
L1542x1286	II	3-23	4	K	1-17	4	M	0	6	0	0.4836	0.4707		
L1542x1287	II	4-4	4	K	4-1	1	A2	0	10	6	1.092	0.9613		
L1542x1369	II	3-30-3	3	K	3-15	1	M	0	2	0	3.083	1.907	ND	29.6
L1542x1449	II	1-8	5	K	3-11	4	G3	0	6	6	1.978	1.573		
L1542x1539	III	3-30	4	K	3-15	1	M	11	7	6	7.977	6.863	ND	66.2
L1542x1565	III	3-30	4	K	3-15	1	M	10	8	4	8.694	2.487	2.78E-06	63.5
L1542x1571	III	3-33	4	K	4-1	1	M	0	0	0	8.262	7.863	8.19E-06	44.2
L1542x1578	III	3-33	6	K	1-5	2	M	0	0	0	12.44	11.11	4.94E-07	69.7
L1542x1601	III	3-33	5	K	1-5	4	M	0	0	0	2.637	2.313	1.13E-05	23.8
L1542x1616	III	3-33	4	K	4-1	1	M	0	0	3	9.65	4.708	1.81E-06	49.3
L1542x1633	III	3-30	4	K	3-15	1	M	10	8	4	8.192	6.651	1.83E-05	67.4
L1542x1639	III	3-33	4	K	2-24	1	M	19	16	7	1.426	1.579	5.31E-06	
L1542x1648	III	3-30	4	K	3-15	1	M	10	8	4	7.479	5.594	1.87E-05	66.6
L1542x1671	III	3-30	4	K	3-15	1	M	10	8	4	7.059	0.943	5.25E-06	46.9
L1542x1690	III	3-33	4	K	2-24	1	M	20	12	5	2.672	3.787	1.03E-05	7.2
L1542x1744	III	3-49	4	K	2D-29	2	M	0	1	0	12.75	12.2	2.63E-07	93.3
L1542x1746	III	3-30	4	K	3-15	1	M	10	8	4	6.538	1.052	3.75E-06	37.3
L1542x1754	III	3-30-3	6	K	3-20	2	M	0	12	6	1.803	2.473	ND	0
L1542x1755	III	3-30	3	K	3-15	1	M	0	8	1	5.87	5.467	ND	48.5
L1542x1761	III	3-74	4	K	4-1	2	M	0	10	5	0.7952	0.7763		
L1542x1762	III	3-33	4	K	4-1	1	M	0	8	6	9.455	6.429	2.22E-06	17.7
L1542x1769	III	3-30	3	K	3-15	2	M	12	8	3	8.598	7.879	1.62E-05	61.5
L1542x1773	III	3-30	4	K	3-15	1	M	11	7	6	6.316	4.212	ND	48.1
L1542x1777	III	3-30	5	K	3-11	2	M	0	1	0	6.691	4.607	ND	56.2
L1542x1811	III	3-30	3	K	3-15	2	M	12	7	3	7.598	6.695	1.30E-05	49
L1542x1837	III	3-33	4	K	2-24	1	M	19	9	7	3.349	4.765	1.32E-05	7.2

L1542x1913	III	3-33	4	K	2-24	1	M	0	7	4	1.064	1.52		
L1542x1914	III	3-33	3	K	3-15	1	M	0	4	0	2.852	3.567	1.07E-05	6.3
L1542x1933	C	3-30	4	K	1-16	4	M	0	10	2	0.602	0.6777		
L1542x1972	C	3-33	4	K	2-24	1	M	0	2	2	2.29	1.455		
L1542x2041	C	3-7	5	K	2-30	1	M	0	11	14	0.7228	0.9048		
L1542x2128	C	1-2	5	K	1D-43	4	M	0	16	6	0.42	0.4535		
L1542x2143	C	4-39	5	K	1-33	2	G1	0	19	9	0.4007	0.4317		
L1542x2151	C	3-33	4	K	1-5	4	M	0	0	1	11.02	9.946	6.36E-07	73.2
L1542x2155	C	3-30	4	K	1-27	3	M	0	1	0	0.7394	0.5246		
L1542x2159	C	3-33	4	K	3-11	2	M	0	0	0	7.528	7.392	8.12E-06	57.7
L1542x2180	C	3-15	4	K	3-15	4	M	0	6	0	0.55	0.6262		
L1542x2191	C	3-7	3	K	4-1	3	A2	22	10	6	0.3979	0.4918		
L1542x2193	C	3-7	3	K	4-1	3	A2	22	10	6	0.5501	0.5291		
L1542x2204	C	3-7	4	K	1-33	5	M	23	26	13	1.298	1.43		
L1542x2207	C	3-33	3	K	1-5	1	M	0	3	3	13.49	12.45	5.64E-08	94.3
D0751x0214	III	4-30-2	4	K	1-27	4	A1	0	41	0	0.7277	0.9047		
D0751x0672	I	3-23	4	K	1-5	2	G1	7	27	26	0.9112	0.965	ND	
D0751x0701	I	3-23	4	K	1-5	2	G2	7	26	15	0.9237	0.897	ND	
D0751x0808	I	3-23	4	K	1-5	2	G2	7	28	13	1.031	0.6726	ND	
D0851x1756	II	3-48	4	K	1-33	3	M	0	0	0	0.4694	0.7221		6.5
D0851x1789	II	1-2	4	K	1-6	4	M	0	0	0	0.4881	0.8195		0
D0851x1790	II	4-4	3	K	3-20	2	G1	0	36	21	0.5166	0.7823		0
D0851x1831	II	1-69	4	K	3-20	2	G1	0	21	5	0.8608	1.021		
D0851x1841	II	4-30-2	5	K	3-15	4	G1	0	23	12	0.5136	0.5684		
D0851x1877	II	3-66	6	K	1-33	4	M	0	0	0	0.4738	0.4698		
D0851x1894	II	4-59	4	K	1-5	4	M	0	0	0	0.5126	0.8587		0
D0851x1985	II	3-23	4	K	1-5	4	A1	0	11	6	0.4404	0.437		
D0851x1996	II	3-9	3	K	1-5	1	M	0	0	0	0.484	0.5757		
D0851x2093	I	3-23	4	K	1-5	1	M	0	18	11	0.4789	0.5586		0.9
D0851x2115	I	4-59	6	K	1-NL1	1	A1	0	28	11	0.7783	0.8589		0
D0851x2118	I	5-a	3	K	2-28	3	M	0	0	1	0.6542	0.7711		
D0851x2168	I	3-23	5	K	1-5	1	M	0	0	0	0.9336	0.8765		
D0851x2218	I	3-30	4	K	2-30	2	M	0	0	0	0.7463	1.004		0
D0851x2248	I	4-59	5	K	3-11	4	A2	0	23	14	0.732	0.9639		
L1471x3246	II	3-33	6	K	3-20	2	M	33	5	1	11.81	10.94	2.70E-07	74
L1471x3374	II	3-33	6	K	3-20	2	M	33	5	1	11.4	10.36	2.85E-07	72.5
L1471x3431	II	3-30-3	4	K	1-5	1	A2	22	43	14	0.54	0.4201		
L1471x3450	II	3-30-3	4	K	1-5	1	M	22	39	15	0.3989	0.5784		
L1471x3536	I	3-21	6	K	2-28	5	M	0	4	0	0.8453	0.8723		
L1471x3639	II	3-33	6	K	3-20	2	M	33	8	1	11.5	10.86	2.44E-07	71.9
L1471x3683	II	3-30-3	4	K	1-5	1	A2	22	41	20	0.5861	0.8821		
L1471x3717	II	3-30-3	4	K	1-5	1	M	22	35	12	0.4909	0.8368		
L1471x3726	II	1-2	4	K	2-28	2	G1	2	6	5	13.42	3.312	1.20E-05	86.6
L1471x3767	II	3-33	6	K	3-20	2	M	33	14	5	12.44	11.24	2.81E-07	83.5

L1471x3768	II	3-33	6	K	3-20	2	M	33	8	3	12.45	10.25	2.23E-07	85.4
L1471x3788	II	3-30-3	4	K	1-5	1	A2	22	39	15	0.9357	0.9204		
L1471x3846	III	3-33	4	K	1-5	1	M	0	1	1	12.23	11.19	1.33E-07	97.2
L1471x3865	III	3-30	3	K	3-20	2	M	25	3	1	13.26	12.27	5.17E-07	80.8
L1471x3870	III	3-15	4	K	2-30	1	M	8	11	1	12.65	12.08	7.90E-08	96.9
L1471x3896	III	3-33	6	K	3-20	2	M	33	7	5	12.98	11.9	5.20E-08	100
L1471x3908	III	3-33	6	K	3-20	2	M	33	7	2	13.24	12.11	5.04E-08	94.1
L1471x3919	III	4-4	6	K	3-20	2	M	57	1	2	10.55	1.375	ND	7.6
L1471x3921	III	3-30	3	K	3-20	2	M	25	5	1	11.28	11.46	4.59E-07	74.1
L1471x3922	III	3-33	5	K	3-11	2	M	31	2	3	11.49	10.43	1.94E-06	79.7
L1471x3945	III	3-33	4	K	3-20	1	M	34	2	0	13.63	12.95	4.35E-08	100
L1471x3960	III	3-33	6	K	3-20	2	M	33	10	3	13.48	11.64	2.60E-09	100
L1471x3965	III	3-33	4	K	1-5	1	G1	27	0	2	11.6	10.85	3.13E-08	96.5
L1471x3975	III	3-33	4	K	2-24	2	M	0	10	1	6.07	3.522	4.76E-06	
L1471x3978	III	3-33	6	K	2-24	2	G1	29	5	2	9.959	8.136	1.68E-05	57.8
L1471x3991	III	1-46	6	K	1-5	1	M	0	0	0	0.7292	0.9019		
L1471x4031	III	3-33	4	K	3-11	4	M	0	0	0	13.5	11.18	4.85E-08	
L1471x4041	III	3-48	3	K	1-17	4	G1	36	10	1	10.96	9.588	1.46E-05	90.9
L1471x4052	III	3-23	3	K	3-20	1	M	16	13	4	4.717	4.808	ND	46.2
L1471x4055	III	3-48	3	K	1-17	4	A1	36	12	6	5.314	8.125	2.44E-05	84.4
L1471x4059	III	3-33	4	K	3-11	1	A1	32	8	5	10.87	8.299	7.76E-06	59.6
L1471x4067	III	3-15	4	K	2-30	1	M	8	12	1	13.48	10.95	7.26E-08	97.6
L1471x4074	III	3-33	4	K	3-11	1	M	32	1	1	6.786	9.45	9.22E-06	51.6
L1471x4087	III	3-30	3	K	3-20	2	G3	25	3	1	12.51	10.41	4.61E-07	80.9
L1471x4092	III	3-33	4	K	3-20	1	M	34	0	0	12.51	10.96	6.24E-08	100
L1471x4115	III	3-30	3	K	3-20	2	G1	25	4	1	12.45	10.58	4.64E-07	86.2
L1471x4130	III	3-33	6	K	3-20	2	M	33	7	2	11.77	12.03	5.10E-08	90.5
L1471x4137	III	3-30	6	K	1-39	2	M	0	0	0	0.9779	1.353		
L1471x4142	III	3-49	4	K	3-20	1	M	38	1	0	13.29	11.07	4.13E-08	99.7
L1471x4151	III	3-33	5	K	3-11	2	M	31	2	2	12.52	10.59	3.90E-06	74.8
L1471x4167	III	1-2	4	K	2-28	2	G1	2	6	5	13.11	3.24	7.90E-06	88.5
L1471x4237	C	4-4	6	K	3-20	2	M	57	1	2	9.696	1.307	ND	9.3
L1471x4239	C	3-23	3	K	3-20	1	M	16	15	5	2.713	3.186	ND	36.5
L1471x4243	C	3-23	3	K	3-20	1	M	16	13	4	1.855	1.833	ND	13.4
L1471x4264	C	3-15	4	K	2-30	1	M	8	12	2	11.26	11.38	1.06E-07	98.9
L1471x4306	C	4-31	4	K	4-1	1	M	0	5	0	1.495	0.9565		
L1471x4310	C	3-33	4	K	1-5	1	G1	27	0	2	12.01	12.25	3.07E-08	100
L1471x4332	C	3-23	4	K	4-1	1	A1	18	27	9	0.497	0.6702		
L1471x4353	C	3-48	3	K	1-17	4	M	36	10	1	8.183	10.06	1.15E-05	96.8
L1471x4377	C	3-33	4	K	3-15	1	M	0	0	0	0.3493	0.3158		
L1471x4396	C	4-4	6	K	3-20	2	M	57	2	2	6.622	0.3291	ND	
L1471x4415	C	3-33	4	K	4-1	1	M	0	0	0	10.75	10.28	9.33E-07	65.7
L1471x4442	C	3-23	4	K	4-1	1	A2	18	23	8	0.4266	0.4788		
L1471x4467	C	3-23	3	K	3-20	1	M	16	14	5	4.064	3.334	ND	41.6

L1471x4476	C	3-33	4	K	3-20	1	G1	34	1	2	11.54	10.7	3.73E-08	100
L1471x4493	C	3-49	4	K	3-20	1	G1	38	5	1	12.07	12.22	2.46E-09	100
L1471x4496	C	3-33	1	K	3-15	3	M	0	0	0	12.41	11.79	5.50E-06	65.7
L1471x4498	C	3-33	4	K	3-11	2	G1	0	9	2	12.36	12.2	6.20E-10	
L1471x4533	C	3-23	4	K	4-1	1	A2	18	23	8	0.4476	0.803		
L1471x4560	C	3-49	4	K	3-20	1	M	38	6	3	13.43	10.72	2.37E-06	94.1
D0972x1157	I	3-7	4	K	2-30	1	M	0	28	10	0.5702	0.6738		
D0972x1460	I	3-23	4	K	1-5	1	M	0	14	11	0.8998	1.063		
D0972x1465	I	3-48	4	K	3-15	4	A1	0	17	7	0.6861	0.913		
D0972x1547	II	3-33	3	K	1-5	1	M	0	5	1	11.18	7.394	1.94E-07	66.1
D0972x1548	II	3-30-3	3	K	3-15	1	M	0	12	7	1.223	0.8995		
D0972x1572	II	4-59	3	K	2-28	2	M	32	1	1	13.26	0.9458	9.78E-06	81.2
D0972x1576	II	3-30-3	3	K	3-11	1	M	8	8	0	10.26	4.737	9.41E-06	71.7
D0972x1593	II	3-30-3	3	K	3-11	4	M	7	7	0	7.148	5.066	9.87E-06	45.9
D0972x1620	II	4-30-2	4	K	2-30	5	G2	0	26	14	0.6419	0.938		
D0972x1647	II	3-30-3	3	K	3-11	4	M	7	2	1	7.559	5.33	9.56E-06	59.4
D0972x1672	II	3-74	5	K	3-20	1	G4	0	28	10	0.3811	0.4916		
D0972x1765	II	4-59	3	K	2-28	2	M	32	0	0	14.15	1.749	1.00E-05	76.8
D0972x1782	II	3-30-3	3	K	3-11	4	M	7	7	1	5.197	1.975	7.53E-06	52.7
D0972x1783	II	3-30-3	3	K	3-11	4	M	7	0	1	7.384	5.169	8.58E-06	53.4
D0972x1788	II	3-30-3	5	K	3-11	1	M	0	9	2	5.017	3.25	7.50E-06	42.5
D0972x1797	II	3-33	4	K	1-5	1	G1	16	0	0	13.13	11.27	1.87E-08	81.7
D0972x1809	II	4-61	4	K	3-11	2	A2	33	40	21	0.6694	0.6674		
D0972x1834	II	3-33	4	K	1-5	2	M	0	0	0	7.102	3.344	4.56E-06	36
D0972x1884	II	3-33	4	K	1-5	1	M	0	0	0	0.5762	0.6022	ND	
D0972x1888	II	3-33	4	K	1-5	1	G1	15	2	0	14.42	11.34	4.59E-09	100
D0972x1949	III	3-33	3	K	1-5	1	G1	0	4	0	12.65	9.392	2.63E-08	96.7
D0972x1954	III	3-33	4	K	1-5	1	G1	0	7	3	13.32	9.602	1.83E-08	86.4
D0972x1985	III	4-59	3	K	2-28	2	M	32	3	0	13.36	1.78	9.93E-06	74.7
D0972x1987	III	3-33	3	K	1-5	3	M	13	0	0	12.37	11.65	2.20E-08	100
D0972x1989	III	3-7	4	K	1-5	4	M	0	13	12	1.007	3.464		
D0972x1994	III	4-59	3	K	2-28	2	M	32	2	1	12.17	0.9443	9.54E-06	
D0972x2001	III	3-33	4	K	1-5	1	G1	0	0	0	13.34	10.97		
D0972x2027	III	4-39	3	K	4-1	1	M	0	8	2	0.6553	0.5225		
D0972x2032	III	3-74	5	K	2-28	4	M	0	0	0	12.86	9.403	2.38E-06	
D0972x2038	III	3-33	4	K	1D-13	4	M	0	0	0	5.404	4.446		
D0972x2073	III	3-33	4	K	1-5	2	G1	17	3	1	12.66	11.9	4.66E-09	92.2
D0972x2100	III	3-33	3	K	1-5	3	G1	13	3	1	14.68	11.34	6.32E-09	86.7
D0972x2102	III	3-21	5	K	1-39	1	G2	0	18	29	0.8011	0.9648		
D0972x2103	III	3-33	3	K	1-5	2	G1	0	5	0	12.14	10.01	6.92E-10	100
D0972x2130	III	3-33	4	K	1-5	1	A1	0	13	7	0.8077	0.9099		
D0972x2140	III	3-33	5	K	1-5	1	G1	0	6	1	13.78	10.51	8.96E-10	100
D0972x2147	III	3-33	4	K	1-5	2	G1	17	3	1	13.12	12.14	4.69E-09	100
D0972x2151	III	3-33	2	K	4-1	1	G1	12	0	0	9.931	6.138	4.95E-06	55.8

D0972x2163	III	3-33	4	K	1-5	1	M	15	0	0	14	10.58	7.04E-09	100
D0972x2164	III	3-33	3	K	1-5	1	G1	0	2	1	13.93	10.86	6.16E-10	100
D0972x2188	III	3-33	3	K	1-5	3	M	13	0	0	12.45	10.92	2.18E-08	89.6
D0972x2219	III	3-33	3	K	1-5	4	M	14	3	1	12.41	11.23	5.72E-09	91.5
D0972x2235	III	3-33	2	K	4-1	1	M	12	0	0	9.846	5.599	5.19E-06	57.5
D0972x2243	III	3-33	4	K	1-5	3	M	0	0	0	13.51	10.79	1.18E-08	100
D0972x2248	III	3-33	4	K	1-5	1	G1	16	1	1	12.44	10.33	1.75E-08	80.8
D0972x2249	III	4-31	4	K	4-1	1	M	25	8	3	3.419	1.68	8.41E-06	29.9
D0972x2251	III	4-59	3	K	2-28	2	M	32	1	0	0.634	0.6896		
D0972x2262	III	3-33	4	K	1-5	2	G1	17	3	2	11.17	9.784	1.27E-07	89.3
D0972x2290	III	3-33	3	K	1-5	4	M	14	0	0	10.06	5.927	1.58E-06	52.9
D0972x2292	III	3-33	4	K	1-5	1	M	16	3	0	13.26	10.14	1.36E-08	97.5
D0773x0980	III	3-49	4	K	1-5	1	M	18	0	0	7.227	4.038	3.43E-06	37.6
D0773x1020	III	3-7	4	K	4-1	4	M	21	1	0	9.597	2.077	4.77E-06	70.7
D0773x1041	III	3-23	4	K	1-5	5	M	5	5	5	10.61	2.411	8.00E-06	65.5
D0773x1090	III	3-49	4	K	4-1	2	M	16	1	0	12.96	11.49	6.56E-07	76.8
D0773x1204	III	3-7	4	K	4-1	4	M	21	2	2	6.622	1.45		63.8
D0773x1210	III	3-33	3	K	1-5	1	M	9	3	4	12.81	12.52	1.14E-08	100
D0773x1216	III	3-48	4	K	2D-29	4	A1	14	9	8	5.532	2.695	5.25E-06	
D0773x1239	III	3-49	4	K	1-5	1	M	18	0	0	7.822	8.304	3.51E-06	41
D0773x1241	III	1-18	4	K	3-11	3	M	1	13	4	2.065	2.911	5.74E-06	0
D0773x1259	III	3-49	4	K	4-1	2	M	16	0	0	13.73	11.21	5.00E-07	72.5
D0773x1284	III	3-7	4	K	4-1	4	M	21	1	2	11.2	3.725	7.06E-06	
D0773x1288	III	3-33	4	K	1-39	3	G1	0	0	0	12.63	11.33		68.3
D0773x1291	III	3-33	6	K	2-30	2	M	12	7	6	1.717	1.545		
D0773x1305	III	3-49	4	K	4-1	2	G1	16	2	5	11.93	10.54	3.78E-09	95.2
D0773x1316	III	3-23	4	K	1-5	1	M	4	18	6	10.65	10.65	4.01E-06	59
D0773x1320	III	3-23	4	K	1-5	1	M	4	13	6	9.334	7.948	2.12E-06	74.7
D0773x1356	III	3-23	4	K	1-5	1	M	4	20	5	7.217	5.02	3.54E-06	69.1
D0773x1366	II	3-23	4	K	1-5	5	M	5	2	2	11.27	1.657	9.32E-06	53.7
D0773x1368	II	3-23	4	K	1-5	5	M	5	7	5	11.08	2.388	8.25E-06	62.1
D0773x1372	II	3-49	4	K	2D-29	1	M	15	0	0	0.739	0.8399		
D0773x1401	II	3-23	4	K	1-5	5	M	5	13	10	11.75	2.874	4.68E-06	
D0773x1403	II	3-23	1	K	4-1	1	M	0	19	12	0.3939	0.4585		
D0773x1419	II	3-23	4	K	1-5	5	M	5	12	11	8.221	1.123	5.06E-06	41.7
D0773x1427	II	3-23	4	K	1-5	1	M	4	15	3	7.325	7.227	4.47E-06	59.4
D0773x1444	II	3-23	6	K	1-5	4	M	6	3	4	6.041	6.926	2.21E-06	34.3
D0773x1450	II	3-23	4	K	1-5	1	A1	4	17	10	10.45	8.756	2.39E-06	60.5
D0773x1463	II	3-23	4	K	1-5	5	M	5	7	9	9.354	1.688	6.37E-06	81.1
D0773x1505	II	3-23	6	K	1-5	1	M	0	12	5	8.985	7.574	1.03E-06	
D0773x1551	II	3-23	4	K	1-5	5	M	5	9	8	10.57	3.291	3.36E-06	74
D0773x1628	II	3-23	4	K	1-5	5	M	5	12	11	11.71	2.683	4.05E-06	82.8
D0773x1780	II	3-33	6	K	2-30	2	M	12	9	1	0.6587	0.7955		
D0773x1810	II	3-21	6	K	1-27	4	M	0	0	0	0.6874	0.8096		

Supplementary Tables

D0873x0588	III	3-7	4	K	4-1	4	M	21	2	0	8.939	1.725	3.41E-06	
D0873x0613	III	4-39	6	K	1-17	2	G1	26	9	7	0.5126	0.5975		
D0873x0614	III	3-33	4	K	1-5	1	G1	0	1	1	12.97	11.2	1.95E-09	
D0873x0615	III	3-7	4	K	4-1	4	M	21	5	0	9.406	2.032	3.15E-06	
D0873x0619	III	1-18	4	K	3-11	3	M	1	13	2	3.024	2.282	7.04E-06	12.4
D0873x0623	III	3-23	4	K	1-5	1	M	4	21	8	8.431	7.87	3.63E-06	54.9
D0873x0647	III	3-33	6	K	1-5	1	M	10	12	3	10.88	10.88	1.99E-09	
D0873x0649	III	1-18	4	K	3-11	3	M	1	18	2	1.475	2.43		
D0873x0668	III	3-30-3	4	K	3-15	1	M	29	7	3	2.911	1.258		
D0873x0689	III	3-49	6	K	2D-29	2	M	17	3	3	11.85	10.21	2.17E-07	81
D0873x0706	III	3-23	4	K	1-5	5	M	5	5	5	8.96	1.433	8.68E-06	51.9
D0873x0785	III	1-18	4	K	3-11	3	M	1	18	5	0.5824	0.3885	7.02E-06	
D0873x0800	III	3-33	4	K	3-11	4	M	13	2	3	10.67	6.324	2.48E-06	60.2
D0873x0828	III	3-30-3	4	K	3-15	1	M	29	7	3	2.392	0.9393		
D0873x0831	III	3-33	6	K	2-30	2	M	12	7	6	1.268	1.181		
D0873x0896	III	3-48	4	K	2D-29	4	A1	14	9	8	4.094	1.841	5.38E-06	
D0873x0898	III	3-23	4	K	1-5	5	M	5	18	14	12.17	2.274	2.41E-06	83.4
D0873x0900	III	3-23	4	K	1-5	1	M	4	15	4	9.106	8.009	3.63E-06	68.2
D0873x0905	III	3-23	4	K	1-5	1	M	4	16	2	7.334	5.722	5.26E-06	58.2
D0873x0922	III	3-33	4	K	1-12	4	M	0	2	1	5.555	3.514	5.89E-06	19.7
D0873x1035	II	3-23	4	K	1-5	5	M	5	9	8	9.235	2.587	3.14E-06	85.3
D0873x1096	II	3-49	6	K	2D-29	2	M	17	0	0	12.84	11.42	4.22E-07	76.8
D0873x1097	II	3-23	4	K	1-5	5	M	5	23	13	11.78	2.705	6.45E-06	59.2
D0873x1158	II	3-7	4	K	1-33	1	M	0	0	0	1.023	0.9401		
D0873x1163	II	3-33	6	K	2-30	2	M	12	11	1	1.73	1.624		0
D0873x1257	II	3-23	4	K	1-5	5	M	5	16	17	13.61	4.286	2.51E-06	81.8
D0873x1264	II	3-23	4	K	1-5	5	M	5	7	8	11.96	2.243	6.27E-06	
D0873x1289	II	1-18	4	K	3-11	3	M	1	6	2	2.232	1.963	9.06E-07	33.5
D0873x1308	II	3-49	6	K	2D-29	2	M	17	0	0	12.81	11.04	5.30E-07	73
D0873x1316	II	3-23	4	K	1-5	1	M	4	15	6	10.43	9.184	2.18E-06	77.6
D0873x1337	II	3-23	4	K	1-5	1	M	4	17	3	6.556	3.265	5.24E-06	51.7
D0873x1342	II	3-23	4	K	1-5	5	M	5	6	8	8.979	1.592	6.33E-06	86.4
L1517x0042	I	3-33	4	L	2-23	3	M	0	0	2	1.808	1.218		
L1517x0201	I	3-33	4	L	2-14	3	M	0	0	0	2.45	2.294	ND	0
L1517x0212	I	3-33	4	L	1-47	2	M	0	0	0	0.6448	0.8429		
L1517x0418	II	1-46	4	L	2-8	2	M	2	19	4	1.841	1.976	ND	1.2
L1517x0480	II	3-13	4	L	3-9	3	M	0	15	11	0.7963	0.6673		
L1517x0498	II	3-9	4	L	2-14	2	M	0	0	0	0.531	0.4273		
L1517x0521	II	4-59	4	L	1-47	3	M	0	7	5	2.609	1.938		
L1517x0552	II	3-23	4	L	1-47	2	M	0	0	0	1.046	0.6868		
L1517x0581	III	1-46	4	L	2-8	2	M	2	19	4	1.006	0.8062		
L1517x0597	III	4-39	4	L	7-43	3	M	0	0	0	0.9917	0.7692		
L1517x0610	III	3-21	4	L	6-57	3	M	0	4	1	1.123	0.9702		
L1517x0622	III	3-74	4	L	1-47	1	M	0	8	6	3.369	2.052	1.77E-07	45

L1517x0632	III	4-39	4	L	2-23	3	M	0	2	5	0.8283	0.8347		
L1517x0713	C	4-39	4	L	3-27	3	M	0	5	4	0.9995	1.18		
L1517x0825	C	3-23	4	L	1-44	2	M	0	6	5	0.948	0.8358		
L1426x0188	I	4-31	6	L	1-44	3	M	0	10	6	1.365	0.5971		
L1426x0222	I	4-39	4	L	3-21	2	A2	12	18	14	0.6723	0.698		
L1426x0453	II	3-21	3	L	1-51	2	A1	0	20	14	0.7385	0.7312		
L1426x0906	III	3-33	6	L	1-44	2	M	0	5	6	0.5693	0.8751		
L1426x1199	C	3-21	4	L	1-44	2	M	0	0	0	0.8812	0.8354		
L1426x1202	C	3-7	5	L	2-11	1	M	0	6	2	0.5638	0.7087		
L1426x1218	C	3-23	4	L	3-1	2	M	0	0	0	0.4397	0.4092		
L1435x1829	C	3-23	4	L	9-49	3	A1	0	19	4	0.9929	1.246		
L1435x1852	C	4-30-4	4	L	2-8	1	M	0	0	2	0.7484	0.9061		
L1435x2489	II	3-74	2	L	2-23	1	A2	36	23	6	1.458	1.406		
L1435x2546	II	1-2	3	L	3-1	2	M	0	0	0	0.653	0.8207		
L1435x2836	III	4-39	6	L	4-69	3	G2	0	5	5	0.5186	0.5424		
L1435x2873	III	3-23	5	L	1-51	3	G3	0	4	1	0.9698	1.186		
L1435x2896	III	5-51	3	L	9-49	3	G3	0	1	1	0.6158	0.6872		
L1542x1205	II	3-30-3	4	L	2-14	2	M	0	9	0	1.238	1.084		
L1542x1248	II	4-39	4	L	7-43	2	M	0	28	17	0.7612	0.6909		
L1542x1512	II	1-2	6	L	3-1	1	G1	0	2	0	1.141	1.06		
L1542x1606	III	3-30	4	L	2-14	2	M	14	1	1	6.724	6.642	1.73E-05	22.6
L1542x1650	III	3-53	4	L	2-14	1	M	0	3	6	0.6666	0.435		
L1542x1698	III	3-23	4	L	2-14	2	M	7	8	8	0.9044	0.6334	ND	
L1542x1906	III	3-23	4	L	2-14	2	M	7	10	9	0.8669	1.144	ND	
L1542x1955	C	3-33	2	L	1-40	1	M	0	1	0	12.9	11.71	1.65E-07	87.2
L1542x2008	C	3-23	4	L	2-14	2	M	7	10	9	1.023	1.09	ND	
L1542x2045	C	3-33	6	L	1-40	1	M	0	0	0	0.3725	0.4506		
L1542x2080	C	3-23	4	L	2-14	2	M	7	8	8	0.6105	0.4767	ND	
L1542x2133	C	3-23	4	L	2-14	2	M	7	11	6	7.235	2.724	1.04E-05	57.4
L1542x2215	III	3-23	4	L	2-14	2	M	7	9	13	0.8415	0.6555	ND	
D0751x0054	III	1-3	4	L	1-47	3	M	2	4	4	0.9378	0.7449	ND	
D0751x0057	III	1-3	4	L	1-47	3	M	2	11	5	1.819	1.357	ND	
D0751x0059	III	1-3	4	L	1-47	3	M	2	12	8	1.63	1.156	ND	
D0751x0121	III	3-48	4	L	1-47	2	G1	0	1	0	6.216	5.379	ND	60.8
D0751x0164	III	1-3	4	L	1-47	3	M	2	15	3	1.186	0.9161	ND	
D0751x0168	III	1-3	4	L	1-47	3	M	2	11	4	2.042	2.333	ND	14.5
D0751x0169	III	1-3	4	L	1-47	3	G1	2	14	9	3.992	2.476	ND	
D0751x0175	III	1-3	4	L	1-47	3	M	2	14	6	1.907	1.483	ND	
D0751x0211	III	1-3	4	L	1-47	3	M	2	15	7	2.056	2.373	ND	25.3
D0751x0259	III	1-3	4	L	1-47	3	M	2	11	4	2.167	1.982	ND	
D0751x0322	III	1-3	4	L	1-47	3	M	2	18	7	4.549	2.847	ND	46.4
D0751x0353	III	1-3	4	L	1-47	3	M	2	13	9	1.911	1.172	ND	
D0751x0371	III	1-3	4	L	1-47	3	M	2	11	4	2.442	1.949	ND	29.6
D0751x0415	II	3-74	4	L	3-1	2	M	0	8	8	0.8449	0.8916		

Supplementary Tables

D0751x0444	II	1-3	4	L	1-47	3	M	2	17	7	0.9967	1.04	ND	
D0751x0449	II	1-3	4	L	1-47	3	M	2	12	4	1.614	1.505	ND	
D0751x0500	II	4-39	3	L	1-40	1	M	16	8	3	3.892	2.183	ND	62.5
D0751x0514	II	4-39	3	L	1-40	1	M	16	8	3	4.863	2.361	ND	69.2
D0751x0547	II	1-3	4	L	1-47	3	M	2	10	5	1.905	2.74	ND	
D0751x0583	II	4-b	5	L	2-8	2	A1	0	24	21	0.8119	1.015		
D0751x0880	III	1-3	4	L	1-47	3	M	2	14	8	2.218	0.9975	ND	
D0751x0894	III	4-59	4	L	2-8	2	M	0	0	0	0.5465	0.8023	ND	4.3
D0751x0901	III	1-3	4	L	1-47	2	M	2	14	5	3.93	1.555	ND	
D0751x0917	III	3-23	4	L	1-47	3	M	0	0	6	0.5807	0.9067		6.7
D0751x0938	III	1-2	4	L	1-51	2	M	1	25	25	1.692	2.772	ND	25.9
D0751x0968	III	1-3	4	L	1-47	2	M	2	15	6	4.355	1.583	ND	
D0851x1569	III	3-30	6	L	2-14	2	M	0	0	0	0.7929	0.7398		
D0851x1570	III	5-51	3	L	2-14	3	G1	0	23	23	0.6657	0.7273		4.7
D0851x1592	III	1-3	4	L	1-47	3	M	2	11	4	3.196	1.565	ND	
D0851x1665	III	1-3	4	L	1-47	3	M	2	14	8	2.319	1.163	ND	
D0851x1682	III	3-74	4	L	2-14	3	M	0	20	21	0.857	0.868		
D0851x1710	III	3-21	5	L	3-1	2	G1	0	1	2	0.6185	0.7629		1.1
D0851x1711	III	1-3	4	L	1-47	3	M	2	16	8	2.239	1.314	ND	
D0851x1742	III	1-3	4	L	1-47	3	M	2	18	7	4.349	2.793	ND	48.9
D0851x1758	II	1-3	4	L	1-47	3	M	2	16	6	3.167	1.59	ND	46.2
D0851x1766	II	3-21	4	L	2-14	1	G1	0	35	25	0.4336	0.5866		0
D0851x1767	II	3-15	6	L	3-21	3	G1	0	27	19	0.4629	0.4804		
D0851x1769	II	1-2	4	L	1-51	2	M	1	12	7	0.6988	0.9236		
D0851x1867	II	1-3	4	L	1-47	3	M	2	8	4	2.311	1.335	ND	
D0851x2031	II	3-49	6	L	2-14	1	M	0	0	0	0.6458	0.6419		
D0851x2137	I	4-59	3	L	2-11	3	M	0	0	0	0.4304	0.503		
D0851x2149	I	4-59	3	L	1-51	2	M	0	0	0	0.587	0.6944		0.7
D0851x2203	I	3-23	4	L	2-8	2	M	0	0	0	0.6995	0.9443		
D0851x2225	I	4-34	3	L	1-47	2	M	0	0	0	0.705	0.9024		
D0851x2235	I	4-59	4	L	2-14	2	M	0	0	2	0.4579	0.5529		0
D0851x2249	I	4-59	2	L	1-47	3	A1	0	18	0	0.8899	1.178		
L1471x3220	II	3-73	4	L	9-49	1	M	0	0	0	0.9894	1.515		
L1471x3269	II	3-33	4	L	2-14	1	M	0	1	3	8.933	9.29	1.02E-06	69.9
L1471x3426	II	3-23	4	L	1-47	1	M	14	13	7	13.2	12.46	1.15E-08	100
L1471x3659	II	3-30	4	L	3-21	3	M	26	7	5	12.36	10.25	6.06E-07	84.6
L1471x3710	II	3-7	3	L	1-51	2	M	42	7	2	9.819	7.174	7.03E-06	71.6
L1471x3878	III	3-7	4	L	1-51	2	M	0	2	3	8.268	6.728	9.11E-06	
L1471x3933	III	3-23	4	L	1-47	1	M	14	15	7	13.22	12.02	1.69E-08	97.9
L1471x3949	III	3-23	4	L	3-1	3	M	0	4	3	1.377	1.391		
L1471x4112	III	3-7	3	L	1-51	2	M	42	7	3	7.924	4.642	6.03E-06	69.4
L1471x4267	C	3-23	4	L	1-47	2	M	14	2	0	11.97	10.32	4.85E-08	100
L1471x4512	C	3-9	6	L	3-21	3	G1	53	0	1	0.5796	0.5952		
D0972x1196	I	3-30-3	4	L	4-69	3	M	9	2	2	3.862	2.383	4.54E-06	40.7

Supplementary Tables

D0972x1271	I	3-7	4	L	2-14	1	M	0	22	8	0.3613	0.4102		0
D0972x1392	I	3-74	1	L	2-23	1	M	0	23	12	0.4888	0.6077		0
D0972x1456	I	4-30-2	3	L	1-44	1	A1	0	16	10	0.7153	0.9698		
D0972x1668	II	3-23	4	L	3-27	3	M	0	15	2	0.4542	0.5092		
D0972x1684	II	4-30-2	4	L	1-44	1	A1	0	13	8	0.5892	0.5809		
D0972x1694	II	3-30	4	L	9-49	1	M	11	2	2	9.853	8.463	6.46E-06	71.3
D0972x1713	II	3-30-3	4	L	4-69	3	M	9	1	2	2.775	1.914	5.80E-06	52.6
D0972x1791	II	3-30	4	L	9-49	1	M	11	11	3	5.135	6.019	1.03E-05	48.9
D0972x1846	II	3-30-3	4	L	4-69	3	M	9	3	2	5.243	2.681	6.87E-06	64.2
D0972x1928	III	3-30-3	4	L	4-69	3	M	9	3	2	3.364	1.71	4.56E-06	26.7
D0972x2031	III	3-30-3	4	L	4-69	3	M	9	3	2	6.097	3.193	6.60E-06	34.6
D0972x2051	III	1-69	4	L	2-23	3	M	0	8	8	0.9424	0.7766		
D0972x2056	III	3-23	4	L	2-11	3	M	0	18	10	1.216	1.132		
D0972x2159	III	4-39	5	L	9-49	2	A1	28	18	10	11.51	9.902	5.06E-08	86.8
D0972x2168	III	1-2	3	L	2-23	2	M	1	0	0	0.7202	0.7922		
D0972x2296	III	4-39	5	L	9-49	2	A1	28	22	15	11.52	9.841	1.41E-07	68.7
D0773x0982	III	3-23	4	L	1-47	2	M	28	0	0	11.38	9.135	2.42E-06	
D0773x1001	III	3-23	4	L	1-47	2	M	7	0	0	9.339	4.461	6.22E-06	73.8
D0773x1006	III	3-23	4	L	1-47	2	M	7	0	0	9.076	5.602	5.14E-06	78.1
D0773x1015	III	3-23	4	L	1-47	2	M	7	0	0	9.309	6.553	5.00E-06	85.9
D0773x1096	III	3-7	4	L	4-69	3	M	22	6	1	8.611	4.817	4.52E-06	78.1
D0773x1194	III	3-23	4	L	4-69	3	M	0	15	8	0.5218	0.9401		
D0773x1199	III	3-23	4	L	1-47	2	M	7	0	0	10.48	7.822	5.85E-06	81.8
D0773x1233	III	3-7	4	L	4-69	3	G1	22	9	1	10.53	5.386	5.32E-07	74
D0773x1256	III	3-74	4	L	9-49	2	M	24	0	0	12.92	12.04	4.68E-08	100
D0773x1340	III	3-23	4	L	1-47	2	M	7	0	0	9.198	6.035	6.01E-06	81.2
D0773x1503	II	3-21	4	L	3-21	2	M	0	0	0	0.3982	0.5058		
D0873x0684	III	3-74	4	L	9-49	2	M	24	0	0	11.3	11.7	3.12E-08	100
D0873x0829	III	3-23	4	L	1-47	2	M	7	0	0	8.505	5.761	6.17E-06	88.7
D0873x0860	III	3-23	4	L	1-47	2	M	28	1	0	10.28	6.782	2.39E-06	64
D0873x0871	III	3-23	4	L	1-47	2	M	7	0	0	10.92	7.193		
D0873x1338	II	3-30	4	L	2-8	3	M	8	9	6	1.076	0.9934		

11. Acknowledgements

My deepest appreciation goes to Prof. Dr. Hedda Wardemann for the opportunity she provided to work on several exciting projects during the course of my PhD. I would like to thank her for all the time and support she offered and her excellent scientific tutelage. I sincerely thank the trial volunteers for their courage and altruism. This project would not have been possible without the support of Dr Benjamin Mordmuller and the clinical team in Tuebingen, Dr Elena Levashina, Dr Giulia Costa and Cornelia Kreschel in Berlin, Lisa Buchaer and Dr Thomas Hoefer in Heidelberg. I convey my thanks to all of them for their collaboration in ideas, expertise and practical work.

I would like to thank Prof. Dr. Arturo Zychlinsky, Prof. Dr. Anja Hauser, Prof. Dr. med. Thomas Doerner and Prof. Dr. Christian Schmitz-Linneweber for offering to be in my thesis committee and for their time in reviewing my thesis.

My sincere thanks go to Dr Christian Busse for the fundamental training he offered in the lab and the countless hours of intellectual discourse. My special thanks go to Tim for coffee, piano and endless thrilling scientific discussions and Gianna for being the best salsa partner. I would like to thank Stefan, Conny and Natalie from Berlin and Dorien, Julia, Ilka, Tizian, Katharina, Claudia and Gemma from Heidelberg for giving me a warm welcome and a warmer stay in Germany. I would like to thank them all for the kind help and presence they always provided both inside and outside the lab. I also appreciate their bravery in trying the Indian cuisine I prepared. I would like to thank the FACS core facility in Berlin and Dr Peter Sehr in EMBL for assisting me with SPR.

To the friends who made my PhD time most memorable, Raj, Cindy, Vandana, Brinda, Muthu, Frida, and Vadim, I convey my cordial thanks.

I would like to thank ZIBI, IMPRS and GRK for their financial support in stipend and travel grants.

Finally, I would like to thank my parents, brother and friends back in India for their love, support and encouragement.